Determining the Role of Agro-Ecosystems in a Changing Climate: Quantification of CO_2 exchange, Carbon allocation and Storage in the Main Agricultural Crops of South Korea.

Dissertation

to attain the academic degree of Doctor of Natural Science (Dr. rer. nat.)

of the Bayreuth Graduate School of Mathematical and Natural Sciences (BayNAT) of the

University of Bayreuth

presented by Steve Lindner

born April 17, 1982 in Zwickau (Germany)

Bayreuth, January 2016

This doctoral thesis was prepared between April 2009 and January 2016 at the Department of Plant Ecology, University of Bayreuth, and was supervised by Dr. habil. Dennis Otieno, Prof. Dr. Bernd Huwe and Prof Dr. John Tenhunen.

Date of submission: 18.01.2016

Date of defence: 28.04.2016

Acting director: Prof. Dr. Stephan Kümmel

Doctoral committee:

P.D. Dr. Dennis Otieno   (1st reviewer)

Prof. Dr. Cyrus Samimi   (2nd reviewer)

Prof. Dr. Gerhard Gebauer   (chairman)

J. Prof. Dr. Angelika Mustroph

Table of contents

Carbon Dioxide Exchange and its Regulation in the main Agro-ecosystems of Haean Catchment in South Korea

Canopy scale CO₂ exchange and productivity of transplanted paddy and direct seeded rainfed rice production systems in S. Korea

Nutritional and developmental influences on components of rice crop light use efficiency

Abstract

Agro-ecosystems, particularly croplands currently constitute 12.6% of the total land area and their coverage is expanding due to the ongoing massive conversion of natural ecosystems into agricultural land, globally. Information regarding how these changes are influencing terrestrial carbon (C) balance is limited. Our current knowledge of CO_2 fluxes and annual C budgets of the resulting croplands originate from extensive monocultural, agricultural landscapes. In most parts of the world, e.g. in Asia however, the agricultural landscapes are characterized by complex, multicultural cropping systems that demand novel approaches to quantify C balances of such croplands due to the challenges associated with the predominantly used CO_2 measurement techniques. The use of portable chambers in this study, allowed direct measurements of net ecosystem exchange (NEE) of CO_2, ecosystem respiration (R_{eco}) and the evaluation of gross primary productivity (GPP) at small spatial scales (plot level), making it possible to key out functional differences of the 5 dominant crops (rice, potato, radish, cabbage and bean) in the Haean catchment of South Korea, which is a model Asian agricultural landscape.

In this multicultural agroecosystem, minimum peak R_{eco} rate during the growing season was 3.8 ± 0.5 µmol m^{-2} s^{-1}, measured in the rice paddies while the highest was 34.4 ± 4.3 µmol m^{-2} s^{-1} measured in the cabbage fields. The highest peak NEE and GPP rates were -38.7 ± 6.6 and 63.0 ± 7.2 µmol m^{-2} s^{-1}, respectively, recorded in the cabbage fields. Parallel measurements conducted on the crops reported peak total biomasses of 0.53 ± 0.07, 0.55 ± 0.12, 1.85 ± 0.51, 2.54 ± 0.35 and 1.01 ± 0.26 kg m^{-2} for radish, cabbage, potato, rice and bean respectively, while the respective maximum leaf area indices (LAI) were 2.8, 3.7, 6.4, 6.3 and 6.7 m^2 m^{-2}. The pattern and magnitudes of biomass and LAI development differed among the major crops likely as a result of differences in planting time, light use efficiencies (α) and carbon allocation patterns. Variations in seasonal patterns, magnitudes and the timing of maximum

NEE and GPP among the crops were the result of differences in LAI and α, while photosynthetic active radiation (PAR) explained more than 90% of the diurnal variations in GPP.

The crop production system also influenced C storage by an agroecosystem. For example, the maximum LAI attained under rainfed rice (RF) agriculture was 4.9 ± 0.5 m^2 m^{-2} compared to 5.4 ± 1.1 m^2 m^{-2} in the conventional paddy rice (PR) production system. The respective peak total aboveground biomasses were 2.16 ± 0.28 and 1.85 ± 0.27 kg m^{-2} while the corresponding grain weights were 1.16 ± 0.09 and 1.19 ± 0.10 kg m^{-2}, amounting to total yields of 6.61 ± 0.22 and 5.99 ± 0.68 t/ha^{-1} for PR and RF, respectively. As long as there was no water stress, patterns of CO_2 uptake and LAI development were similar between flooded and rainfed rice, suggesting that rice production may not be pegged on flooding per se. Paddy system, however, was less efficient in nutrient use. For example, when we applied similar nitrogen (N) amounts to rainfed and paddy rice fields, the rainfed rice showed higher leaf N content. Reasons for such differences were however, not clear. Overall, N input significantly influenced plant productivity, LAI development, C partitioning and leaf- and ecosystem level CO_2 exchange. In rice, nutrient addition stimulated plant growth by a head start and an early burst in leaf area. An N−input of 115 kg N ha^{-1} increased aboveground biomass by 56%. This was also reflected in the grain yield, which increased by 58%. Fertilized rice developed higher proportion of leaves in the upper layers, increasing light interception and light use efficiency. Since LAI controlled GPP, the overall result was an increased CO_2 uptake as a result of higher N-input.

The study demonstrated that the active period of atmospheric C uptake is extended in multicultural, agroecosystem landscape due to the staggered timing of maximum CO_2 uptake among crops, thus offering an ecological advantage by prolonging the period of high CO_2 uptake. Flooding agriculture (paddy) offered no economic advantage as long as soil moisture

was not limiting, since similar yields were recorded. The fact that paddy rice had lower leaf N than rainfed rice suggests that some of the N in PR might have been lost into the atmosphere or seeped underground. Thus water logged cropping system could be a source of environmental pollution. Increased N-availability promoted productivity by an accelerated canopy development and increased LAI, enabling higher PAR absorption throughout the season.

In general, increasing respiration losses (CO_2) alongside high productivity and significant CO_2 emissions during the fallow season could nevertheless result in a long-term net C release and, therefore, lower the carbon mitigation potential of croplands. Although N-fertilization increased productivity and carbon gain capacity, an N surplus can lead to negative environmental impacts through surface and groundwater pollution.

Zusammenfassung

Agrarökosysteme, insbesondere Feldkulturflächen bedecken derzeit 12,6% der gesamten weltweiten Landfläche und unterliegen derzeit einer fortlaufenden Ausbreitung auf Kosten einer massiven Umwandlung natürlicher Ökosystemen in Ackerland.

Informationen über den Einfluss dieser Änderungen auf die global-terrestrische Kohlenstoff−(C)−Bilanz sind weiterhin begrenzt. Unsere bisherigen Kenntnisse über CO_2−Flüsse und jährlichen Kohlenstoffbudgets der entstandenen Kulturflächen stammen von großflächigen, monokulturell bewirtschafteten Agrarflächen. Der Großteil der agrarwirtschaftlich genutzten Flächen auf der Erde, zum Beispiel in Asien, sind jedoch charakterisiert durch komplexe, multikulturelle landwirtschaftliche Systeme und es bedarf differenzierter Methoden, um die Kohlenstoffbilanzen solcher Kulturflächen zu quantifizieren. Die in der vorliegenden Studie verwendeten mobilen Messkammern erlaubten eine direkte Messung des Netto-Ökosystemaustausches (NEE) von CO_2, der Ökosystemrespiration (R_{eco}) und die Berechnung der Bruttoprimärproduktion (GPP) von kleinen Arealen (Plot-Flächen), um funktionelle Unterschiede der fünf dominanten Nutzpflanzen (Reis, Kartoffel, Rettich, Kohl und Bohne) im Haean-Gebiet in Süd-Korea, repräsentativ für asiatische Agrarlandschaften, zu ermitteln.

In diesem multikulturellen Agrarökosystem, wurde die geringste maximale Ökosystemrespirations-Rate während der Wachstumsperiode mit $3,8 \pm 0,5$ µmol m^{-2} s^{-1} in Nassreis und die maximale R_{eco}-Rate von $34,4 \pm 4,3$ µmol m^{-2} s^{-1} in Kohlfeldern gemessen. Die höchsten maximalen NEE und GPP-Raten wurden mit $-38,7 \pm 6,6$ und $63,0 \pm 7,2$ µmol m^{-2} s^{-1} in Kohlfeldern ermittelt. Die parallelen Messungen des maximalen Blattflächenindexes (LAIs) ergaben für Rettich, Kohl, Kartoffel, Reis und Bohne entsprechend 2,8; 3,7; 6,4; 6,3 und 6,7 m^2 m^{-2}. Die Verteilung und Größe der Biomasse sowie die Blattflächenentwicklung unterschieden sich zwischen den Nutzpflanzen hauptsächlich aufgrund unterschiedlicher

Pflanzzeiten, Lichtnutzungseffizienzen (α) und Kohlenstoffallokationen. Schwankungen in der saisonalen Verteilung, Betrag und Zeitpunkt des Auftretens des maximalen NEE und GPP zwischen den Nutzpflanzen waren das Resultat unterschiedlicher LAI und α, wohingegen die photosynthetisch aktive Strahlung (PAR) mehr als 90% der täglichen Schwankungen der GPP erklärten.

Das landwirtschaftliche Anbausystem beeinflusste ebenfalls die pflanzliche Kohlenstoffspeicherung. Zum Beispiel war der maximale LAI von Trockenreis (RF) bei ausschließlicher Bewässerung durch Niederschläge $4,9 \pm 0,5$ m^2 m^{-2}, im Vergleich zu $5,4 \pm 1,1$ m^2 m^{-2} in konventioneller Nassreis-Kultivierung (PR). Die maximale oberirdische Biomasse (Trockengewicht) betrug $2,16 \pm 0,28$ und $1,85 \pm 0,27$ kg m^{-2}, wohingegen das Korngewicht $1,16 \pm 0,09$ und $1,19 \pm 0,10$ kg m^{-2} bei einem Gesamtertrag von $6,61 \pm 0,22$ und $5,99 \pm 0,68$ t/ha^{-1}, entsprechend für PR und RF, betrug. Die CO_2-Aufnahme und die Entwicklung des LAI zeigte zwischen PR und RF einen ähnlichen Verlauf bei angemessener Wasserversorgung; dadurch wurde der Reisanbau nicht nur auf geflutete Felder beschränkt. Es wurde jedoch durch die Flutung des agrarwirtschaftlichen Systems, im untersuchten Beispiel bei Nassreis eine verringerte Stickstoff-(N)-Nutzung sichtbar. So wurden in unserem Versuch die gleiche Menge an Stickstoffdünger im RF und PR Feld ausgebracht, wobei der Trockenreis letztendlich einen höheren Blattstickstoffgehalt zeigte. Ein klarer Grund für diesen Unterschied konnte jedoch in dieser Studie nicht festgestellt werden. Insgesamt beeinflusste allerdings eine erhöhte Stickstoffzugabe die Produktivität der Nutzpflanzen, die Blattflächenentwicklung, Kohlenstoffallokation und den Blatt- und Ökosystem-CO_2−Gaswechsel. Das Wachstum von Reis wurde durch die Nährstoffzugabe gefördert, insbesondere durch eine frühere und stärkere Entwicklung der Blattfläche. Eine Stickstoffzugabe von 115 kg N ha^{-1} erhöhte die oberirdische Biomasse um 56%. Zugleich ergab sich eine von 58%. Gedüngter Reis entwickelte einen höheren Anteil an Blättern in den oberen Bestandsschichten und zeigte eine erhöhte Strahlungsaufnahme und

Lichtnutzungseffizienz. Da die GPP stark abhängig vom LAI war, ergab sich letztendlich eine erhöhte CO_2-Aufnahme als Folge der gesteigerten Stickstoffzugabe.

Diese Studie demonstrierte, dass der Zeitraum für eine aktive Aufnahme an atmosphärischem Kohlenstoff in einer multikulturellen Agrarlandschaft durch ein Aufeinanderfolgen der Perioden mit maximaler CO_2-Aufnahme der entsprechenden Nutzpflanzen verlängert wurde und bietet daher einen ökologischen Vorteil durch einen verlängerten Zeitraum mit hoher CO_2-Aufnahme.

Nassreiskultivierung in Feldern mit gefluteten Böden zeigte keinen ökonomischen Vorteil gegenüber dem Trockenreisanbau, solange die Bodenfeuchte keinen limitierenden Einfluss hatte, da sich die Erträge in beiden Systemen (PR und RF) wenig unterschieden. Der Nassreis entwickelte jedoch im Vergleich zum Trockenreis einen geringeren Stickstoffgehalt in den Blättern und weist daher auf einen Verlust von N in die Atmosphäre oder den Boden hin. Daher können geflutete Agrarökosysteme eine Ursache für Umweltverschmutzung darstellen. Die erhöhte Stickstoffversorgung begünstigte die Produktivität durch eine beschleunigte Entwicklung des Bestandes und Bildung eines höheren LAI, wodurch eine größere Lichtabsorption während der gesamten Vegetationsperiode ermöglicht wurde.

Allgemein lässt sich sagen, dass gesteigerte respiratorische Verluste (CO_2) bei erhöhter Produktivität und signifikanter CO_2-Emissionen während der Brache jedoch das Kohlenstoff-Minderungspotenzial von landwirtschaftlichen Flächen verringern könnten. Zwar steigert die Stickstoffdüngung die Produktivität und Kohlenstoffaufnahmekapazität, ein Stickstoffüberschuss führt jedoch zu negativen Einflüssen auf die Umwelt durch Oberflächen- und Grundwasserverschmutzung.

Acknowledgements

List of figures

List of tables

List of abbreviations and symbols

Abbreviation/ Symbol	Definition	Unit
A	Leaf assimilation rate	$\mu mol\ CO_2\ m^{-2}\ s^{-1}$
A_{max}	Photosynthetic rate at normal CO_2 concentration and saturating PAR	$\mu mol\ CO_2\ m^{-2}\ s^{-1}$
$A_{max,30}$	Photosynthetic rate at 30°C and saturating PAR	$\mu mol\ CO_2\ m^{-2}\ s^{-1}$
APAR	Daily integrated PAR intercepted by canopy	$MJ\ m^{-2}\ d^{-1}$
a.s.l.	above sea level	m
AWS	automatic weather station	
BD	bulk density	$g\ cm^{-3}$
C	Carbon	
C_a	Ambient CO_2 concentration	$\mu mol\ CO_2\ mol^{-1}\ air$
CEC	cationic exchange capacity	$cmol_c\ kg^{-1}$
cf.	compare	
C_i	Intercellular CO_2 concentration	$\mu mol\ CO_2\ mol^{-1}\ air$
CO_2	Carbon dioxide	
C_{org}	organic soil carbon	$g\ kg^{-1}$
C_{tot}	total organic carbon content	$cmol_c\ kg^{-1}$
cv.	cultivar	
DAT	Day after transplanting	
DOY	Day of year	
EC	Eddy covariance technique	
e.g.	for example	
et al.	and others	
ETR	Electron transport rate	$\mu mol\ electrons\ m^{-2}\ leaf\ s^{-1}$
fPAR	Fraction of incident integrated PAR to absorbed PAR	%
GLA	Green leaf area	m^2
GLAI	Green leaf area index	$m^2\ m^{-2}$
g_m	Mesophyll conductance to CO_2	$mmol\ CO_2\ m^{-2}\ leaf\ s^{-1}$
GPP	Gross primary production	$\mu mol\ CO_2\ m^{-2}\ s^{-1}$
GPP_{max}	Daily maximum GPP at saturating light	$\mu mol\ CO_2\ m^{-2}\ s^{-1}$
GPP_{int}	Daily integrated GPP	$g\ C\ m^{-2}\ d^{-1}$
g_s	Stomatal conductance to CO_2	$mmol\ CO_2\ m^{-2}\ leaf\ s^{-1}$
$J_{max,30}$	Maximum electron transport rate at leaf temperature 30°C	$\mu mol\ electrons\ m^{-2}\ leaf\ s^{-1}$
J_p	Electron transport rate that is used by CO_2 fixation process	$\mu mol\ electrons\ m^{-2}\ leaf\ s^{-1}$
K	Potassium	
K_L	Light attenuation efficiency	
K_N	Nitrogen attenuation efficiency	
K_p	Coefficiency controlling correlation between LAI and LAI	
K_{vi}	Coefficiency controlling correlation between NDVI and LAI	

Abbreviation/ Symbol	Definition	Unit
LA	Leaf area	m^2
LAI	Leaf area index	$m^2\,m^{-2}$
LAUC	leaf area in the upper canopy	
L_{gs}	Percent limitation due to finite stomatal conductance	%
L_{gm}	Percent limitation due to finite mesophyll conductance	%
L_{total}	Percent limitation due to finite CO_2 diffusion conductance	%
LUE	Light use efficiency	
LUE_{abs}	Light use efficiency based on absorbed PAR	$g\,C\,MJ^{-1}$
LUE_{ins}	Instantaneous canopy light use efficiency	$\mu mol\,CO_2\,\mu mol^{-1}$ photons
LUE_{inc}	Daily mean light use efficiency based on incident PAR	$g\,C\,MJ^{-1}$
N	Nitrogen	
N_a	Leaf nitrogen content per leaf area	$g\,m^{-2}$ leaf
NEE	Net ecosystem exchange	$\mu mol\,CO_2\,m^{-2}\,s^{-1}$
N_{min}	mineralized nitrogen content	$g\,kg^{-1}$
N_{tot}	total nitrogen content	$g\,kg^{-1}$
N_{total}	Canopy nitrogen content per ground	$g\,m^{-2}$ ground
NPP	Net primary production	$\mu mol\,CO_2\,m^{-2}\,s^{-1}$
NPP_{int}	daily integrated NPP	$g\,C\,m^{-2}\,d^{-1}$
NDVI	Normalized difference vegetation index	
$NDVI_{max}$	Maximum normalized difference vegetation index	
$NDVI_{min}$	Minimum normalized difference vegetation index	
P	Phosphorous	
PAI	Plant area index	$m^2\,m^{-2}$
PAR	Photosynthetically active radiation	$\mu mol\,photons\,m^{-2}\,s^{-1}$
PPFD	Photosynthetic photon flux density	$MJ\,m^{-2}$
Pg	Petagram	
ppm	Parts per million	
PR	Paddy rice	
R^2	coefficient of determination	
R_{day}	non-photorespiratory CO_2 evolution	$\mu mol\,CO_2\,m^{-2}$ leaf s^{-1}
R_{eco}	Ecosystem respiration rate	$\mu mol\,CO_2\,m^{-2}$ ground s^{-1}
ref.	refer to	
RF	Rainfed rice	
rH	relative humidity	%
R_p	Plant respiration rate	$\mu mol\,CO_2\,m^{-2}$ ground s^{-1}
R_{soil}	Soil respiration rate	$\mu mol\,CO_2\,m^{-2}$ ground s^{-1}
S.E.	standard error	
SLA	Specific leaf area	$cm^2\,g^{-1}$
SOM	Soil organic matter	$g\,kg^{-1}$
SD	Standard deviation	

Abbreviation/ Symbol	Definition	Unit
T_{air}	Air temperature above plant canopy	°C
T_{soil}	Soil temperature at 10 cm depth	°C
var.	variety	
$V_{cmax,30}$	Maximum carboxylation rate at leaf temperature 30°C	μmol CO_2 m^{-2} leaf s^{-1}
VPD	Vapor pressure difference	kPa
VWC	Volumetric water content	%
α	Slope of assimilation-light response curve, equivalent to LUE_{ins}	μmol CO_2 μmol^{-1} photons
β	Saturating value of light response curve under infinitely high PAR	μmol CO_2 m^{-2} s^{-1}
$(\beta + \gamma)_{1500}$	average maximum canopy uptake capacity	μmol CO_2 m^{-2} s^{-1}
γ	estimation of the average respiration	μmol CO_2 m^{-2} s^{-1}
$\Gamma*$	Chloroplast CO_2 compensation point	μmol CO_2 mmol^{-1}
Ψ	Water potential	MPa

Chapter 1

1. Synopsis

1.1. General introduction

1.1.1. Agroecosystems of the world

Evidence of agricultural activities can be traced back to 12000 years ago (Barker, 2006). Since then, cultivation of plants and domestication of animals replaced hunting and gathering as core means of feeding human population around the globe. The shift from foraging to agriculture, also known as the Neolithic revolution, became fully developed by 3000 B.C. (Usha Rao and Pandey, 2007). Neolithic revolution occurred simultaneously in China, India, Indochina, Central Asia, Near East, Mediterranean, Ethiopia, Mesoamerica and northeastern South America (Vavilov and Freier, 1951), although indications are that the diverse vegetation of South East Asia was most ideal for the evolution of agriculture (Usha Rao and Pandey, 2007). The development and expansion of agriculture to produce food, fiber etc. was characterized by the conversion of natural ecological systems to agricultural ecosystems (agroecosystems) (Conway, 1987). Today, wheat, corn and rice provide more than 60% of the world's calories, replacing about 53, 43, 31, and 21% of Asian, Africa, American and European land masses, respectively, that were formally natural ecosystems and accounting for 38% of the total lost natural ecosystems globally (FAOSTAT, 2015). This shift from natural to agricultural ecosystems has radically transformed the natural landscapes, since it involved the replacement of natural vegetation by crops that have different growth cycles and functions.

Agricultural development has had significant impacts on the global climate as a result of the increased emission of carbon dioxide (CO_2) and other greenhouse gases into the atmosphere. The emitted greenhouse gasses trap heat within the atmosphere causing climate warming (so

called "greenhouse effect"), with the highest climate forcing potential of 57% coming from CO_2 (Johnson et al., 2007). The global expansion of the agroecosystems during the Agrarian revolution has been singled out as one of the main contributors to the sharp rise in the atmospheric CO_2 concentrations between 14th and 19th Centuries (Thirsk, 1997) and whose impacts are still being felt to date as exemplified in the sharp rise in the atmospheric CO_2 concentrations (Monnin et al., 2001). For example, the pre-industrial levels of atmospheric CO_2 concentration were estimated at around 280 ppm (IPCC, 2001), but this has since risen to the current concentration of 380-400 ppm, surpassing the 370 ppm reported in 2001 (Keeling and Whorf, 2004). It is estimated that between 1850 and 1990 alone, approximately 123 Pg of carbon was released into the atmosphere in the form of CO_2 as a result of agricultural land use (Bonan, 2002). This has been mainly due to high losses of soil carbon through soil respiration (Béziat et al., 2009). Future predictions show that atmospheric CO_2 concentrations may reach 500 ppm by the end of the 21st Century (IPCC, 1996).

Significant progress has been made in the monitoring of changes in the atmospheric CO_2 concentrations. Today, the ecosystem CO_2 fluxes are measured in more than four hundred research locations around the globe (Baldocchi, 2008) linked to AmeriFlux and Fluxnet-Canada (Law, 2005; Coursolle et al., 2006) networks in North America, the Biosphere Amazon (LBA) in South America (Keller et al., 2004), the EuroFlux and CarboEurope networks in Europe (Valentini et al., 2000; Ciais et al., 2005), OzFlux in Australasia, China Flux (Yu et al., 2006) and AsiaFlux in Asia (Saigusa et al., 2005) and AfriFlux in Africa (Williams et al, 2007). These measurements show that ecosystems gaining the most carbon (negative sign) tend to be evergreen forests, which have all year-round growing seasons and small pools of decomposing detritus in the soil. For example, the net carbon fluxes over subtropical evergreen mixed forest were in the range of -441.2 and -563.0 $gC \cdot m^{-2} \cdot y^{-1}$ (Chunlin et al., 2006). Net carbon fluxes at a successional forest of maple and aspen at Camp

Borden in southern Ontario, Canada, are on the order of -100 to -280 gC m^{-2} y^{-1} (Lee et al., 1999), while mature sites in Canada covered with aspen were in the range of -139 to -361 gC m^{-2} y^{-1}, jack pine stands reached 23 to – 41 gC m^{-2} y^{-1} and black spruce sites -21 to -68 gC m^{-2} y^{-1} (Amiro et al., 2006). The net carbon fluxes over much of the United States and Europe forests range between 146 and -757 gC m^{-2} y^{-1} (Falge et al., 2002), while for the cool-temperate deciduous forest in Japan, the rates range from -237 to -309 gC m^{-2} y^{-1} (Saigusa et al., 2005).

While knowledge on the contribution of natural ecosystems to the global C-budget has significantly grown (Falge et al., 2002; Kato et al., 2008), there is still need for increased quantitative research to establish the contributions of agroecosystems to the global C-budget. Although croplands are able to fix large amounts of CO_2 annually through photosynthesis, most of the fixed carbon is likely released in 1 to 2 years following harvest and subsequent decomposition or consumption (West et al., 2011), but the proportions are not known. Previous studies assessing C-fluxes and C-budget of agroecosystems are from extensive monocultural agricultural landscapes of maize and soybean in North America (Pattey et al., 2002; Suyker et al., 2004; Baker and Griffis, 2005; Bernacchi et al., 2005; Hollinger et al., 2005; Suyker et al., 2005; Verma et al., 2005), rice in Asia (Miyata et al., 2000; Campbell, 2001A; Saito et al., 2005, Alberto et al., 2007), sugar beet in Belgium (Moureaux et al., 2006, Aubinet et al., 2009), winter wheat and triticale in Germany (Baldocchi, 1994; Ammann et al., 1996; Anthoni et al., 2004; Moureaux et al., 2008; Béziat et al., 2009), and sunflower, rapeseed or maize in south-west France (Béziat et al., 2009). Efforts to quantify CO_2 exchange of the natural and agroecosystems have widely relied on the eddy covariance (EC) technique (Aubinet et al., 2000; Wohlfahrt et al., 2005; Pavelka et al., 2007), which applies best in open habitats (from hundreds of m^2 to km^2) where fluxes are related to clearly defined vegetation types (footprint), such as in monocultural, agricultural landscapes. Little is

however known about multicultural agricultural landscapes (Soegaard et al., 2003; Béziat et al., 2009; Zhao et al., 2012), especially the patchy landscapes (Mack et al., 1990; Schmid, 2002; Göckede, et al. 2004; Rebmann et al., 2005), due to the challenges that characterize this CO_2 quantification technique. Fragmented agroecosystems are, however, widespread in some parts of the world e.g. in Asia and Africa, where they dominate and cannot be overlooked. The main objective in most CO_2 flux studies in croplands has been to upscale the actual field measurements to landscape (Soegaard et al., 2003) or regional (Migletta et al., 2007) scales, however, flux measurements in complex topographies or patchy vegetation using the EC methodology is biased and likely to be inaccurate (Baldocchi, 2008).

1.1.2. Agroecosystems in Asia

In Asia, the agricultural landscape is characterized by patchy, multicultural cropping systems co-dominated by rice paddies and dryland crops. South Korea, for example, has a rugged terrain, with fragmented agricultural landscape characterized by small plots grown with multicultural crops that have different timing and functions. About 70% of the country is mountainous, with elevations of up to 2000 m a.s.l. separated by deep and narrow valleys. Rice paddies are found in the valley bottom, where flooding is possible, while dryland crops grow on the slopes mainly through rainfed agriculture. These cultivation systems (flooding vs rainfed production) and also the different crop types are likely to influence patterns of CO_2 exchange within the agricultural landscape. In such heterogeneous landscapes, therefore, noble approaches are required that can improve the accuracy of C-budgeting of the agroecosystems (Sheehy and Mitchell, 2013).

In South Korea, agricultural intensification due to the rising food demands (Cassman, 1999) has also been associated with increased nitrogen (N) fertilizer use (Frink et al., 1999; Bashkin

et al., 2002). With its current N application rate of 313 kg N ha^{-1} $year^{-1}$, South Korea stands as a global leader in N input (Kim et al., 2008). Most of the applied N is, however, leached away during the heavy monsoonal rainfall, with negative environmental impacts such as surface and groundwater pollution (Kettering et al., 2012; Bartsch et al., 2013). On the other hand, N-nutrition in agricultural crops potentially increases LAI development and radiation interception by the vegetation. In most crops, N-concentration is curvilinearly correlated with canopy CO_2 assimilation (Evans, 1989; Weerakoon et al., 2000). Increase N-input results in increased leaf growth, chlorophyll formation and amount of Ribulose 1-5 Bisphosphate Carboxylase/Oxygenase (Rubisco) enzyme (Ookawa et al., 2004). Positive linear relationship between the amount of Rubisco and the N concentration in mature leaves is demonstrated through increased light use efficiencies in the vegetation, which eventually results in higher light-saturated photosynthetic rate (A) (Makino et al., 1997). The efficiency with which plants acquire resources (e.g. nitrogen uptake and radiation absorption) and resource conversion into biomass and yield are a measure of plant productivity (Kato et al., 2006A).

In this study, we addressed challenges associated with measuring CO_2 fluxes of agroecosystems in Asia, typically characterized by a rugged terrain and a multicultural agricultural landscape, using portable ecosystem CO_2 measurement chambers (Chapter 2) in order to identify key drivers regulating CO_2 fluxes and biomass production of agricultural crops. Measurements of net ecosystem CO_2 exchange (NEE), ecosystem respiration (R_{eco}) and gross primary productivity (GPP) were done at small spatial scales (plot level), making it possible to key out functional differences within the heterogeneous cropping landscape in the Haean-myeon catchment, which is a representative of the South Korean agricultural landscape. In the third chapter, a new rice cultivar (*Oryza sativa* L. subsp. Japonica cv. Unkwang) was cropped in a typical East Asia monsoonal climate as rainfed and conventional

paddy production system in order to assess the effects of the two dominant crop production practices (flooding vs. rainfed) on crop productivity, leaf and ecosystem-level CO_2 exchange and nutrient utilization. Chapter four addresses the role of N-input on plant structural and physiological adjustments related to carbon gain and productivity.

1.1.3. Study Hypotheses and Objectives

The study was guided by the following general hypotheses:

- CO_2 exchange and productivity of the multicultural agroecosystems are a function of climate, leaf area and N-nutrient supply.

- Nitrogen fertilization leads to an increased canopy leaf area, alters nitrogen investments, and induces changes in leaf gas exchange and biomass production.

- Growing season CO_2 uptake of the agroecosystems is determined by the duration and magnitude of green Leaf Area Index (LAI) and resource use efficiency.

The main research objectives were:

Objective 1: To determine drivers of seasonality and magnitudes of CO_2 exchange and productivity of the main agricultural crops in South Korea (Study 1)

Mixed multicultural cropping in a heterogeneous landscape complicates the estimation of agroecosystem CO_2 exchange and its drivers. Current knowledge of CO_2 fluxes and annual C budgets of croplands originates mostly from measurements conducted on extensive monocultural agricultural landscapes (Suyker et al., 2004; Moureaux et al., 2008; Hoyaux et al., 2008). Information regarding mixed croplands, particularly the type that exists in the Asian agricultural landscapes, is still scarce. Due to the overlapping production phases caused by varied timing and growing lengths of different crops, the quantification of CO_2 fluxes and the contribution of respective crops require that each crop type is assessed independently. The

widely accepted EC technique mostly applies in open habitats, with clearly defined footprints (Aubinet et al., 2000; Wohlfahrt et al., 2005; Pavelka et al., 2007). Its application in multicultural, agricultural landscapes is therefore limited, since it is difficult to discern between the respective crops (Zhao et al., 2012). We employed the portable chamber method to determine the seasonal patterns and magnitudes of CO_2 exchange and productivity of the five dominant crop types grown together in a heterogeneous agricultural landscape in South Korea.

The specific objectives were to:

- Determine the seasonal patterns and magnitudes of CO_2 exchange and productivity of the five main crop types grown in the multi-cultural South Korean agricultural landscape.

- Identify key drivers regulating CO_2 fluxes and biomass production and how the intensity of regulation relates to C-storage in the fragmented agricultural landscape in the Haean catchment.

The specific hypothesis guiding this study was that:

- Differences in timing and magnitudes of GPP and R_{eco} among crops lead to a high spatial variability in CO_2 exchange and C-storage in a typical multicultural East Asian agricultural system.

Objective 2: To quantify the impacts of different cultivation approaches on rice productivity (Study 2)

Canopy photosynthesis rate determines the carbon uptake throughout the day, but the C-balance that is used in growth is the balance between photosynthesis and respiration. While respiration remains relatively constant most of the day, higher daily canopy assimilation rates increase the amount of carbohydrates available for growth, resulting in a long-term increased

biomass production and yield (Monteith and Moss, 1977). Although recent research indicated that paddy rice planted in rainfed fields can develop comparable or even higher aboveground biomasses in years with adequate rainfall during the growing season (Katsura et al., 2010), yield reductions of 10-40% (Tuong and Bouman, 2001) can occur under aerobic soil conditions. Paddy soils are submerged for much of the growing season and therefor differs from that of many other crops due to the induces changes in micro-environmental conditions when compared to other terrestrial ecosystems (Zaho, et al., 2008; Alberto et al., 2013). In this study, measurements of seasonal trends of canopy CO_2 exchange, leaf area development and biomass C-partitioning were conducted throughout a growing season in a paddy and rainfed Unkwang rice field to compare the carbon uptake capacity and productivity in both environments. The cultivation of Unkwang rice in a rainfed environment rather then in a conventional paddy system may limit production or shifts the demands of carbohydrates due to an expected increased development of the root system. Previous studies were conducted to compare the canopy and ecosystem gas exchange of paddy and rainfed rice (Miyata et al., 2000; Alberto et al., 2009), nevertheless, measurements from temperate monsoon regions are still rarely reported.

The specific objective was:

- To determine how growing conditions influence canopy processes and yield of a rice cultivar grown under both rainfed and conventional paddy conditions.

The specific hypothesis guiding this study was:

- That under adequate soil moisture supply, the rice grown in a rainfed system maintains similar rates of CO_2 uptake, C-allocation pattern and light use efficiency compared to that in a paddy system.

Objective 3: To determine the impact of fertilization on rice productivity (Study 3)

Nitrogen (N) availability has been identified as one of the factors that determine productivity of the agro ecosystems (Weerakoon et al., 2000). Previous researches show that N-fertilization results in an increased plant height and increased tillering (Koyama and Niamsrichand, 1973; Bandaogo et al., 2015), earlier and higher leaf area index development through increased number and leaf size and higher specific leaf area (Sinclair and Horie, 1989, Gimenez et al., 1994), and a greater number of spikelets per panicle (Koyama et al., 1973). Increased canopy development as a result of increased N-input enhances canopy photosynthetic capacity through provision of a large photosynthetic area for light interception (Kato et al., 2006A). Higher N-input also increases chlorophyll formation, thus facilitation the photosynthetic efficiency of the chloroplasts. As a result, CO_2 uptake rate by the plants can be expressed as a function of the amount of light intercepted by the canopy (canopy size) and the light conversion efficiency (biochemical processes related to chlorophyll content) by which absorbed light is converted into chemical energy (Monteith, 1972). Light use efficiency (LUE) can change significantly with phenology of the crop (Gimenez et al., 1994; Alberto et al., 2013), influencing the capacity to assimilate carbon dioxide by a given crop species (Kiniry et al., 1989). In paddy rice, LUE ranges between 1.52 and 2.1 g C MJ^{-1} during elongation growth and from 0.73 to 1.22 g C MJ^{-1} at post-anthesis of spikelets formation (Campbell et al., 2001B). N fertilization of rice, therefore, supports rapid canopy development in order to realize high light interception. At leaf level, higher N input facilitates chlorophyll formation. The combine effects ensure relatively higher photosynthetic activity, plant growth and yield (Gimenez et al., 1994; Okami et al., 2013). Hence, increments in the amount of photosynthetic production with nutrient additions may be ascribed to changes in the capacity for light interception and light conversion efficiency. We conducted leaf-level gas exchange and chlorophyll fluorescence measurements on rice leaves to identify which

component of the CO_2 exchange process is most influenced by N addition. Additionally, canopy developments of 3 rice fields with three nutrient treatment levels were monitored, in order to examine how N-input affects canopy leaf area, biomass allocation pattern, biomass production and leaf gas exchange.

The specific objectives of this study were to:

- Examine the extent to which increased nutrient supply leads to increased canopy leaf area, altered nitrogen investments, changes in leaf gas exchange and biomass production.

The following hypothesis guided the formulation of this study:

- Increasing nutrient supply to the rice crop leads to an acceleration in the rate of canopy development (rate of increase in LAI) and overall carbon gain.
- Variation in leaf function in rice grown with different nutrient supply and under varying light environments within the crop canopy is largely explained by variations in leaf nitrogen allocation and nitrogen-driven gas exchange.

1.2. List of manuscripts and specification of individual contributions

The three different studies described in this thesis have been presented as three separate manuscripts. Manuscript 1 is published in the Agriculture, Ecosystems and Environment journal, Manuscript 2 and 3 are submitted to Agriculture and Forest Meteorology. The following list specifies the contributions of the individual authors to each manuscript.

Manuscript 1

Authors	Lindner, Steve; Otieno, Dennis; Lee, Bora; Xue, Wei; Arnhold, Sebastian; Kwon, Hyojung; Huwe, Bernd; Tenhunen, John
Title	Carbon Dioxide Exchange and its Regulation in the main Agro-ecosystems of Haean Catchment in South Korea
Status - DOI	published - 10.1016/j.agee.2014.09.005
Journal	Agriculture, Ecosystems and Environment
Contributions	S. Lindner concept (95%), manuscript writing (90%), data collection (85%), data analysis (95%), figures and tables (100%), discussion (85%)

Steve Lindner is the corresponding Author. The study was designed by Steve Lindner and Bora Lee. Data collection was done by Steve Lindner and Bora Lee supported by local Korean labors (see acknowledgements). Samples were analyzed at the Department of Plant Ecology at the University of Bayreuth by Margarete Wartinger (see acknowledgements). Data was analysed by Steve Lindner and Bora Lee. The results were discussed by Steve Lindner, Dennis Otieno, Wei Xue, Sebastian Arnhold, Hyojung Kwon, Bernd Huwe and John Tenhunen. Figures and tables were created by Steve Lindner. Steve Lindner wrote the first draft of the manuscript. Revision and rewriting of the manuscript was done by Steve Lindner and Bora Lee.

Manuscript 2

Authors   Steve Lindner, Wei Xue, Bhone Nay-Htoon, Jinsil Choi, Yannic Ege,

Nikolas Lichtenwald, Fabian Fischer, Jonghan Ko, John Tenhunen,

Dennis Otieno

Title   Canopy scale CO_2 exchange and productivity of transplanted

paddy and direct seeded rainfed rice production systems in S.

Korea

Status   Under review

Journal   Agriculture and Forest Meteorology

Contributions   S. Lindner   concept (90%), manuscript writing (90%),

data collection (50%), data analysis (95%), figures and tables (100%),

discussion (85%)

Steve Lindner is the corresponding Author. The study was designed by Steve Lindner, Xue
Wei and Bhone Nay-Htoon. Data collection was done by Steve Lindner, with the support of 4
student assistants Nikolas Lichtenwald, Fabian Fischer, Yannic Ege and Jinsil Choi. Samples
were analyzed at the Department of Plant Ecology at the University of Bayreuth by Margarete
Wartinger (see acknowledgements). Data was analysed by Steve Lindner and Wei Xue. The
results were discussed by Steve Lindner, Wei Xue, Dennis Otieno, Bhone Nay-thoon,
Jonghan Ko and John Tenhunen. Figures and tables were created by Steve Lindner. Steve
Lindner wrote the first draft of the manuscript. Revision and rewriting of the manuscript was
done by Steve Lindner and Wei Xue.

Manuscript 3

Authors	Wei Xue; Steve Lindner; Bhone Nay-Htoon; Maren Dubbert; Dennis Otieno, Jonghan Ko; Hiroyuki Muraoka; Christiane Werner; John Tenhunen; Peter Harley
Title	Nutritional and developmental influences on components of rice crop light use efficiency
Status - DOI	published - 10.1016/j.agrformet.2016.03.018
Journal	Agriculture and Forest Meteorology
Contributions	S. Lindner data collection (20%), data analysis (20%), discussion (30%), manuscript editing (10%)

Wei Xue is the corresponding Author. The study was designed by Wei Xue. Data collection was done by Wei Xue and Steve Lindner. Samples were analyzed at the Department of Plant Ecology at the University of Bayreuth by Margarete Wartinger (see acknowledgements). Data was analysed by Wei Xue and Steve Lindner. The results were discussed by Wei Xue, Steve Lindner, Dennis Otieno, Bhone Nay-thoon, Jonghan Ko, Maren Dubbert, Hiroyuki Muraoka, Christiane Werner, Peter Harley and John Tenhunen. Figures and tables were created by Wei Xue. Wei Xue wrote the first draft of the manuscript. Revision and rewriting of the manuscript was done by Wei Xue and Steve Lindner.

1.3. General materials and methods

1.3.1. General description of the study sites

Study 1 was conducted in the Haean-myeon Basin, while Studies 2 and 3 were carried out at the Chonnam National University's research farm.

The Haean-myeon Basin (128° 50'–128° 11' E, 38° 13' –38° 20° N), is part of the Yanggu County in the Gangwon Province, South Korea (see Figure 1). The elevation of the area (in total 62.7 km^2) ranged from 340 m at the bottom of the catchment to 1320 m at the ridges, with an average slope of 28.4%. The climate of the "punchbowl" shaped basin (see Figure 2) is temperate, with a mean annual air temperature of 10.5 °C in the valley bottom and ca. 7.5°C on the northern ridge. The annual precipitation during the last 12 years ranged between 930 and 2299 mm year[1], 50% of which fall during the summer monsoon between June and July (Korean Meteorological Administration, 2011). The bed rock is Precambrian Gneiss at the higher elevations, with Jurassic biotite granite intrusion that was subsequently eroded and deposited in the catchment bottom (Kwon et al., 1990). Due to the long-term addition of sandy soil on the top layer of the agricultural fields by farmers, the soil is mainly artificial and characterized as Anthrosols (FAO, 2006). The texture of the top layers (0–30 cm) for the dryland field sites is either sandy loam or loamy sand (Kettering et al., 2012). The cultivated land is grown with paddy rice (ca. 30% of the area under crop), and dryland crops (radish – 24%, beans – 13%, potato – 10% and cabbage – 5%) (Yanggu County Office Annual Report, 2010).
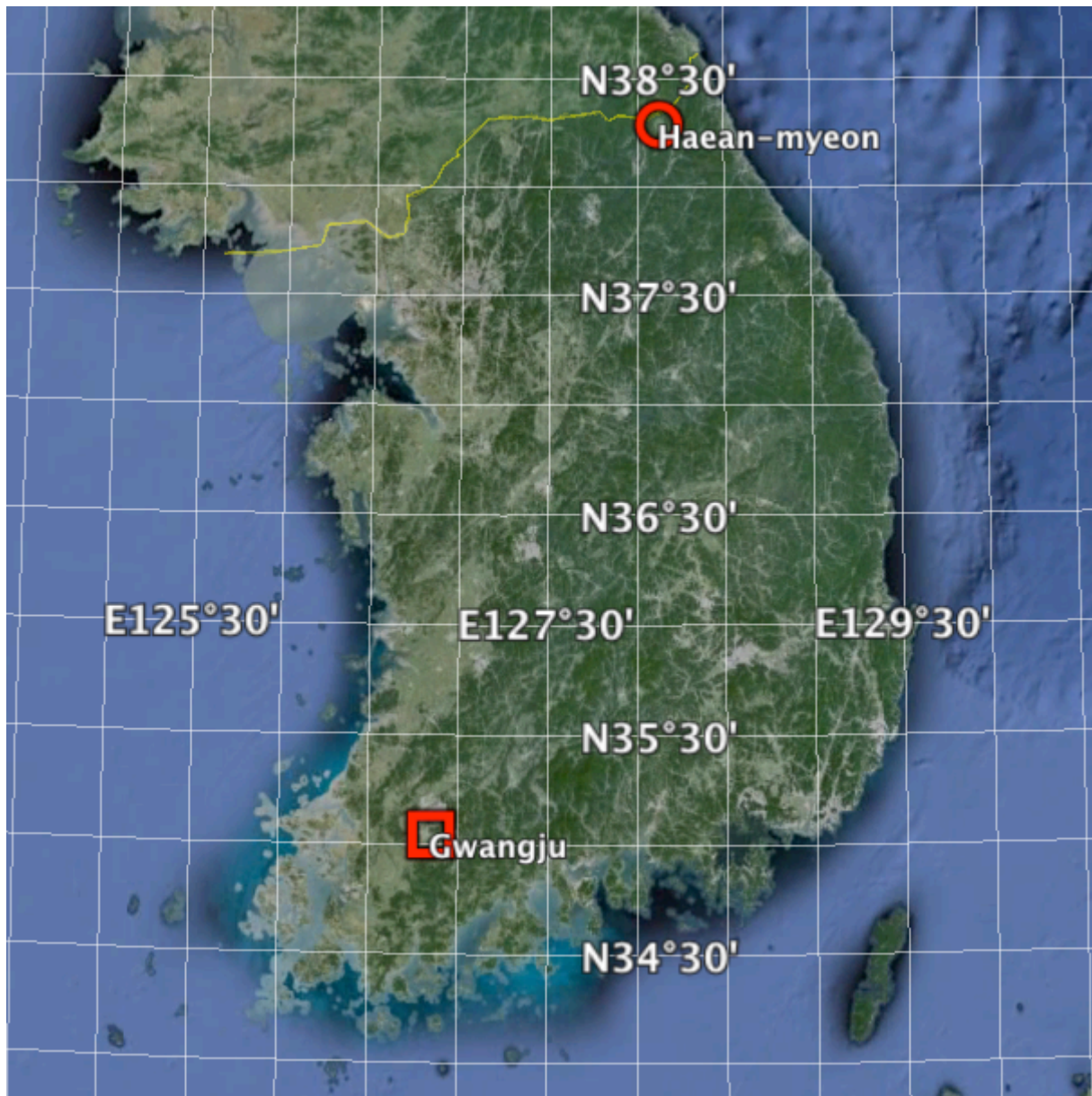
Figure 1: **Overview of the South Korean peninsula with the study sites Haean-myeon and Gwangju (Image Landsat, ©google earth).**

Figure 2: **Overview of the Haean Basin in the Yanggu County, the punchbowl shaped basin is an example of the heterogeneous landscape of South Korea (©S. Lindner).**

The Chonnam National University's research farm (35° 10' N, 126° 53' E, alt. 33m) is located in Gwangju (see Figure 1), Chonnam province, South Korea. Chonnam province is one of the major rice growing regions of S. Korea, with a typical East Asian monsoon climate, a mean annual temperature of 13.8°C and precipitation of between 1391 and 1520 mm/yr (1981–2010). More than 60% of precipitation occurs during the summer monsoon season (July to August). The top soil layer (0 – 30 cm) is categorized as loam.

1.3.2. Experimental design and field management

The experimental fields for study 1 (see Figure 3) comprised rain-fed crop fields of radish (*Raphanus sativus*), potato (*Solanum tuberosum* L.), white cabbage (*Brassica oleracea* var. capitata) and soybean (*Glycine max* (L.) Merr.) and irrigated rice (*Oryza sativa* L.). For each crop, we selected 3 representative, approx. 0.1 ha of the fields. Tillage, fertilization of the

fields, planting/harvesting dates and paddy irrigation program were done according to the local management practices/program (see Kim et al., 2008; Kettering et al., 2012). Weed and pests were controlled by herbicides and pesticides, respectively. Basal fertilizer application was done 7 – 10 days before planting.
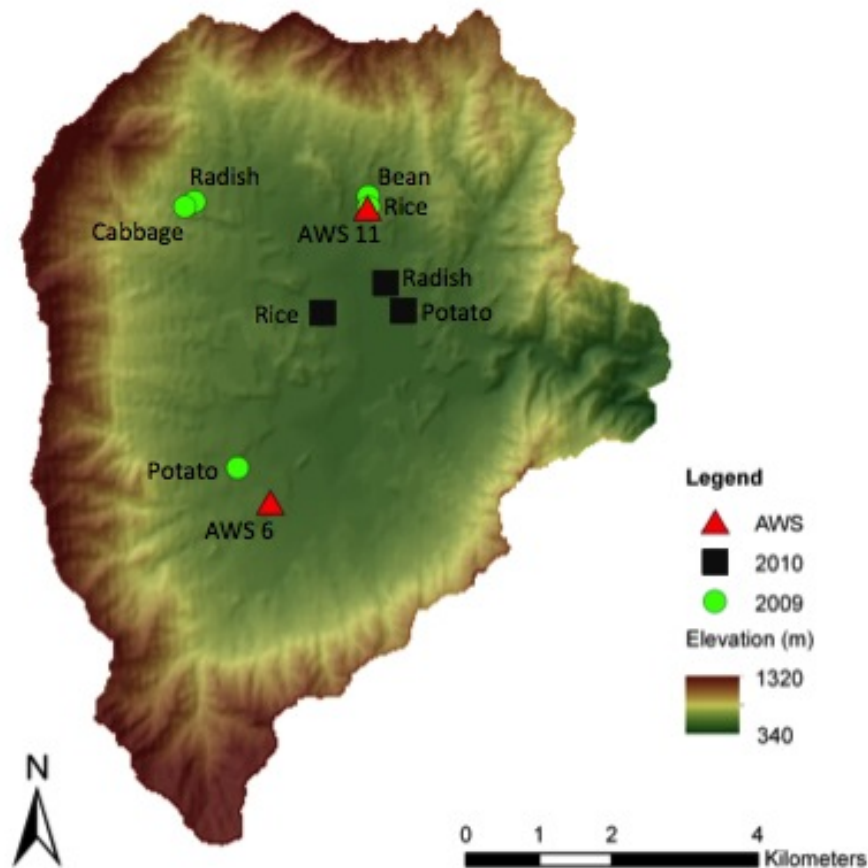
Figure 3: Distribution of the field sites in 2009 and 2010 in Haean catchment in South Korea (©S. Arnhold).

In study 2, an improved rice variety, *Oryza sativa* subsp. Japonica cv. Unkwang (Iksan 435 x Cheolweon 54) was cultivated as flooded paddy crop (PR) and as rainfed crop (RF) in two adjacent (separated by 100 m) experimental rice fields (see Figure 4). PR was planted in a block measuring 73.0 m x 19.5 m, surrounded with a perimeter cement wall. Sampling was confined to 8 m by 8 m sub-plot at the center of the block to minimize edge effects. In the RF

field, we demarcated 3 replicate plots measuring 37.5 m x 28.0 m for our measurements. These plots were randomly selected, but restricted to the center of the fields to avoid edge effects. In both PR and RF, the sample plots were accessed using footbridges to minimize disturbances of the soil and canopy. The rice seedlings were grown for 4 weeks as seedling mats in the greenhouse, before being transplanted into the PR field, whereas in RF the rice was directly seeded. Fertilization rate of 115 kgN/ha (80% as basal dosage and 20% during the tillering stage) for PR and RF were done before transplanting and at seeding stages, respectively, at a ratio of 11 : 6 : 5 (N : P : K), following the recommendations of the Ministry of Agriculture, Food and Rural Affairs (MAFRA), Republic of Korea. Rice in RF and PR were planted at a distance of 10 cm and a line spacing of 30 cm at a seed-density of 50.48 kg/ha. The PR field was kept flooded from 5 days before transplanting until the heading stage (late July). Irrigation water in PR was applied when the water level decreased below 5 cm above the soil surface. The RF field was never irrigated and relied entirely on the ambient rainfall. Weeds and insects were controlled with herbicides and insecticides, respectively.
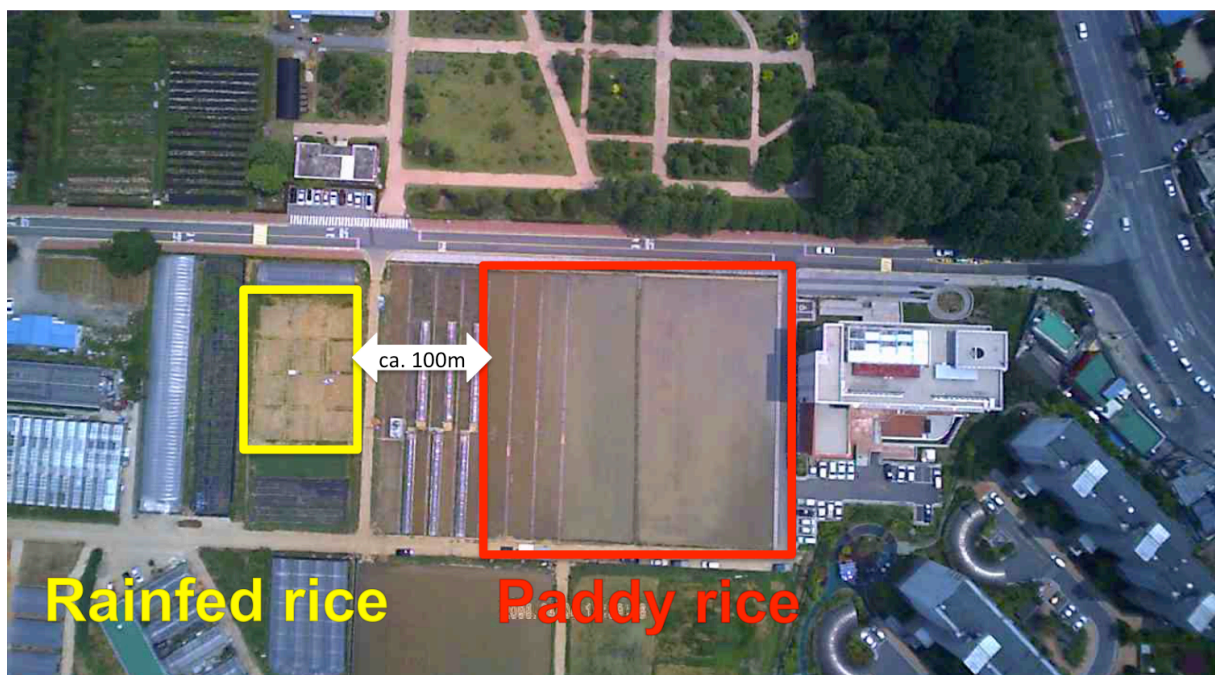
Figure 4: Overview of the study location at the Chonnam National University research farm in Gwangju, South Korea, with the rainfed (yellow square) and paddy (red square) rice field (©F. Fischer).

In study 3, Unkwang (*Oryza sativa* cv. Unkwang) was cultivated in 4 paddy fields (see Figure 5 and 6) with different application of nitrogen fertilizer. Fertilization rates were adapted to 0, 50, 115 and 180 kg N ha^{-1}, with addition of phosphate and potassium based on mass ratio of 11:5:6 for N-P-K. 80% of N fertilizer was applied two days before planting (18th of May, 138 DOY) and 20% at the tillering stage after 19 days past transplanting (157 DOY). Each field was surrounded by a perimeter cement wall resulting in an area of 73.0 m x 19.5 m for the 115 kg N ha^{-1} treatment, while measuring 73.0 m x 7.0 m for the 0, 50 and 180 kg N ha^{-1} treatments. Data acquired in the 50 kg N ha^{-1} field is excluded from further analysis in Chapter 4.

Figure 5: Fertilizer treatments (P1: 0 , P2: 50, P3: 180, P4: 115 kgN ha^{-1}) of the paddy rice in Gwangju during the growth season 2013 (©F. Fischer).
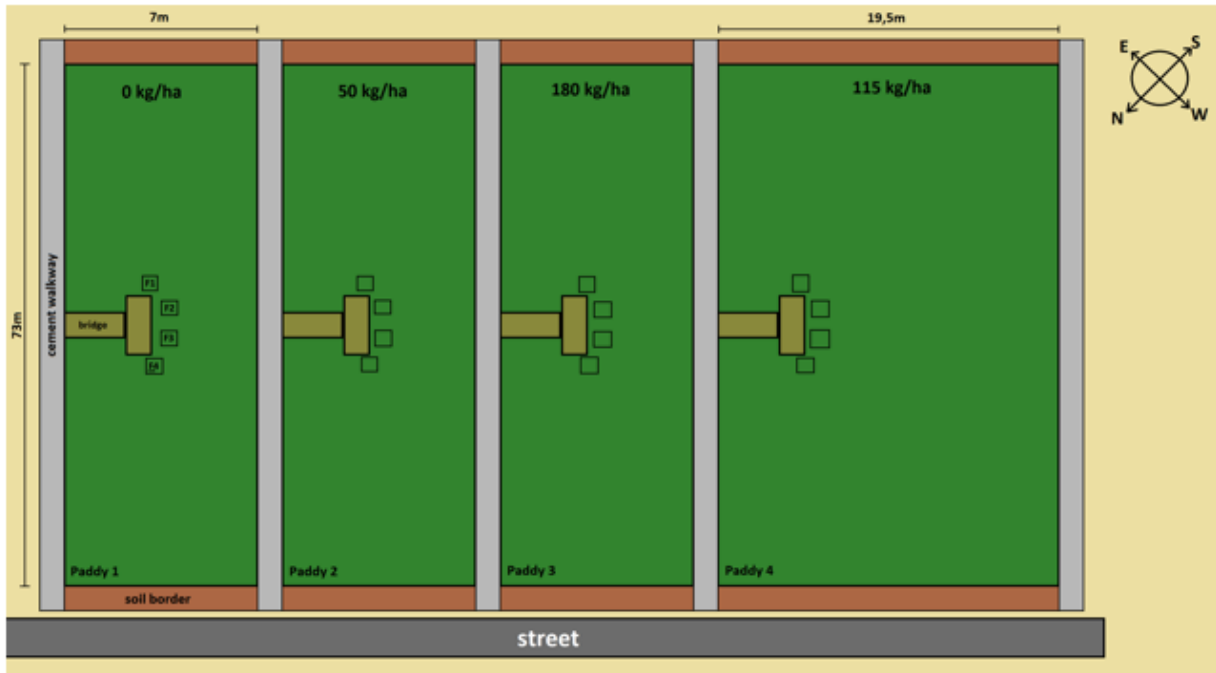
Figure 6: **Schematic overview of the experimental field setup for paddy rice in 2013, Gwangju. Four different nitrogen fertilization rates were applied (0, 50, 115, 180 kgN/ha) (©N. Lichtenwald).**

1.4. Measurements

1.4.1. Microclimate

In the Haean-catchment and in Gwangju, air temperature, humidity, precipitation and global radiation were continuously measured with a 2 m high automatic weather stations (AWS, WS−GP1, Delta−T Devices Ltd., UK). Data were taken every 5 min, averaged and logged half-hourly. Additional discontinuous records of photosynthetic photon flux density (PPFD, LI−190, LI−COR, USA) within the transparent CO_2 measurement chamber (approx. 50 cm above ground surface), air temperature (T_{air}) at 20 cm height inside and outside the CO_2 chamber (Digital thermometer, Conrad, Hirschau, Germany) and soil temperature (T_{soil}) at 10 cm soil depth (soil thermometer, Conrad, Hirschau, Germany) within the soil frames were taken during the CO_2 flux measurements. Data were recorded every 15 seconds alongside CO_2 fluxes. This allowed closer monitoring of the microclimate, in order to relate the CO_2 fluxes to the actual conditions within the chambers during measurements.

1.4.2. Soil water content

In both study sites, Haean and Gwangju, Volumetric Soil Water Content (VWC) in the plots was determined using both the gravimetric method and also by continuous measurements with the EC−5 soil moisture sensors (Decagon, WA, USA) installed at 10 and 30 cm soil depths. Data were logged every 30 min using EM50 data-logger (Decagon, WA, USA). For gravimetric VWC determination, three replicates of soil cores were obtained with a 3 cm-diameter soil corer down to 30 cm. The gravimetric methodology was not applicable in paddy condition. Each sample was immediately weighed to determine the fresh weight. The samples were later oven dried at 105°C to a constant weight before determining their dry weights. Soil moisture content was determined as the relative change in weight between fresh and dry weights.

1.4.3. Ecosystem CO$_2$ flux measurements

For the measurement of CO$_2$ exchange by the crops, the chamber methodology was applied. The ecosystem CO$_2$ flux measurement chambers were set on soil frames measuring 39.5 by 39.5 cm, which acted as a base for the chambers (see Figure 7) to prevent any gas leakage. On each crop field, four soil frames (collars) enclosing healthy, representative crops (crop plots) and two frames without vegetation (soil plots) were established 4-5 days before the commencement of CO$_2$ flux measurements for study 1 (see chapter 2 for more details). For the studies 2 and 3, 4 soil frames enclosing representative crops and 3 bare plots were established in each treatment block (see chapter 3 and 4 for more details).

Most CO$_2$ flux measurements were performed on sunny days. After flux measurements, all the soil frames were replaced on to new locations for the next round of measurements. Detailed description of the measurements conducted in the respective plots are provided in the respective chapters (see chapter 2, 3 and 4). On any measurement day, NEE and R$_{eco}$ were sequentially observed with a systematic rotation over all plots. Gross Primary Production (GPP) was calculated as:

GPP = -NEE + R$_{eco}$ **Equation 1**

where R$_{eco}$ is the sum of plant respiration (R$_{Plant}$) and soil respiration.

Plant net primary production (NPP), denoted as net carbon gain per ground meter over given time after subtracting carbon loss by plant respiration from GPP during the same time period (Campbell et al., 2001A) was determined as:

NPP = -NEE + R$_{soil}$ **Equation 2**
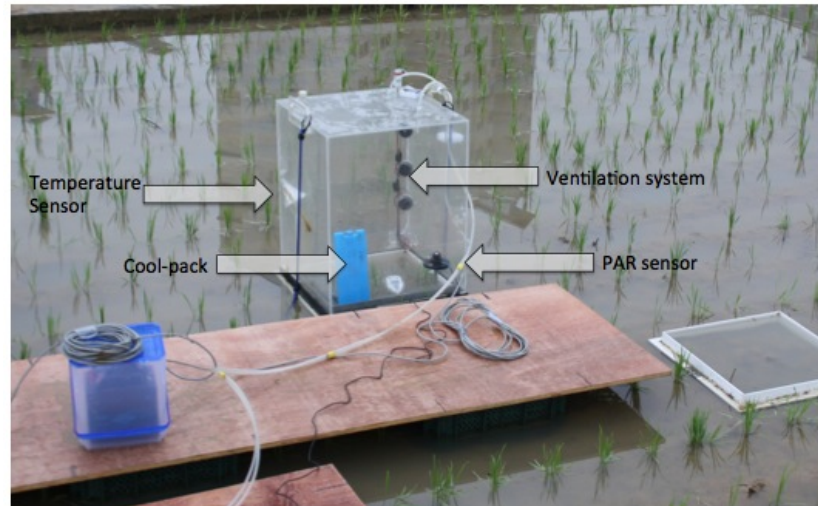
Figure 7: Picture of the transparent CO_2 measurement chamber used for NEE measurement in our experiments.

1.4.4. Analyses of nutritional influence on components of carbon gain capacity

For assessment of nutritional influences on plant growth in study 3, biomass productivity and carbon gain capacity in paddy rice, measurements of canopy structure, light and nitrogen distribution, leaf physiology in canopy profiles and GPP were carried out at the low, normal and high nutrient groups. Diurnal courses of plant canopy gas exchange were measured on DOY 157, 167, 174, 200, 219. On each measuring day, chamber measurements rotated from one plot to the next until completion of one cycle in one group, and then was moved to the next nutrient group. Diurnal gas exchange and chlorophyll fluorescence measurements in the sunlit (uppermost), second, third and fourth mature leaves of the high fertilization group were conducted using a portable gas-exchange and chlorophyll fluorescence system (GFS 3000 and PAM Flourometer 3050 F, Heinz Walz GmbH, Effeltrich, Germany) on 57 (DOY 197) and 73 DAT (DOY 213) set to track ambient environmental conditions external to the leaf cuvette. The diurnal course of leaf gas exchange in the uppermost leaves was periodically measured in the low, normal and high fertilization groups. Photosynthetic determinants $V_{cmax,30}$ and $J_{max,30}$ were derived from the linear phase and saturation phase of assimilation vs. CO_2 response curve measured at leaf temperature 30°C, based on methods referred by

Sharkey et al. (2007). CO_2 curves were commenced according to the sequence of CO_2 concentration 1500, 900, 600, 400, 200, 100 to 50 μmol mol^{-1} after leaves had acclimated to the cuvette microenvironment (CO_2 concentration of 400 μmol mol^{-1} and saturating PAR of 1500 μmol m^{-2} s^{-1}). Relative humidity (rh) was controlled to ca. 60% and light intensity at 1500 μmol m^{-2} s^{-1}. Assimilation rate, stomatal conductance and fluorescence signals were recorded after new steady-state readings were obtained. At least three replicated measurements of CO_2 curve were conducted at tillering and grain filling stage at the low and normal nutrient groups. The variable J_p method of Harley et al. (1992) for estimating mesophyll conductance was applied to data on the ETR-limited portions of CO_2 response curves. Using values of V_{cmax} and J_{max} determined from CO_2 response measurements, rates of net assimilation were predicted assuming different values of chloroplastic CO_2 concentration (C_c), the CO_2 partial pressure at the site of fixation, which is jointly determined by fixation rate, stomatal and mesophyll conductances. The limitations on photosynthetic capacity resulting from finite stomatal and mesophyll conductance were evaluated by comparing measured A_{400} at $C_a = 400$ with rates predicted assuming infinite stomatal and/or mesophyll conductance by method from Harley et al. (1986).

On 26, 33, 54, 72 and 86 DAT (corresponding to DOY 166, 173, 194, 212 and 226), three planted hills consisting of fifteen plants (five seedlings comprising one planted bundle) from each treatment were harvested, and total leaf area of each was determined with an LI-3100 leaf area meter. On 54 and 72 DAT the standing canopy in each fertilization treatment was stratified into vertical layers, each layer 15 cm in thickness. Leaf and stem area and biomass in each stratified layer were measured. On 43 DAT (DOY 183), three typical hills from each treatment were randomly selected to record individual leaf laminar area. Grain yield determinations were obtained at four sampling plots (0.5 × 0.5 m) at the end of the growing season at 113 DAT (DOY 253), and were weighed after air-drying.

Vertical profiles of incident light were determined either the day before or on the day of plant sampling (54 and 72 DAT) with light data loggers (HOBO, Onset Computer Corporation, Bourne, MA) mounted on thin rods with vertical spacing of 15 cm from base 0 cm to top of the canopy, and where multiple rods were placed along a transect diagonal to the planted rows. Data was logged every 15 min on two consecutive days when the measurements of stratified leaf area were made for nutrient groups. The HOBO logger light values were periodically compared to PAR measured with a LI-COR quantum sensor to develop a calibration curve and to estimate the PAR profiles. PAR was assumed to be attenuated through the canopy according to the Lambert-Beer law. Leaf nitrogen distribution in profiles was computed in similar way to that of light attenuation.

1.4.5. Empirical description of canopy responses

Empirical description of the measured NEE and GPP was performed with a non-linear least squares fit of the data to a hyperbolic light response model, also known as the Michaelis-Menten or rectangular hyperbola model (Owen et al., 2007)

NEE= (α*β*PAR/(α*PAR+β))+γ   **Equation 3**

where α is the initial slope of the curve and an approximation of the canopy light utilization efficiency (CO_2/ photon), β is the maximum NEE of the canopy ($\mu mol\ CO_2\ m^{-2}\ s^{-1}$), PAR is photosynthetic photon flux density ($\mu mol\ photon\ m^{-2}\ s^{-1}$), γ is an estimate of the average ecosystem respiration occurring during the observation period ($\mu mol\ CO_2\ m^{-2}\ s^{-1}$). Since the rectangular hyperbola may saturate very slowly in terms of light, we used the value calculated from α*β*PAR/(α*PAR+β) for high light intensity levels (PAR = 1500 $\mu mol\ photons\ m^{-2}\ s^{-1}$)

in this study. This value approximates the potential maximum GPP and can be thought of as the average maximum canopy uptake capacity during each observation period (noted here as $(\beta + \gamma)_{1500}$). The parameters $(\beta + \gamma)_{1500}$ (e.g. NEE at PAR = 1500 μmol m^{-2} s^{-1}) and γ were estimated for each day using NEE data from the four measurement plots per day.

Statistical analysis and best fits for light and temperature response curves were performed using Sigma Plot version 11.0.

Analysis of short-term temperature sensitivity of R_{eco} was made for the daytime R_{eco} using the Lloyd & Taylor respiration equation (Lloyd and Taylor, 1994; their Eq. (11)).

$$R_{eco} = R_{ecoRef,283}\,exp^{(E_0(1/(283.15-T_0))-(1/(T_K-T_0)))} \qquad \textbf{Equation 4}$$

where T_K is soil temperature (in K), E_0 is a parameter describing R_{eco} sensitivity to temperature, T_0 is a temperature scale parameter (kept constant at $T_0 = -46.02°C$) and $R_{ecoRef,283}$ (μmol CO_2 m^{-2} s^{-1}) is the ecosystem respiration rate at reference temperature (283.15K = 10°C).

1.4.6. Above- and belowground biomass sampling

Aboveground biomass was determined from the 39.5 cm x 39.5 cm plots where the CO_2 fluxes were measured with the chambers. The aboveground biomass was sorted into leaves, grains, culms and dead material. Respective leaf areas (LA) and green leaf areas (GLA) were determined with leaf area meter (LI−3000A, LI−COR, USA) from the sampled leaves. All the biomass was oven-dried to a constant weight at 85°C for at least 48 hours. Leaf area index (LAI) and green leaf area index (GLAI) was determined from total LA or GLA within the 39.5 cm by 39.5 cm ground area and expressed per unit square meter. Using an 8 cm diameter soil corer, soil cores were obtained from the middle of the collar, after aboveground biomass

harvest, down to 30 cm. The cores were divided in 0-10, 10-20 and 20-30 cm each, washed under running tap water, before oven-drying the sieved (2 mm mesh size) belowground biomass.

1.4.7. Plant C/N determination

Sub-samples from the dried biomass of the respective collars (for CO_2 flux measurements) were ball-milled into fine powder, re-dried at 80°C and kept in a desiccator for further analysis. A small fraction of the dried samples (< 1 g) was analyzed for total carbon/ nitrogen (C/N) content (%) using C:N Analyzer 1500 (Carlo Erba Instruments, Milan, Italy).

1.5. General results and discussions

1.5.1. Drivers of seasonality and magnitudes of CO$_2$ exchange and productivity

Chapter 2 examined CO$_2$ exchange, carbon allocation patterns and biomass development of 5 dominant crops in the Haean catchment. The results demonstrated significant differences among crops in their biomass and LAI developments. These differences were attributed mainly to differences in carbon allocation patterns and quantum yield (α). For example in cabbage, only 4% of the total biomass was allocated to the roots and the rest was directed to the aboveground biomass for leaf development (Table 3). On the other hand, radish allocated more carbon to the roots throughout the growing period. The distinct carbon allocation patterns had implications for the overall plant growth, given that preferential allocation to the aboveground structures, especially during the early stages of crop development, was associated with higher assimilation and rapid growth. At the ecosystem scale, rapid LAI development was associated with higher GPP and NEE rates, given that R$_{eco}$ was largely temperature-controlled (Figure 14).

In this multicultural agroecosystem, seasonality and the magnitudes of NEE and GPP among the crops tended to reflect the patterns of LAI development, with strong variations among crops. This compared very well with Suyker et al. (2005), who also found a strong relationship between LAI development and GPP/ NEE for maize and soybean.

Our findings demonstrate that the variations among crops that were not linked to LAI were due to differences in α, which is more or less a genetic conformation. The average peak GPP in this study was 36.8 ±16.0 µmol m^{-2} s^{-1}, while the average peak NEE was –22.6 ±7.7 µmol m^{-2} s^{-1}, rates that are comparable to those measured in some monocultural crop fields in Asia and elsewhere. For example, peak GPP was around –40.9 µmol m^{-2} s^{-1} in rice paddies in southern Korea (Moon et al., 2003) and peak NEE rates were –29.5 µmol m^{-2} s^{-1} in western Japan (Saito et al., 2005). The peak NEE in monocultures of bean in Europe and USA ranged

from -6.8 to -21.1 μmol m^{-2} s^{-1} (Falge et al. 2002, Suyker et al. 2005, Hernandez-Ramirez et al. 2011), while the maximum NEE rates in this study measured in potato and cabbage fields were -29.4 ± 0.4 and -38.7 ± 6.6 μmol m^{-2} s^{-1}, respectively. We however, observed strong differences in the timing and the duration of peak NEE rates among the different crops. The peak NEE rates reported for the agroecosystems are usually higher than rates observed in most natural ecosystems (Kato et al., 2008; Kwon et al., 2010). With regard to the atmospheric CO_2 uptake however, crops tend to have a relatively short vegetative period, which limits the duration of CO_2 uptake. For example, in our study, some crops only lasted $2-3$ months, from germination to maturity. In multicultural agriculture landscape the sawing of crops is staggered, thus there was an extended period of peak GPP and NEE, increasing the active period of atmospheric C uptake. We consider this as an ecological advantage of the multicultural agroecosystems found in S. Korea and other parts of Asia.

The observed rapid growth rates and higher NEE measured were attributed to high nutrient availability due to high fertilization rates, as N fertilization generally stimulates canopy LAI development, leaf photosynthesis through increased light use efficiency and biomass growth (Cheng et al., 2009). Net primary production in most terrestrial ecosystems, including agroecosystems, is correlated with nitrogen availability (Holland and Braswell, 1997; Frageria and Baligar, 2001; Huang et al., 2007) and foliar N concentrations scales directly with the maximum C assimilation over whole canopies (Baret et al., 2007; Gitelson et al., 2014). Standard fertilizer N application rates recommended by the Rural Development Administration of South Korea (RDA) are 238 kg N ha^{-1} for highland cabbage, 252 kg N ha^{-1} for highland radish, 137 kg N ha^{-1} for highland potato, 30 kg N ha^{-1} for beans, and 90-100 kg N ha^{-1} for paddy rice (RDA, 2006). The average fertilizer N consumption in South Korea was however estimated to be 313 kg N ha^{-1} yr^{-1} (Kim et al., 2008). While N-nutrition has a strong affect on LAI development and light interception (Weerakoon et al., 2000), biomass

production requires an ample supply of assimilates, which depends on the daily PAR. At saturating PAR, biomass production increases linearly with N-supply (Lawlor, 2002) (see chapter 4 for more details). N is a substrate for the synthesis of amino acids and, therefore, of proteins. Rapid CO_2 assimilation rate requires correspondingly large amounts of the light harvesting chlorophyll–protein complexes (LHCP), electron transport and $NADP^+$-reducing components of thylakoids, and the CO_2 assimilating enzyme Ribulose 1-5 Bisphosphate Carboxylase/Oxygenase (Rubisco), plus other enzymes required for CO_2 assimilation in the stroma (Lawlor, 2002). The major protein of the chloroplast and leaf (Evans, 1983; Sage et al., 1987) is Rubisco, but Rubisco has low catalytic rate per mass of protein, so the rates of CO_2 assimilation commonly determined in C_3 leaves requires a large amount of Rubisco (up to 30% of the N in the leaves). Differences revealed in GPP_{max} between the crops in this study are therefor not only caused by LAI, but also caused by quantum yield (α). The latter is determined by Rubisco concentration and activity, which depends on N-supply.

While LAI and α explained seasonal GPP and NEE fluctuations ($R^2 = 0.40 - 0.98$), more than 90% of the diurnal changes were due to fluctuations in PAR during the day. On a daily basis, GPP was a non-linear function of PAR, saturating at PAR > 1000 $\mu mol\ m^{-2}\ s^{-1}$. Although these observations are not unique, and have been reported for monocultural crops elsewhere (Suyker et al., 2005, Baldocchi, 1994), this study demonstrated that under similar environmental conditions, different crops respond in a relatively similar manner. Differences that are observed among them are majorly dictated by the patterns of C-partitioning and quantum yield.

The CO_2 exchange of agricultural crops is quite variable and mainly driven by agricultural practice and the climate (Jans et al., 2010), with obvious responses to season length, nutrient availability, and management measures (Owen et al., 2007). Croplands are intensively managed and exposed to frequent and persistent disturbance, perhaps more so than grasslands

and unlike many forest ecosystems, even those subject to some management. Since nearly all crops are sown and harvested annually, and are often grown in rotation, the impact of the previous or actual crop management can have a greater effect in croplands than in perennial grasslands or forest ecosystems (Smith et al., 2010). This influences the seasonal changes of ecosystem CO_2 fluxes, which are closely related to the changes in physiological activity of the ecosystem and occur in response to meteorological conditions.

Natural ecosystems at temperate latitudes, where the period for carbon assimilation (growing season) can be restricted by temperature, light and moisture conditions, as well as by leaf phenology (Keeling et al., 1996; Jackson et al., 2000), respiratory carbon losses occur simultaneously throughout the year (Janssens et al., 2001) and are mainly regulated by temperature and moisture conditions (Lloyd and Taylor, 1994), but GPP and R_{eco} may have dissimilar periods of activity (Falge et al., 2002) depending on the light, temperature and moisture conditions over the course of the year. In natural ecosystems, factors are often auto-correlated with the seasonal distributions of air/ soil temperature and soil moisture, whereas in agroecosystems, the crops are not planted until the temperatures and moisture conditions are most favorable for development of the respective crop. Since the agroecosystems monitored in this study was situated within a temperate monsoonal climatic zone, water availability was not a major factor controlling R_{eco} or limited GPP. GPP significantly (P < 0.05, $R^2 = 0.67$) influenced R_{eco}, which was due to increased maintenance respiration as root biomass increased (Gifford, 1994; Ma et al., 2007). Differences in R_{eco} observed among crops were, therefore, likely the result of variable GPP. This is in agreement with Janssens et al. (2001), Law et al. (2002), Aubinet et al. (2009), showing that ecosystem respiration is proportional to productivity, as the delivery of assimilates to the roots and exudation of sugars by roots into the soil stimulates root and soil respiration, respectively. Similar to studies of Jans et al. (2010), where a contribution of root respiration to soil respiration of up to 61%

during the cultivation period was reported.

In most cases, R_{eco} was also positively correlated with air temperature, as temperature is particular significant and affects the rates of biochemical processes, therefore determining the potential, with maximum potential occurring at an optimum temperature or within an optimum temperature range (Lawlor, 2002).

1.5.2. The role of cultivation approaches on CO_2 exchange productivity

In the Haean catchment (Chapter 2), which is a model S. Korean agroecosystem, 30% of the cultivated land is under rice cultivation (Yanggu County Office, 2010). Our chapter 3 focuses on rice crop. The two main rice production methods in S. Korea are flooded (paddy) and rainfed (upland) rice. To investigate differences arising from these rice production methods, the study investigated the same rice variety (Unkwang), which has been developed for both rainfed and paddy conditions, to minimize differences that may arise due to genotypic differences. The rice was grown under similar environmental and fertilization regimes.

The relative humidity (rH) in paddy rice was around 78% at midday on sunny days compared to 53% in the rainfed field. The interplay between high rH and cooler air temperatures in the flooded rice resulted in a lower mean daily VPD in comparison to the rainfed rice field. In the rainfed rice fields, high VPD and lower soil moisture content may results in low tissue water potentials (Ψ) and plants, therefore, respond by closing their stomata, consequently lowering CO_2 uptake and production (Maruyama and Kuwagata, 2008). Although leaf-level experiments indicate that stomatal closure causes a proportionately greater decrease in transpiration than in photosynthesis because of additional diffusive resistances of CO_2 (Cowan, 1982), other studies suggest that when water availability or hydraulic capacity of the whole plant system is limited, stomata adjust to maintain a sustainable water flow and minimize the possibility of xylem cavitation (Mencuccini and Grace, 1996), thereby reducing

CO_2 assimilation. In this study however, rainfed rice exhibited higher GPP at similar LAI (labeled as GLAI in chapter 3) compared to paddy rice due to a higher leaf N content and specific leaf weight, which resulted in a higher light use efficiency and improved productivity. This resembles the results demonstrated in chapter 2, where seasonal differences in GPP were due to variations in LAI and α, while PAR determined the daily fluctuations in GPP.

Furthermore, there were no significant differences in yield for both cultivations (yielding 6.61 $\pm$ 0.22 in paddy rice and 5.99 $\pm$ 0.68 t ha^{-1} in rainfed rice). Root water uptake by rainfed rice was, therefore, adequate to sustain C assimilation despite the fact that the plants were grown under non-water saturated soils. We note that in our case, soil water content remained > 37.2%, which are soil moisture conditions reported to be not limiting C assimilation or overall productivity (Alberto et al., 2009). This result is similar to previous studies, where GPP of non-flooded rice was less sensitive to increasing VPD compared to flooded rice fields (Alberto et al., 2009, 2012, 2013) and equally large biomass values were achieved at an adequate supply of water (Kato et al., 2006), as it was present in this study.

Chapter 3 revealed that as long as soil moisture is not limiting, the ultimate determinants of crop productivity appear to be N availability and radiation (PAR). Thus, leaf N content was correlated with aboveground biomass, α and GPP, irrespective of the growing conditions (paddy or rainfed). The findings agree with what we reported in chapter 2 for a wide range of crops.

1.5.3. Role of fertilization on crop productivity

The previous studies pointed to the important role of N-input in crop productivity (Makino et al., 1997). In chapter 4, we explored further the effect of N fertilization on leaf-level process, which ultimately determine plant productivity. Previous studies have emphasized the

important role of Nutrient application in the productivity of the agroecosystems (Holland and Braswell, 1997). In chapter 2 and 3, we observed that LAI development and light use efficiency (α) are key determinants of productivity in the agroecosystem. Leaf area and chlorophyll developments are both controlled by N-availability (Evans, 1989; Li et al., 2009). To minimize limitations due to water stress, the study was performed on paddy rice.

Generally, N addition stimulated leaf area development and yield. N-input rates of 115 and 180 kg N ha^{-1} increased aboveground biomass by 56% and 62%, respectively. This was also reflected in the grain yield, which increased by 58% and 73%, respectively, compared to the unfertilized treatment (0 kg N ha^{-1}). The study showed that N-application rates beyond the 115 kg N ha^{-1} does not further improve grain yield production and could only be a source of environmental pollution (Good et al., 2007). This is valuable information with regard to environmental management.

In relation the results observed in chapter 2 and 3, where LAI was correlated with GPP, this study showed that for rice, LAI development was due to increase in leaf numbers and leaf size. These changes are facilitated by N fertilization and leads to higher GPP. Furthermore, N−fertilized rice also developed a higher proportion of leaves in the upper canopy, where leaves experienced higher light conditions. As demonstrated in the previous studies, higher total leaf N content (labeled as N_a in chapter 4) was associated with higher quantum yield and photosynthesis. N−fertilization increases net photosynthetic rates by increasing the amounts of rate limiting enzymes (Yoshida 1981; Campbell et al., 2001a; Niinemets, 2007). This we demonstrated through a linear correlation between leaf N-content and the maximum carboxylation rate (V_{cmax}) and maximum electron transport rate (J_{max}), explaining the importance of N in determining the amounts of rate-limiting enzymes in the Calvin cycle (especially Rubisco) and the electron transport chain (Lawlor, 2002).

The relationship between light use efficiency and the percentage of total leaf area above 45 cm (termed as leaf area of upper canopy, LAUC) was linear, demonstrating the importance of leaf area development on canopy on light fixation. This linearity was only possible when N-was not limiting, demonstrating the important role played by N in light interception and fixation. The greatest benefit arising from increased N-availability is the burst in productivity early in the elongation stage that stimulates rapid canopy development and increases LAI. Thus, development of aboveground biomass is accelerated in fertilized plots, enabling them to maintain their advantageous LAI throughout development. This leads to greater PAR absorption in fertilized plots, enhancing both GPP and light use efficiency.

1.6. General conclusion and recommendation

This study investigated CO_2 exchange and carbon balance of agroecosystems comprising a multicultural cropping system in a complex terrain of South Korea. Crops differed in their patterns and magnitudes of biomass and LAI development, which was likely the result of differences in light use efficiencies and carbon allocation patterns. Both LAI and light use efficiency were the key determinants of the seasonal patterns and magnitudes of NEE and GPP, while on a daily basis, PAR explained more than 90% of their diurnal variations.

Significant variations in respiration rates among the crops were observed. Since they were grown on similar soils, with no water stress during the growing season, we assume that spatial differences in R_{eco} among the fields were due to differences in GPP. This argument is based upon the observed positive correlation between GPP and R_{eco} for the surveyed crops.

The timing of maximum CO_2 assimilation (GPP_{max}) differed among the crops, thus, even though maximum CO_2 uptake in the respective crops only lasted a couple of weeks, the effect of the staggered peak GPP resulted in extended period of high CO_2 uptake. These differences

among crops were significant and are considered as an ecological advantage in these multicultural agroecosystems found in S. Korea and other regions of Asia.

The balance between GPP and R_{eco} determines daily and seasonal NEE (Owen et al., 2007), and, therefore, the sink or source strength of C in the agricultural ecosystem. The only process of CO_2 uptake is photosynthesis and the only pool in which C can be sequestered is the soil.

Although crops in agricultural fields showed generally high CO_2 uptake rates, a short growing season length compared to i.e. forest ecosystems can lead to a low-to-moderate annual net CO_2 uptake (Anthoni et al., 2004). Introducing double cropping may help to increase the length of crop carbon uptake and shortens period of soil carbon release in the fallow land. Annual crops are harvested each year, and therefore provide no long-term storage of carbon in aboveground biomass, but soils can sequestrate atmospheric CO_2 when large quantities of crop residues and organic manure must be returned to the soil (Huang et al., 2009).

Especially for rice, enhanced fluxes of CO_2 from drained soil were caused by the removal of the barrier to gas transport from the soil surface to the air caused by the floodwater (Miyata et al., 2000).

Nevertheless, flooding and puddling of the soil are commonly practiced in paddy rice to provide abundant water, enhance nutrient availability, increase diffusion rates and mass flow, conferring much fertility to soils and stability to the ecosystem (Bachelet et al., 1995). Due to the growing scarcity of water worldwide, replacing the conventional irrigated paddy rice production by an alternative rainfed rice cultivation is seen as a promising way to maintain crop productivity under water scarcity (Tuong and Bouman, 2003). In this study, the surveyed Unkwang rice cultivar planted in rainfed fields under monsoon climate, without prolonged drought, had comparable canopy carbon gain capacity, leaf canopy size and biomass accumulation to the flooded paddy cultivation. This could be a promising water

conserving strategy in the rice productions systems. A serious environmental problems encountered in intensive paddy rice systems is a downstream water pollution and emission of ammonium volatilization due to surplus of organic nitrogen fertilizer application (Fillery et al., 1986; Ju et al., 2009).

The results of this study revealed that no benefits occurred when N > 115 kg N ha^{-1} was applied. The extra N above this rate most likely becomes a source of environmental pollution. Selecting an appropriate rate of N fertilizer is, therefore, necessary in order to minimize environmental impacts arising from agriculture, while sustaining crop productivity.

1.7. References

Alberto, M.C.R., Wassmann, R., Hirano, T., Miyata, A., Kumar, A., Agnes, P., Amante, M., 2009: CO_2/heat fluxes in rice fields: Comparative assessment of flooded and non-flooded fields in the Philippines. Agricultural and Forest Meteorology 149 ,1737–1750.

Alberto, M.C.R., Hirano, T.,Miyata ,A., Wassmann, R., Kumar, A., Padre, A., Amante, M., 2012: Influence of climate variability on seasonal and interannual variations of ecosystem CO_2 exchange in flooded and non–flooded rice fields in the Philippines. Field Crops Research 134, 80–94.

Alberto, M.C.R.,, Buresh, R.J., Hirano, T., Miyata, A.. Wassmann, R., Quilty, J.R., Correa, T.Q., Sandro, J., 2013: Carbon uptake and water productivity for dry-seeded rice and hybrid maize grown with overhead sprinkler irrigation. Field Crops Research 146, 51–65.

Ammann, C., Meixner, F.X., Busch, J., Lösch, R., 1996: CO_2 and H_20 Gas Exchange of a Triticale Field: II. Micrometeorological Flux Studies and Comparison With Upscaling From Porometry. Physics and Chemistry of the Earth 21, 151-155.

Amiro, B.D., Barr, A.G., Black, T.A., Iwashita, H., Kljun, N., McCaughey, J.H., Morgenstern, K., Murayama, S., Nesic, Z., Orchansky, A.L., Saigusa, N., 2006: Carbon, energy and water fluxes at mature and disturbed forest sites, Saskatchewan, Canada. Agricultural and Forest Meteorology 136, 237–251.

Anthoni, P.M., Freibauer, A., Kolle, O., Schulze, E.D., 2004: Winter wheat carbon exchange in Thuringia, Germany. Agricultural and Forest Meteorology 121, 55- 67.

Aubinet, M., Grelle, A., Ibrom, A., Rannik, U., Moncrieff, J., Foken, T., Kowalski, A.S., Martin, P.H., Berbiger, P., Bernhoefer, C., Clement, R., Elbers, R., Granier, A., Grunwald, T., Morganstern, K., Pilegaard, K., Rebmann, C., Snijders, W., Valentini, R., Vesala, T., 2000: Estimates of the annual net carbon and water exchange of forests: the EUROFLUX methodology. Advances in Ecological Research 30, 113–175.

Aubinet M., Moureaux C., Bodson B., Dufranne D., Heinesch B., Suleau M., Vancutsem F., Vilret, A., 2009: Carbon sequestration by a crop over a 4-year sugar beet/winter wheat/seed potato/winter wheat rotation cycle. Agricultural and Forest Meteorology 149, 407-418.

Bachelet, D., Kern, J., Tölg, M., 1995: Balancing the rice carbon budget in China using spatially-distributed data. Ecological Modelling 79, 167-177.

Baker, J.M., Griffis, T.J., 2005: Examining strategies to improve the carbon balance of corn/soybean agriculture using eddy covariance and mass balance techniques. Agricultural and Forest Meteorology 128, 163-177.

Baldocchi, D., 1994: A comparative study of mass and energy exchange rates over a closed C_3 (wheat) and an open C_4 (corn) crop: II. CO_2 exchange and water use efficiency. Agricultural and Forest Meteorology 67, 291-321.

Baldocchi, D., 2008: Breathing of the terrestrial biosphere: lessons learned from a global network of carbon dioxide flux measurement systems, Australian Journal of Botany 56, 1–26.

Bandaogo, A., Bidjokazo, F., Youl, S., Safo, E., Abaidoo, R., Andrews, O., 2015: Effect of fertilizer deep placement with urea supergranule on nitrogen use efficiency of irrigated rice in Sourou Valley (Burkina Faso). Nutrient Cycling in Agroecosystems 102, 79–89.

Baret, F., Houles, V., & Guerif, M. (2007). Quantification of plant stress using remote sensing observations and crop models: The case of nitrogen management. Journal of of Experimental Botany 58, 869–880.

Barker, G; 2006: The Agricultural Revolution in Prehistory : Why did Foragers become Farmers?: Why did Foragers become Farmers? OUP Oxford, Agriculture, 616 pages.

Bartsch, S., Peiffer, S., Shope, C.L., Arnhold, S., Jeong, J.J., Park, J.H., Eum, J., Kim, B., Fleckenstein, J.H., 2013: Monsoonal-type climate or land-use management: Understanding their role in the mobilization of nitrate and DOC in a mountainous catchment. Journal of Hydrology 507, 149–162.

Bashkin, V.N., Park, S.U., Choi, M.S., Lee, C.B., 2002: Nitrogen budgets for the Republic of Korea and the Yellow Sea Region. Biogeochemistry 57/58, 387–403.

Bernacchi, C. J., Hollinger, S. E., Meyers, T., 2005: The conversion of the corn/soybean ecosystem to no-till agriculture may result in a carbon sink. Global Change Biology 11, 1867–1872.

Béziat, P., Ceschia, E., Dedieu, G., 2009: Carbon balance of a three crop succession over two cropland sites in South West France. Agricultural and Forest Meteorology 149, 1628–1645.

Bonan, G., 2002. Ecological climatology: concepts and applications. Cambridge University Press, Cambridge, p. 678.

Busch, J., 2001: Characteristic values of key ecophysiological parameters in the genus Carex. Flora, 196, 405–430.

Campbell, C.S., Heilman, J.L., McInnes, K.J., Wilson, L.T., Medley. J.C., Wu, G., Cobos, D.R., 2001A: Diel and seasonal variation in CO_2 flux of irrigated rice. Agricultural and Forest Meteorology 108, 15–27.

Campbell, C.S., Heilman, J.L., McInnes, K.J., Wilson, L.T., Medley, J.C., Wu, G., Cobos, D.R., 2001B: Seasonal variation in radiation use efficiency of irrigated rice. Agricultural and Forest Meteorology, 110, 45–54. Chen,

Carrara, A., Janssens, I.A., Yuste, J.C., Ceulemans, R., 2004: Seasonal changes in photosynthesis, respiration and NEE of a mixed temperate forest. Agricultural and Forest Meteorology 126, 15–31.

Cassman, K.G., 1999: Ecological intensification of cereal production systems: Yield potential, soil quality, and precision agriculture. Proceedings of the National Academy of Sciences 96, 5952–5959.

Cheng, X., Luo, Y., Su, B., Verburg, P.S.J., Hui, D., Obrist, D., Arnone, J.A., Johnson, D.W., Evans, R.D., 2009: Responses of net ecosystem CO_2 exchange to nitrogen fertilization in experimentally manipulated grassland ecosystems Agricultural and Forest Meteorology 149, 1956–1963.

Colmer, T.D., Gibberd, M.R., Wiengweera, A., Tinh, T.K., 2003. The barrier to radial oxygen loss from roots of rice (*Oryza sativa* L.) is induced by growth in stagnant solution. Journal of Experimental Botany 49, 1431–1436.

Conway,G.R., 1987: The Properties of Agroecosystems. Agricultural Systems 24, 95-117.

Cowan, I., 1982: Regulation of water use in relation to carbon gain in higher plants. Physiological Plant Ecology II. Springer, pp. 589–613.

Ciais, P., Reichstein, M., Viovy, N., Granier, A., Ogee, J., Allard, V., Aubinet, M., Buchmann, N., Bernhofer, C., Carrara, A., Chevallier, F., De Noblet, N., Friend, A.D., Friedlingstein, P., Grunwald, T., Heinesch, B., Keronen, P., Knohl, A., Krinner, G., Loustau, D., Manca, G., Matteucci, G., Miglietta, F., Ourcival, J.M., Papale, D., Pilegaard, K., Rambal, S., Seufert, G., Soussana, J.F., Sanz, M.J., Schulze, E.D., Vesala, T, Valentini, R., 2005: Europe-wide reduction in primary productivity caused by the heat and drought in 2003. Nature 437, 529-533.

Coursolle, C., Margolis, H.A., Barr, A.G., Black, T.A., Amiro, B.D., McCaughey, J.H., Flanagan, L.B., Lafleur, P.M., Roulet, N.T., A Bourque, C.P., Arain, M.A., Wofsy, S.C., Dunn, A., Morgenstern, K., Orchansky, A.L., Bernier, P.Y., Chen, J.M., Kidston, J., Saigusa,

N., Hedstrom, N., 2006: Late-summer carbon fluxes from Canadian forests and peatlands along an east-west continental transect. Canadian Journal of Forest Research 36, 783-800.

Chunlin, W., Guirui, Y., Guoyi, Z., Junhua, Y., Leiming, Z., Xu, W., Xuli, T., Xiaomin, S., 2006: CO_2 flux evaluation over the evergreen coniferous and broad-leaved mixed forest in Dinghushan, China. Science in China Series D: Earth Sciences 49, 127-138.

Evans, J.R., 1983: Nitrogen and photosynthesis in the flag leaf of wheat (Triticum aestivum L.). Plant Physiology 72, 297-302.

Evans, J.R., 1989: Photosynthesis and nitrogen relationships in leaves of C3 plants. Oecologia 78, 9-19.

Falge, E., Baldocchi, D., Tenhunen, J., Aubinet, M., Bakwin, P. , Berbigier, P., Bernhofer, C., Burba, G., Clement, R., Davis, K.J., Elbers, J.A., Goldstein, A.H., Grelle, A., Granier, A., Guðmundsson, J., Hollinger, D., Kowalski, A.S., Katul, G., Law, B.E., Malhi, Y., Meyers, T., Monson, R.K., Munger, J.W., Oechel, W., Paw U, K.T., Pilegaard, K., Rannik, Ü., Rebmann, C., Suyker, A., Valentini, R., Wilson, K., Wofsy, S., 2002: Seasonality of ecosystem respiration and gross primary production as derived from FLUXNET measurements. Agricultural and Forest Meteorology 113, 53–74.

FAOSTAT, 2015. FAOSTAT online database at http://faostat3.fao.org/browse/E/*/E

Fillery, I., Simpson, J., De Datta, S., 1986: Contribution of ammonia volatilization to total nitrogen loss after applications of urea to wetland rice fields. Fertilizer Research 8, 193–202.

Food and Agriculture Organization of the United Nations (FAO). 2006. Guidelines for soil description, fourth ed. Rome.

Flanagan, L.B., Johnson, B.G., 2005: Interacting effects of temperature, soil moisture and plant biomass production on ecosystem respiration in a northern temperate grassland. Agricultural and Forest Meteorology 130, 237–253.

Fageria, N.K., Baligar, V.C., 2001: Lowland rice response to nitrogen fertilization. Communications in Soil Science and Plant Analysis 32, 1405 — 1429

Frink, C.R., Waggoner, P.E., Ausubel, J.H., 1999: Nitrogen fertilizer: Retrospect and prospect. Proceedings of the National Academy of Sciences 96, 1175–1180.

Giardina, C.P., Ryan, M. G., Binkley, D., Fownes, J.H., 2003: Primary production and carbon allocation in relation to nutrient supply in a tropical experimental forest. Global Change Biology 9, 1438–1450.

Gifford, R.M., 1994. The global carbon-cycle: a viewpoint on the missing sink. Australian Journal of Plant Physiology 21, 1-15.

Gimenez, C., Connor, D.J., Rueda, F., 1994: Canopy development, photosynthesis and radiation–use efficiency in sunflower in response to nitrogen. Field Crops Research 38, 15–27.

Gitelson, A.G., Peng, Y., Arkebauer, T.J., Schepers, J., 2014: Relationships between gross primary production, green LAI, and canopy chlorophyll content in maize: Implications for remote sensing of primary production. Remote Sensing of Environment 144, 65–72.

Good, A.G., Johnson, S.J., De Pauw, M., Carroll, R.T., Savidov, N., Vidmar, J., Lu, Z., Taylor, G., Stroeher, V., 2007: Engineering nitrogen use efficiency with alanine aminotransferase . Canadian Journal of Botany 85, 252–262.

Göckede, M., Rebmann, C., Foken, T., 2004: A combination of quality assessment tools for eddy covariance measurements with footprint modelling for the characterisation of complex sites. Agricultural and Forest Meteorology 127, 175-188.

Hanson, P.J., Edwards, N.T., Garten, C.T., Andrews, J.A., 2000: Separating root and soil microbial contributions to soil respiration; a review of methods and observations. Biogeochemistry 48, 115–146.

Harley, P.C., Tenhunen, J.D., Lange, O.L., 1986: Use of an analytical model to study limitation on net photosynthesis in Arbutus unedo under field conditions. Oecologia, 70, 393–401.

Harley, P.C., Loreto, F., Dimarco, G., Sharkey, T.D., 1992: Theoretical considerations when estimating the mesophyll conductance to CO_2 flux by the analysis of the response of photosynthesis to CO_2. Plant Physiology, 98, 1429–1436.

Hernandez-Ramirez, G., Hatfield, J.L., Parkin, T.B., Sauer, T.J., Prueger, J.H., 2011: Carbon dioxide fluxes in corn–soybean rotation in the midwestern U.S.: inter- and intra-annual variations, and biophysical controls. Agriculture and Forest Meteorology 151, 1831-1842.

Holland, E.A., Braswell, B.H., Lamarque, J.F., Townsend, A., Sulzman, J., Müller, J.F., Dentener, F., Brasseur, G., Levy H., Penner, J.E., Roelofs, G.J., 1997: Variations in the predicted spatial distribution of atmospheric nitrogen deposition and their impact on carbon uptake by terrestrial ecosystems. Journal of Geophysical Research 102, 15849–15866.

Hollinger, D.Y., Kelliher, F.M., Byers, J.N., Hunt, J.E., McSeveny, J. E., Weir, P.L., 1994: Carbon dioxide exchange between an un-disturbed old-growth temperate forest and the atmosphere, Ecology 75, 134–150.

Hossen, M., Mano, M., Miyata, A., Baten, M., Hiyama, T., 2011: Seasonality of ecosystem respiration in a double–cropping paddy field in Bangladesh. Biogeosciences Discussions 8, 8693–8721.

Hoyaux, J., Moureaux, C., Tourneur, D., Bodson, B., Aubinet, M., 2008: Extrapolating gross primary productivity from leaf to canopy scale in a winter wheat crop. Agricultural and Forest Meteorology 148, 668–679.

Huang, Y., Zhang, W., SUN, W., Zheng, X., 2007: Net primary production of chinese croplands from 1950 to 1999. Ecological Applications 17, 692–701.

Huang, Y., Yu, Y., Zhang, W., Sun, W., Liu, S., Jiang, J., Wu, J., Yu, W., Wang, Y., Yang, Z., 2009: Agro-C: A biogeophysical model for simulating the carbon budget of agroecosystems. Agricultural and Forest Meteorology 149, 106–129.

IPCC (Intergovernmental Panel of Climate Change), 1996: Climate change 1995: the science of climate change. Cambridge University Press, Cambridge, UK.

IPCC (Intergovernmental Panel of Climate Change), 2001: Climate Change 2001 – The Scientific Basis. Cambridge University Press, 881 pp.

Jackson, R.B., Lechowicz, M.J., Li, X., Mooney, H.A., 2000: The roles of phenology, growth, and allocation in global terrestrial productivity. In: Mooney, H.A., Saugier, B., Roy, J. (Eds.), Terrestrial Global Productivity: Past, Present, and Future. Academic Press, San Diego, US, pp. 61–82.

Jans, W.W.P., Jacobs, C. M.J., Kruijt, B., Elbers, J.A., Barendse, S., Moors, E. J., 2010: Carbon exchange of a maize (*Zea mays* L.) crop: Influence of phenology. Agriculture, Ecosystems and Environment 139, 316–324.

Janssens, I.A., Lankreijer, H., Matteucci, G., Kowalski, A.S., Buchmann, N., Epron, D., Pilegaard, K., Kutsch, W., Longdoz, B., Grünwald, T., Montagnani, L., Dore, S., Rebmann, C., Moors, E. J., Grelle, A., Rannik, Ü., Morgenstern, K., Oltchev, S., Clement, R., Guðmundsson, J., Minerbi, S., Berbigier, P., Ibrom, A., Moncrieff, J., Aubinet, M., Bernhofer, C., Jensen, N.O., Vesala, T., Granier, A., Schulze, E.D., Lindroth, A., Dolman, A.J., Jarvis, P.G., Ceulemans, R., Valentini, R., 2001: Productivity overshadows temperature

in determining soil and ecosystem respiration across European forests. Global Change Biology, 7, 269–278.

Johnson, J.M.F., Franzluebbers, A.J., Weyers, S.L., Reicosky, D.C., 2007: Agricultural opportunities to mitigate greenhouse gas emissions. Environmental Pollution 150, 107-124.

Ju, X.T., Xing, G.X., Chen, X.P., Zhang, S.L., Zhang, L.J., Liu, X.J., Cui, Z.L., Yin, B., Christie, P., Zhu, Z.L., 2009: Reducing environmental risk by improving N management in intensive Chinese agricultural systems. Proceedings of the National Academy of Sciences, USA 106, 3041–3046.

Kato, Y., Kamoshita, A., Yamagishi, J., Abe, J., 2006A: Growth of Three Rice (*Oryza sativa* L.) Cultivars under Upland Conditions with Different Levels of Water Supply 1. Nitrogen Content and Dry Matter Production. Plant Production Science 9, 422-434.

Kato, Y., Abe, J., Kamoshita, A., Yamagishi, J., 2006B: Genotypic variation in root growth angle in rice (Oryza sativa L.) and its association with deep root development in upland fields with different water regimes. Plant Soil 287, 117–129.

Kato, Y., Kamoshita, A., Yamagishi, J., Imoto, H., Abe, J., 2007: Growth of Rice (Oryza sativa L.) Cultivars under Upland Conditions with Different Levels of Water Supply 3. Root System Development, Soil Moisture Change and Plant Water Status. Plant Production Science 10, 3–13.

Kato, T., TANG, Y., 2008: Spatial variability and major controlling factors of CO_2 sink strength in Asian terrestrial ecosystems: evidence from eddy covariance data. Global Change Biology 14, 2333–2348.

Katsura, K., Okami, M., Mizunuma, H., Kato, Y., 2010: Radiation use efficiency, N accumulation and biomass production of high–yielding rice in aerobic culture. Field Crops Research, 117, 81–89.

Keeling, C.D., Chin, J.F.S., Whorf, T.P., 1996: Increased activity of northern vegetation inferred from atmospheric CO2 observations. Nature 382, 146–149.

Keeling, C.D., Whorf, T.P., 2004: Atmospheric Carbon Dioxide Concentrations at 10 Locations Spanning Latitudes 82°N to 90°S. DOI: 10.3334/CDIAC/atg.ndp001.2004

Keller, M., Alencar, A., Asner, G.P., Braswell, B., Bustamante, M., Davidson, E., Feldpausch, T., Fernandes, E., Goulden, M., Kabat, P., Kruijt, B., Luizao, F., Miller, S., Markewitz, D., Nobre, A.D., Nobre, C.A., Priante, N., da Rocha, H., Dias, P.S., von Randow, C., Vourlitis, G.L., 2004: Ecological research in the large-scale biosphere- atmosphere experiment in Amazonia: Early results. Ecological Applications 14, 3-16.

Kettering, J., Park, J.H., Lindner, S., Lee, B., Tenhunen, J., Kuzyakov, Y., 2012: N fluxes in an agricultural catchment under monsoon climate: A budget approach at different scales. Agriculture, Ecosystems and Environment 161, 101 – 111.

Kim, T., Kim, G., Kim, S., Choi, E., 2008: Estimating riverine discharge of nitrogen from the South Korea by the mass balance approach. Environmental Monitoring and Assessment 136, 371–378.

Kiniry, J., Jones, C., O'toole, J., Blanchet, R., Cabelguenne, M., Spanel, D., 1989: Radiation–use efficiency in biomass accumulation prior to grain–filling for five grain–crop species. Field Crops Research 20, 51–64.

Kondo, M., Pablico, P.P., Aragones, D.V., Agbisit, R., Abe, J., Morita, S., Courtois, B., 2003: Genotypic and environmental variations in root morphology in rice genotypes under upland field conditions. Plant and Soil 255, 189–200.

Korea Meteorological Administration, 2011: A white paper on Changma.

Kotula, L., Ranathunge, K., Steudle, E., 2009: Apoplastic barriers effectively block oxygen permeability across outer cell layers of rice roots under deoxygenated conditions: roles of apoplastic pores and of respiration. New Phytologist, 184, 909–917.

Koyama, T., Chammek, C., Niamsrichand, N., 1972: Soil–plant nutrition studies on tropical rice V. Yield components as affected by the timing of top–dressing of nitrogen in the Bangkhen paddy field. Soil Science and Plant Nutrition 18, 233–245.

Koyama, T., Niamsrichand, N., 1973: Soil–plant nutrition studies on tropical rice VI. The effect of different levels of nitrogenous fertilizer application on plant growth, grain yield, and nitrogen utilization by rice plants. Soil Science and Plant Nutrition 19, 265–274.

Kwon, Y.S., Lee, H.Y., Han, J., Kim, W.H., Kim, D.J., Kim, D.I., Youm, S.J., 1990: Terrain analysis of Haean Basin in terms of earth science. Journal of the Korean Earth Science Society 11, 236–241.

Kwon, H.J., Park, T. Y., Hong, J., Lim, J.H., Kim, J., 2010: Seasonality of Net Ecosystem Carbon Exchange in Two Major Plant Functional Types in Korea
Asia-Pacific Journal of Atmospheric Sciences 45, 149-163.

Lai, C.T., Katul, G., Butnor, J., Siqueira, M., Ellsworth, D., Maier, C., Johnsen, K., Mckeand, S., Oren, R., 2002: Modelling the limits on the response of net carbon exchange to fertilization in a south-eastern pine forest. Plant, Cell and Environment 25, 1095–1119.

Larsen, K.S., Ibrom, A., Beier, C., Jonasson, S., Michelsen, A., 2007: Ecosystem respiration depends strongly on photosynthesis in a temperate heath. Biogeochemistry 85, 201–213.

Law, B.E., Falge, E., Gu, L., Baldocchi, D.D., Bakwin, P., Berbigier, P., Davis, K., Dolman, A.J., Falk, M., Fuentes, J.D., Goldstein, A., Granier, A., Grelle, A., Hollinger, D., Janssens, I.A., Jarvis, P., Jensen, N.O., Katul, G., Mahli, Y., Matteucci, G., Meyers, T., Monson, R., Munger, W., Oechel, W., Olson, R., Pilegaard, K., Paw U, K.T., Thorgeirsson, H., Valentini, R., Verma, S., Vesala, T., Wilson, K., Wofsy, S., 2002: Environmental controls over carbon dioxide and water vapor exchange of terrestrial vegetation
Agricultural and Forest Meteorology 113, 97–120.

Law, B., 2005: Carbon dynamics in response to climate and disturbance: Recent progress from multi-scale measurements and modeling in AmeriFlux. Plant Responses to Air Pollution and Global Change, Springer-Verlag Tokyo 2005, 205-213.

Lawlor, D.W., 2002: Carbon and nitrogen assimilation in relation to yield: mechanisms are the key to understanding production systems. Journal of Experimental Botany 53, 773–787.

Lawson, T., Craigon, J., Tulloch, A.M., Black, C.R., Colls, J.J., Landon, G., 2001: Photosynthetic responses to elevated CO_2 and O_3 in field-grown potato (*Solanum tuberosum*). Journal of Plant Physiology 158, 309–323.

Lee, X., Fuentes, J.D., Staebler, R.M., Neumann, H.H., 1999: Long-term observation of the atmospheric exchange of CO2 with a temperate deciduous forest in southern Ontario, Canada. Journal OF Geophysical Research104, 15975–15984.

Li, Y., Gao, Y., Xu, X., Shen, Q., Guo, S., 2009: Light-saturated photosynthetic rate in high-nitrogen rice (*Oryza sativa* L.) leaves is related to chloroplastic CO_2 concentration. Journal of Experimental Botany 60, 2351–2360.

Lloyd, J., Taylor, J.A., 1994: On the temperature dependence of soil respiration. Functional Ecology 8, 315–323.

Ma, S., Baldocchi, D.D., Xu, L., Hehn, T., 2007: Inter-annual variability in carbon dioxide exchange of an oak/grass savanna and open grassland in California. Agric. For. Meteorol 147, 157–171.

Mack, A.R., Desjardins, R.L., MacPherson, J.I., Schuepp, P.H., 1990: Relative photosynthesis activity of agricultural lands from airborne carbon dioxide and satellite data. International Journal of Remote Sensing 11, 237–251.

Makino, A., Sato, T., Nakano, H., Mae, T., 1997. Leaf photosynthesis, plant growth and nitrogen allocation in rice under different irradiances. Planta 203, 390–398.

Maruyama, A., Kuwagata, T., 2008: Diurnal and seasonal variation in bulk stomatal conductance of the rice canopy and its dependence on developmental stage. Agricultural and Forest Meteorology 148, 1161–1173.

McDonald, M.P., Galwey, N.W., Colmer, T.D., 2002: Similarity and diversity in adventitious root anatomy as related to root aeration among a range of wetland and dryland grass species. Plant Cell and Environment, 25, 441–451.

Mencuccini, M., Grace, J., 1996: Hydraulic conductance, light interception and needle nutrient concentration in Scots pine stands and their relations with net primary productivity. Tree Physiology 16, 459–468.

Migletta, F., Gioli, B., Hutjes, R.W.A., Reichstein, M., 2007: Net regional ecosystem CO_2 exchange from airborne and ground-based eddy covariance, land-use maps and weather observations. Global Change Biology 13, 548–560.

Ministry of Agriculture, Food and Rural Affairs (MAFRA), Republic of Korea. Found at http://english.mafra.go.kr

Miyata, A., Leuning, R., Denmead. O.T., Kim, J., Harazono, Y., 2000: Carbon dioxide and methane fluxes from an intermittently flooded paddy field. Agricultural and Forest Meteorology 102, 287–303.

Monnin, E., Indermühle, A., Dällenbach, A., Flückiger, J., Stauffer, B., Stocker, T.F., Raynaud, D., Barnola, J.M., 2001: Atmospheric CO_2 Concentrations over the Last Glacial Termination. Science 5, 112-114.

Monteith, J., 1972: Solar radiation and productivity in tropical ecosystems. Journal of Applied Ecology 9, 747–766.

Monteith, J.L., Moss, C., 1977: Climate and the efficiency of crop production in Britain [and discussion]. Philosophical Transactions of the Royal Society B: Biological Sciences, 281, 277–294.

Moog ,P.R., Brüggemann, W., 1998: Flooding tolerance of Carex species. II. Root gas–exchange capacity. Planta, 207, 199–206.

Moon, B.K., Hong, J., Lee, B.R., Yun, J.I., Park, E.W., Kim, J., 2003: CO_2 and energy exchange in a rice paddy for the growing season of 2002 in Hari, Korea. Korean Journal of Agriculture and Forest Meteorologie 5, 51–60.

Moureaux C., Debacq A., Bodson B., Heinesch B., Aubinet, M., 2006: Annual net ecosystem carbon exchange by a sugar beet crop. Agricultural and Forest Meteorology 139, 25-39.

Moureaux, C., Debacq, A., Hoyaux, J., Suleau, M., Tourneur, D., Vancutsem, F., Bodson, B., Aubinet, M., 2008: Carbon balance assessment of a Belgian winter wheat crop (Triticum aestivum L.). Global Change Biology 14, 1353-1366.

Naklang, K., Fukai, S., Nathabut, K., 1996: Growth of rice cultivars by direct seeding and transplanting under upland and lowland conditions. Field Crops Research 48, 115-123.

Niinemets, U. 2007. Photosynthesis and resource distribution through plant canopies. Plant Cell and Environment, 30, 1052–1071. Niinemets,

Okami, M., Kato, Y., Yamagishi, J.; 2013: Grain Yield and leaf area growth of direct–seeded rice on flooded and aerobic soils in Japan. Plant Production Science, 16, 276–279.

Ookawa, T., Naruoka, Y., Sayama, A., Hirasawa, T., 2004: Cytokinin effects on ribulose-1,5-bisphosphate carboxylase/oxygenase and nitrogen partitioning in rice during ripening. Crop Science 44, 2107–2115.

Ollinger, S.V., Richardson, A.D., Martin, M.E., Hollinger, D.Y., Frolking, S.E., Reich, P.B., Plourde, L.C., Katul, G.G., Mungere, J.W., Oren, R., Smith, M.L., Paw U, K.T., Bolstad, P.V., Cook, B.D., Daya, M.C., Martin, T.A., Monson, R.K., Schmid, H.P., 2008: Canopy nitrogen, carbon assimilation, and albedo in temperate and boreal forests: Functional relations and potential climate feedbacks. Proceedings of the National Academy of Sciences of the United States of America 105, 19336–19341.

Owen, K.E., Tenhunen, J., Reichstein, M., Wang, Q., Falge, E., Geyer, R., Xiao, X., Stoy, P., Ammann, C., Arain, A., Aubinet, M., Aurela, M., Bernhofer, C., Chojnicki, B.H., Granier, A., Gruenwald, T., Hadley, J., Heinesch, B., Hollinger, D., Knohl, A., Kutsch, W., Lohila, A., Meyers, T., Moors, E., Moureaux, C., Pilegaard, K., Saigusa, N., Verma, S., Vesala, T., Vogel, C., 2007: Linking flux network measurements to continental scale simulations: ecosystem carbon dioxide exchange capacity under under non-water-stressed conditions. Global Change Biology 13, 734–760.

Pattey, E., Strachan, I.B., Desjardins, R.L. and Massheder, J., 2002: Measuring nighttime CO_2 flux over terrestrial ecosystems using eddy covariance and nocturnal boundary layer methods. Agricultural and Forest Meteorology 113, 145-153.

Pavelka, M., Sedlák, P., Acosta, M., Czerny, R., Taufarová, K., Janous, D., 2007: Chamber techniques versus eddy covariance method during nighttime measurements. International Scientific Conference, Polana nad Detvou, Slovakia.

Peng, S., Bouman, B., Visperas, R.M., Castaneda, A., Nie, L., Park, H.K., 2006: Comparison between aerobic and flooded rice in the tropics: Agronomic performance in an eight-season experiment. Field Crops Research 96, 252–259.

Raich, J.W., Tufekcioglu, A., 2000: Vegetation and soil respiration: correlations and controls. Biogeochemistry 48, 71–90.

Ranathunge, K., Kotula, L., Steudle, E., Lafitte, R., 2004: Water permeability and reflection coefficient of the outer part of young rice roots are differently affected by closure of water

channels (aquaporins) or blockage of apoplastic pores. Journal of Exponential Botany 55, 433–447.

RDA (Rural Development Administration of Korea) (Ed.), 2006: The standard rate of chemical fertilizer for crops, Suwon-si.

Rebmann, C., Göckede, M., Foken, T., Aubinet, M., Aurela, M., Berbigier, P., Bernhofer, C., Buchmann, N., Carrara, A., Cescatti, A., Ceulemans, R., Clement, R., Elbers, J.A., Granier, A., Grünwald, T., Guyon, D., Havránková, K., Heinesch, B., Knohl, A., Laurila, T., Longdoz, B., Marcolla, B., Markkanen, T., Miglietta, F., Moncrieff, J., Montagnani, L., Moors, E., Nardino, M., Ourcival, J.M., Rambal, S., Rannik, Ü., Rotenberg, E., Sedlak, P., Unterhuber, G., Vesala, T., Yakir, D., 2005: Quality analysis applied on eddy covariance measurements at complex forest sites using footprint modelling. Theoretical and Applied Climatology 80, 121-141.

Sage, R.F., Pearcy, R.W., Seemann, J.R., 1987: The nitrogen use efficiency of C_3 and C_4 plants. I. Leaf nitrogen, growth, and biomass partitioning in *Chenopodium album* (L.) and *Amaranthus retroflexus* (L.). Plant Physiology 84, 954–958.

Saigusa, N., Yamamoto, S., Murayama, S., Kondo, H., 2005: Inter-annual variability of carbon budget components in an AsiaFlux forest site estimated by long-term flux measurements. Agricultural and Forest Meteorology 134, 4-16.

Saito, M., Miyata, A., Nagai, H., Yamada, T., 2005: Seasonal variation of carbon dioxide exchange in rice paddy field in Japan. Agricultural and Forest Meteorology 135, 93–109.

Schmid, H.P., 2002: Footprint modeling for vegetation atmosphere exchange studies: a review and perspective. Agricultural and Forest Meteorology 113, 159–183.

Sharkey, T.D., Bernacchi, C.J., Farquhar, G.D., Singsaas, E.L., 2007: Fitting photosynthetic carbon dioxide response curves for C3 leaves. Plant Cell and Environment, 30, 1035–1040.

Sheehy, J.E., Mitchell, P.L., 2013: Designing rice for the 21st century: the three laws of maximum yield. Discussion Paper Series 48. Los Baños (Philippines): International Rice Research Institute.

Sinclair, T.R., Horie, T., 1989: Leaf nitrogen, photosynthesis, and crop radiation use efficiency: a review. Crop Science 29, 90–98.

Smith, P., Lanigan, G., Kutsch, W.L., Buchmann, N., Eugster, W., Aubinet, M., Ceschia, E., Béziat, P., Yeluripati, J.B., Osborne, B., Moors, E.J., Brut, A., Wattenbach, M., Saunders, M., Jones, M., 2010: Measurements necessary for assessing the net ecosystem carbon budget of croplands. Agriculture, Ecosystems and Environment 139, 302–315.

Soegaard, H., Jensen, N.O., Boegh, E., Hasager, C.B., Schelde, K., Thomsen, A., 2003: Carbon dioxide exchange over agricultural landscape using eddy correlation and footprint modelling. Agricultural and Forest Meteorology 114, 153–173.

Suyker A.E., Verma S.B., Burba G.G., Arkebauer T.J., Walters D.T., Hubbard K.G., 2004: Growing season carbon dioxide exchange in irrigated and rainfed maize. Agricultural and Forest Meteorology, 124, 1-13.

Suyker A., Verma S., Burba G., Arkebauer T.J., 2005: Gross primary production and ecosystem respiration of irrigated maize and irrigated soybean during a growing season. Agricultural and Forest Meteorology 131, 180-190.

Thirsk, J., 1997: Alternative Agriculture: A History : From the Black Death to the Present Day. OUP Oxford, Business & Economics.

Tuong, B.A.M., Bouman, T.P., 2000: Field water mangement to save water and increase its productivity in irrigated lowland rice. Agricultural Water Management 49, 11-30.

Tuong, T.P., Bouman, B.A.M., 2003: Rice production in water–scarce environments, in: J.W. Kijne; R. Barker and D. Molden (eds.), Water Productivity in Agriculture: Limits and Opportunities for Improvement. pp. 53–67.

Usha Rao, I., Pandey, B.K., 2007: Origin and Introduction of Crop Plants, Cereals and Pulses. Economy Botany, 1-34.

Valentini, R., Matteucci, G., Dolman, A.J., Schulze, E.D., Rebmann, C., Moors, E.J., Granier, A., Gross, P., Jensen, N.O., Pilegaard, K., Lindroth, A., Grelle, A., Bernhofer, C., Grünwald, T., Aubinet, M., Ceulemans, R., Kowalski, A.S., Vesala, T., Rannik, Ü., Berbigier, P., Loustau, D., Gu, J., Thorgeirsson, H., Ibrom, A., Morgenstern, K., Clement, R., Moncrieff, J., Montagnani, L., Minerbi, S., Jarvis, P.G., 2000: Respiration as the main determinant of carbon balance in European forests. Nature 404, 861 - 865.

Vavilov, N.I.; Freier, F., 1951: Studies on the origin of cultivated plants.

Verma S.B., Dobermann A., Cassman K.G., Walters D.T., Knops J.M., Arkebauer T.J., Suyker A.E., Burba G.G., Amos B., Yang, H., 2005: Annual carbon dioxide exchange in irrigated and rainfed maize-based agroecosystems. Agricultural and Forest Meteorology 131, 77-96.

Weerakoon, W.M.W., Ingram, K.T., Moss, D.N., 2000: Atmospheric carbon dioxide and fertilizer nitrogen effects on radiation interception by rice. Plant Soil 220, 99–106.

West, T.O., Bandaru, V., Brandt, C.C., Schuh, A.E., Ogle, S.M., 2011: Regional uptake and release of crop carbon in the United States. Biogeosciences Discussions, 8, 631–654.

Williams, C.A, Hanan, N.P., Neff, J.C., Scholes, R.J., Berry, J.A., Denning, A.S., Baker, D.F., 2007: Africa and the global carbon cycle. Carbon Balance and Management 2, 3.

Wohlfahrt, G., Anfang, C., Bahn, M., Haslwanter, A., Newesely, C., Schmitt, M., Drösler, M., Pfadenhauer, J., Cernusca, A., 2005: Quantifying nighttime ecosystem respiration of a meadow using eddy covariance, chambers and modelling. Agricultural and Forest Meteorology 128, 141-162.

Yanggu County Office (Ed.), 2010. Yanggu Statistical Yearbook 2009, Yanggu.

Yoshida, S., 1981. Fundamentals of Rice Crop Science. IRRI, P.O. Box 933, Manila, Philippines.

Yu, G.R., Wen, X.F., Sun, X.M., Tanner, B.D., Lee, X., Chen, J.Y., 2006: Overview of chinaflux and evaluation of its eddy covariance measurement. Agricultural and Forest Meteorology 137, 125-137.

Zhao, X.S., Huang, Y., Jia, Z.J., Liu, H.Z., Song, T., Wand, W.S., Shi, L.Q., Song, C.C., Wang, Y.Y., 2008: Effects of the conversion of marshland to crop- land on water and energy exchanges in northeastern China. Journal of Hydrologie 355, 181–191.

Zhao, P., Lüers, J., 2012: Improved determination of daytime net ecosystem exchange of carbon dioxide at croplands, Biogeosciences Discussions, 9, 2883-2919.

Chapter 2

2. Carbon Dioxide Exchange and its Regulation in the main Agro-ecosystems of Haean Catchment in South Korea

Lindner, Steve[1]; Otieno, Dennis[1]; Lee, Bora[1]; Xue, Wei[1]; Arnhold, Sebastian[2]; Kwon, Hyojung[3]; Huwe, Bernd[4] and Tenhunen, John[1]

(1) Department of Plant Ecology, Universitätsstraße 30, University of Bayreuth, 95447 Bayreuth, Germany.

(2) Department of Ecological Services, University of Bayreuth, ZAPF Buildung 4, Nürnberger Str. 38, 95447 Bayreuth, Germany.

(3) Department of Forest Ecosystems and Society, Oregon State University, 321 Richardson Hall, Corvallis, OR 97331, United States of America.

(4) Department of Soil Physics, Universitätsstraße 30, University of Bayreuth, 95447 Bayreuth, Germany.

2.1. Abstract:

The Asian agricultural landscape, which accounts for approximately 12.6% of the world's agricultural land, is highly heterogeneous due to the multicultural cropping system. Information regarding CO_2 exchange and carbon (C) balance of these agro-ecosystems is scarce, even though they are likely to immensely contribute to the global C budget. Net Ecosystem CO_2 Exchange (NEE) and Ecosystem respiration (R_{eco}) were measured between 2009 and 2010 on 5 dominant crops (potato, rice, radish, cabbage and bean) in the Haean catchment of South Korea, using a closed chamber system to quantify CO_2 fluxes in this agricultural landscape characteristic of the Asian cropping system. Parallel measurements were conducted on leaf area index (LAI), plant biomass and climatic variables, mainly photosynthetic active radiation (PAR), air temperature, soil temperature and soil moisture. Biomass and LAI development differed among the crops likely as a result of differences in light use efficiencies (α) and carbon allocation patterns. The peak total biomass for radish, cabbage, potato, rice and bean were 0.53 ± 0.07, 0.55 ± 0.12, 1.85 ± 0.51, 2.54 ± 0.35 and 1.01 ± 0.26 kg m^{-2}, respectively, while the respective maximum LAI were 2.8, 3.7, 6.4, 6.3 and 6.7 m^2 m^{-2}. Variations in seasonal patterns, magnitudes and the timing of maximum NEE and gross primary production (GPP) among the crops were likely the result of differences in LAI and α. The lowest peak R_{eco} rate was 3.8 ± 0.5 μmol m^{-2} s^{-1}, measured on rice paddies while the highest was 34.4 ± 4.3 μmol m^{-2} s^{-1} measured on the cabbage fields. The maximum NEE rates were -29.4 ± 0.4 and -38.7 ± 6.6 μmol m^{-2} s^{-1}, measured in potato and cabbage fields, respectively. Peak GPP rates in potato and cabbage fields were 39.5 ± 0.6 and 63.0 ± 7.2 μmol m^{-2} s^{-1}, respectively. PAR explained more than 90 % of the diurnal variations in GPP, while LAI and α determined the seasonal trends of maximum GPP. The timing of maximum CO_2 assimilation (GPP_{Max}) differed among the crops, thus even though maximum CO_2 uptake in the respective crops only lasted a couple of weeks, the effect of

staggered peak GPP resulted in extended period of high CO_2 uptake. These differences among crops were significant, hence modeling approaches need to consider the heterogeneity in ecosystem CO_2 exchange associated with these multicultural agriculture landscapes.

2.2. Introduction

There is a general consensus regarding the contribution of natural ecosystems such as forests, wetlands, grasslands, savannas and the tundra to the global carbon (C) budget. However, agro-ecosystems, particularly croplands which currently constitute 12.6% of the total land area (FAO, 2014) have been less regarded (Gilmanov et al., 2010; Smith et al., 2010). Due to their small spatial coverage, croplands were for a long time considered moderate contributors to the global atmospheric C pool (Smith and Falloon, 2005), but this is changing owing to the ongoing massive conversion of natural ecosystems such as forests and grasslands into croplands, increasing their spatial coverage globally (Desjardins et al., 2007; Corbin et al., 2010). Crop production is seasonal nature hence as a result of their expansion, they are likely to play an increasingly important role as drivers of annual and inter-annual fluctuations in the global atmospheric CO_2 concentrations (Moreaux et al., 2008).

Our current knowledge on CO_2 fluxes and annual C budgets of croplands originate from measurements conducted on extensive monocultural agricultural landscapes such as maize and soybean rotations in North America (Hollinger et al., 2005; Pattey et al., 2002; Suyker et al., 2004, 2005; Hernandez-Ramirez et al., 2011); corn, soybean, wheat (Falge et al., 2002a; Corbin et al., 2010); maize, winter wheat and barley (Sus et al., 2010; Jans et al., 2010) in central and northern Europe. Similar data are available for sugar beet (Moureaux et al., 2006; Aubinet et al. 2009), winter wheat (Hoyaux et al., 2008; Moreaux et al., 2008; Dufranne et al., 2011; Schmidt et al., 2012), potato (Aubinet et al., 2009) and triticale (Béziat et al., 2009) from other parts of Europe. Results from long-term measurements of net ecosystem CO_2 exchange (NEE) in 17 flux sites in Europe for 45 cropping periods were summarized by Moors et al. (2010). Soegaard et al. (2003) reported CO_2 fluxes over a mixed agricultural landscape in western Denmark planted with winter wheat, winter barley, spring barley, maize and grass. In Asia, Lei and Yang (2010), Qun and Huizhi (2013) reported annual CO_2 fluxes

and C storage for winter wheat and summer maize rotation fields representative of the main cropping system in the North China plains. Data on rice field CO_2 fluxes are available from North America (Campbell et al., 2001), Korea (Moon et al., 2003), Japan (Saito et al., 2005), and China (Ren et al., 2011).

In Asia, most of the agricultural landscape is characterized by multicultural cropping systems comprising relatively small (1 to 2 hectares) land holdings (Pookpakdi, 1996). Although smaller than the world average holding range of 3.7 hectares, combined, these farms contribute around 20% of the world's agricultural land and must play a critical role in the global C budget. Fragmentation of the landscape through multicultural cropping is also likely to induce strong fluctuations in C fluxes through varied timing and growing lengths of different crop types and might be contributing to the oscillations observed in the atmospheric CO_2 concentration during the year. In a multicultural landscape, quantifying CO_2 fluxes and C budgeting for the respective ecosystem patches (small farms) is a major challenge. Also, linking CO_2 fluxes at landscape scales to the agricultural yields is difficult, especially when the production phases of the crops are overlapping.

Quantification of CO_2 exchange between ecosystems and the atmosphere have been achieved with the two widely accepted measurement techniques, namely the chamber (CT) and the eddy covariance (EC) techniques (Aubinet et al., 2000; Pavelka et al., 2007; Wohlfahrt et al., 2005). While the EC technique applies best in open habitats (from hundreds of m^{-2} to km^{-2}) where fluxes are related to clearly defined vegetation types (footprint), the use of portable chambers allows direct evaluation of NEE, ecosystem respiration (R_{eco}) and gross primary productivity (GPP) at small spatial scales (plot level), making it possible to key out functional differences within a heterogeneous landscape like mixed farming systems in the Asian agricultural landscape. In this study, we focused on CO_2 exchange on fields of major crops

grown in the heterogeneous agricultural landscape of the Haean-myun catchment to: (1) determine the seasonal patterns and magnitudes of CO_2 exchange and productivity of five main crop types, (2) identify factors that regulate CO_2 fluxes and biomass production and the intensity of regulation among different crops in the fragmented agricultural landscape in the Haean catchment. We hypothesized that in a multicultural agricultural system, differences in the timing and magnitudes of GPP and R_{eco} among crops lead to a high spatial variability of CO_2 exchange.

2.3. Materials and Methods

2.3.1. Study site

The study was conducted in the Haean Basin (128° 5' to 128° 11' E, 38° 13' to 38° 20' N), Yanggu County in Gangwon Province, South Korea. The elevation of the area (in total 62.7 km^2) ranged from 340 m at the bottom of the catchment to 1320 m at the ridges, with an average slope of 28.4%. The climate of the "punchbowl" shaped basin is temperate, with a mean annual air temperature of 10.5°C in the valley bottom and ca. 7.5°C on the northern ridge. The annual precipitation during the last 12 years ranges between 930 and 2299 mm/yr, 50% of which fall during the summer monsoon between June and July. The rock bed is Precambrian Gneiss at the higher elevations, with Jurassic biotite granite intrusion that was subsequently eroded and deposited in the catchment bottom (Kwon et al., 1990). Due to the long-term addition of sandy soil on the top layer of the agricultural fields by farmers, the soil is mainly artificial and characterized as Anthrosols (FAO, 2006). The texture of the top layers (0 – 30 cm) for the dryland field sites is either sandy loam or loamy sand, with a bulk density (BD) of 1.23 g cm^{-3}, pH 5.8, soil organic matter (SOM) of 10.7 g kg^{-1}, cationic exchange capacity (CEC) of 10.3 cmol$_c$ kg^{-1}, total nitrogen content (N$_{tot}$) of 0.61 g kg^{-1}, total organic carbon content (C$_{tot}$) of 6.04 g kg^{-1}, mineralized nitrogen (N$_{min}$) before fertilization averaged for the experimental sites is 93 kg NO$_3$ ha^{-1} and 98 kg NH$_4$ ha^{-1} (Kettering et al., 2012). Averaged for rice paddies, BD is 1.14 g cm^{-3}, pH 6.2, SOM of 17.2 g kg^{-1}, CEC of 12.2 cmol$_c$ kg^{-1}, N$_{tot}$ of 0.81 g kg^{-1}, C$_{tot}$ of 8.72 g kg^{-1}, N$_{min}$ before fertilization is 9.96 kg NO$_3$ ha^{-1} and 98 kg NH$_4$ ha^{-1} (Kettering et al., 2012).

The cultivated land is grown with paddy rice (ca. 30% of the area under crop), and dryland crops (radish – 24%, beans – 13%, potato – 10% and cabbage – 5%) (Yanggu County Office, 2010).

2.3.2. Description of the experimental plots

The experimental sites (see Figure 8) comprised rain-fed crop fields of radish (*Raphanus sativus*), potato (*Solanum tuberosum* L.), white cabbage (*Brassica oleracea* var. *capitata*) and soybean (*Glycine max* (L.) Merr.) and irrigated rice (*Oryza sativa*). For each crop, we selected 3 representative, approx. 0.1 ha of the fields. Tillage, fertilization of the fields, planting/harvesting dates and paddy irrigation program were done according to the local management practices/program (see Kim et al., 2008; Kettering et al., 2012). Weed and pests were controlled by herbicides and pesticides, respectively. Basal fertilizer application was done 7 – 10 days before planting. Planting/transplanting information is summarized in Table 1.

Table 1: Planting and harvesting dates of the respective crops during 2009 and 2010. Data are expressed in day of year (DOY).

	Year	Crop				
		Rice	*Radish*	*Potato*	*Cabbage*	*Bean*
Planting date	2009	140	152	110	140	125
Harvest date		289	253	247	198	258
Planting date	2010	144	161	116		
Harvest date		290	243	273		
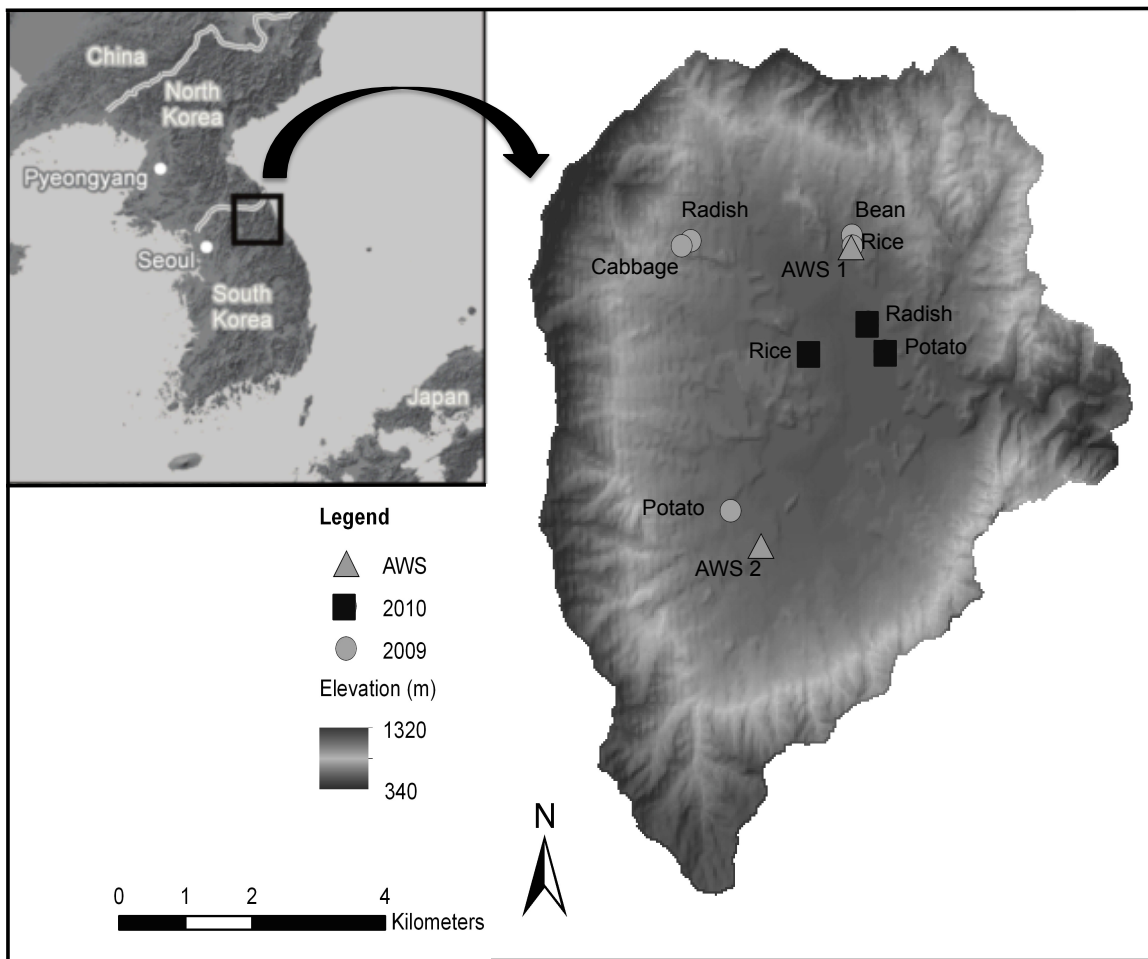
Figure 8: Location of the Haean-myeon catchment on the Korean peninsula with the experimental sites where our measurements were conducted during 2009 (circles) and 2010 (squares). Locations of the Automatic weather stations are indicated with triangles.

2.3.3. Measurements

2.3.3.1 Microclimate

Between 2009 and 2010, air temperature, humidity, precipitation and global radiation were continuously measured with 2 m high automatic weather stations (AWS, WS-GP1, Delta-T Devices Ltd., UK). Data were taken every 5 minutes, averaged and logged half-hourly. Additional discontinuous records of photosynthetic photon flux density (PPFD, LI−190, LI−COR, USA) within the transparent CO_2 measurement chamber (approx. 50 cm above ground surface), air temperature (T_{air}) at 20 cm height inside and outside the CO_2 chamber (Digital thermometer, Conrad, Hirschau, Germany) and soil temperature (T_{soil}) at 10 cm soil

depth (Soil thermometer, Conrad, Hirschau, Germany) within the soil frames were taken during the CO_2 flux measurements. Data were recorded every 15 s alongside CO_2 fluxes. This allowed closer monitoring of the microclimate, in order to relate the CO_2 fluxes to the actual conditions within the chambers during measurements.

2.3.3.2 Ecosystem CO_2 flux measurements

On each field per crop, four soil frames (collars) enclosing healthy, representative crops (crop plots) and two frames without vegetation (soil plots) were established 4-5 days before the commencement of CO_2 flux measurements. Collars on soil plots were installed one month before planting and also removed 2 weeks after harvesting. Each collar enclosed an area measuring 38 cm by 38 cm. The collars provided a 2 cm wide base for CO_2 measurement chambers. Most CO_2 flux measurements were performed on sunny days, when peak (midday) light intensities reached ~ 1500 µmol m^{-2} s^{-1} (Table 2). The measurements were adapted to the management regimes in Haean and were not conducted within two days after fertilization, irrigation or pesticide/herbicide application. After flux measurements, all the soil frames were replaced on to new locations for the next round of measurements. Measurements were carried out between 10-14 h (4 cycles per day), at least once a month between June and October 2009, while the measurements in 2010 were conducted between 9-18 h (8 cycles per day).

Table 2: Day of Year (DOY) when CO$_2$ chamber measurements were conducted on the respective plots in 2009 and 2010. Measurements before planting or after harvest are enclosed in brackets.

Year	Crop				
	Rice	*Radish*	*Potato*	*Cabbage*	*Bean*
2009	147	(153)	(134)	(139)	169
	155	163	138	148	179
	156	176	159	162	202
	164	196	174	177	235
	175	213	189	197	
	203	253	220		
	260				
2010	181	205	152		
	208	227	157		
	232	243	174		
	261	(280)	186		
			210		
			(280)		

NEE and R$_{eco}$ were sequentially observed with a systematic rotation over all plots using manually operated closed CO$_2$ measurement chambers (Li et al., 2008; Otieno et al., 2012). The 40 x 40 x 54 cm^3 chambers of our system were constructed of transparent Plexiglas (3 mm XT type 20070; light transmission 95%). Dark chambers for measuring R$_{eco}$ were constructed of opaque PVC, covered with opaque insulation, with reflective aluminum surface on the outside. Using extension bases, chamber height was adjusted to the canopy height. Chambers were placed on the plastic frames that were inserted 7 cm into the ground. They were sealed to the collars with a flexible rubber gasket and then firmly secured using elastic bands fastened onto the ground from two sides. Increased air pressure in the chamber was avoided by a 12 mm opening at the top of the chamber, which was closed after the chamber had been firmly secured on the base collar and before any records were taken. Circulation of air within the chamber was provided by three fans yielding a wind speed of 1.5 m s^{-1}. Change in chamber CO$_2$ concentration over time was assessed with a portable, battery operated infrared gas analyzer (LI–820, LI–COR, USA).

Once steady state was attained, data were logged every 15 sec for 2 min. In all cases data were recorded within 3–5 min of placing the chamber onto the collars. CO_2 fluxes were calculated from a linear regression describing the time dependent change in CO_2 concentration within the chamber. Influence of the CO_2 concentration change on plant physiological response was ignored. By mounting dry ice packs inside and at the back of the chamber in the airflow, temperature during measurements could be maintained within 1°C relative to ambient. GPP was calculated from R_{eco} and NEE according to Equation 5:

$$GPP = -NEE + R_{eco}$$ **Equation 5**

At the end of each day of CO_2 flux measurement, the soil frames, except those established on the bare soil plots (no vegetation) were replaced onto new locations for the next round of measurements.

2.3.3.3 Above- and belowground biomass sampling

After CO_2 flux measurements, all the aboveground plant material within the 38 x 38 cm area enclosed by the collars was excised to ground level. The aboveground biomass was sorted into leaves, stems and dead material. After sorting, the respective leaf areas (LA) were determined with leaf area meter (LI−3000A, LI−COR, USA). Using an 8 cm diameter soil corer, soil cores were obtained from the middle of the collar, after aboveground biomass harvest, down to 30 cm. The cores were divided in 0-10, 10-20 and 20-30 cm each, washed under running tap water, before oven-drying the sieved (2 mm mesh size) belowground biomass. All the biomass was oven dried to a constant weight at 85°C for at least 48 hours. Leaf area index (LAI) was determined from total LA within the 38 cm by 38 cm soil collars and then expressed per unit square meter for the respective crop fields.

2.3.3.4 Soil water content

Volumetric Water Content (VWC) within the collars was determined through gravimetric method. Within each plot, two sets of soil cores were obtained with a 3 cm-diameter soil corer down to 30 cm. Each sample was immediately weighed to determine the fresh. Samples were later oven dried at 105°C to a constant weight before determining their dry weights. Gravimetric soil moisture content was determined as the relative change in weight between fresh and dry weights. In 2010, additional VWC at -10 and -30 cm depth, within each collar was measured using EC–5 soil moisture sensors (Decagon, WA, USA). The soil moisture sensors were installed at least two weeks before and replaced to new plots after CO_2 flux measurements.

2.3.3.5 Empirical description of canopy responses

Empirical description of the measured NEE and GPP was performed with a non-linear least squares fit of the data to a hyperbolic light response model, also known as the Michaelis-Menten or rectangular hyperbola model (Owen et al., 2007)

$$NEE = -\frac{\alpha * \beta * PAR}{\alpha * PAR + \beta} + \gamma$$

Equation 6

where α is the initial slope of the curve and an approximation of the canopy light utilization efficiency (CO_2/ photon), β is the maximum NEE of the canopy (μmol CO_2 m^{-2} s^{-1}), PAR is photosynthetic photon flux density (μmol photon m^{-2} s^{-1}), γ is an estimate of the average ecosystem respiration occurring during the observation period (μmol CO_2 m^{-2} s^{-1}). Since the rectangular hyperbola may saturate very slowly in terms of light, we used the value calculated from $\alpha\beta$*PAR/(α*PAR+β) for high light intensity levels (PAR = 1500 μmol photons m^{-2} s^{-1}) in this study. This value approximates the potential maximum GPP and can be thought of as

the average maximum canopy uptake capacity during each observation period (noted here as $(\beta+\gamma)_{1500}$). The parameters $(\beta+\gamma)_{1500}$ (e.g. NEE at PAR = 1500 μmol m^{-2} s^{-1}) and γ were estimated for each day using NEE data from the four measurement plots per day.

Statistical analysis and best fits for light and temperature response curves were performed using Sigma Plot version 11.0.

Analysis of short-term temperature sensitivity of R_{eco} was made for the daytime R_{eco} using the Lloyd & Taylor respiration equation (Lloyd and Taylor, 1994; their Eq. (11)).

$$\mathbf{R_{eco} = R_{ecoRef,283}}\mathit{exp}^{(E_0(1/(283.15-T_0))-(1/(T_K-T_0)))} \qquad \textbf{Equation 7}$$

where T_K is soil temperature (in K), E_0 is a parameter describing R_{eco} sensitivity to temperature, T_0 is a temperature scale parameter (kept constant at $T_0 = -46.02°C$) and $R_{ecoRef,283}$ (μmol CO_2 m^{-2} s^{-1}) is the ecosystem respiration rate at reference temperature (283.15K = 10°C).

2.4. Results

2.4.1. Microclimate

Weather conditions during 2009 and 2010 are summarized in Figure 9. In both years, daily maximum solar radiation approached the annual maximum of 28 ± 2 MJ m^{-2} d^{-1} in June and then declined gradually to low values of approximately 17 MJ m^{-2} d^{-1} by mid September (Figure 9A & B, PAR measured within the chamber is shown as discrete points). Air temperature increased steadily from spring, reaching maximum values of 25°C in August (Figure 9C & D). The amount of rainfall received between May and October was 1300 mm in 2009 and 1283 mm in 2010 (Figure 9E & F). Intensive rainfall occurred during the summer monsoon, from late June to July 2009 and 2010. In 2010, the month of September also received large amounts of rainfall. VWC in the dryland crop fields ranged between 15.8 and 30.2% (Figure 9E & F). For rice paddies the plots remained saturated (VWC = 40 – 45.1%) throughout the growing period. The mean daily vapour deficit (VPD) during the vegetation period was around 0.67 ± 0.35 kPa, the highest values occurring in May for both years (Figure 9G & H).
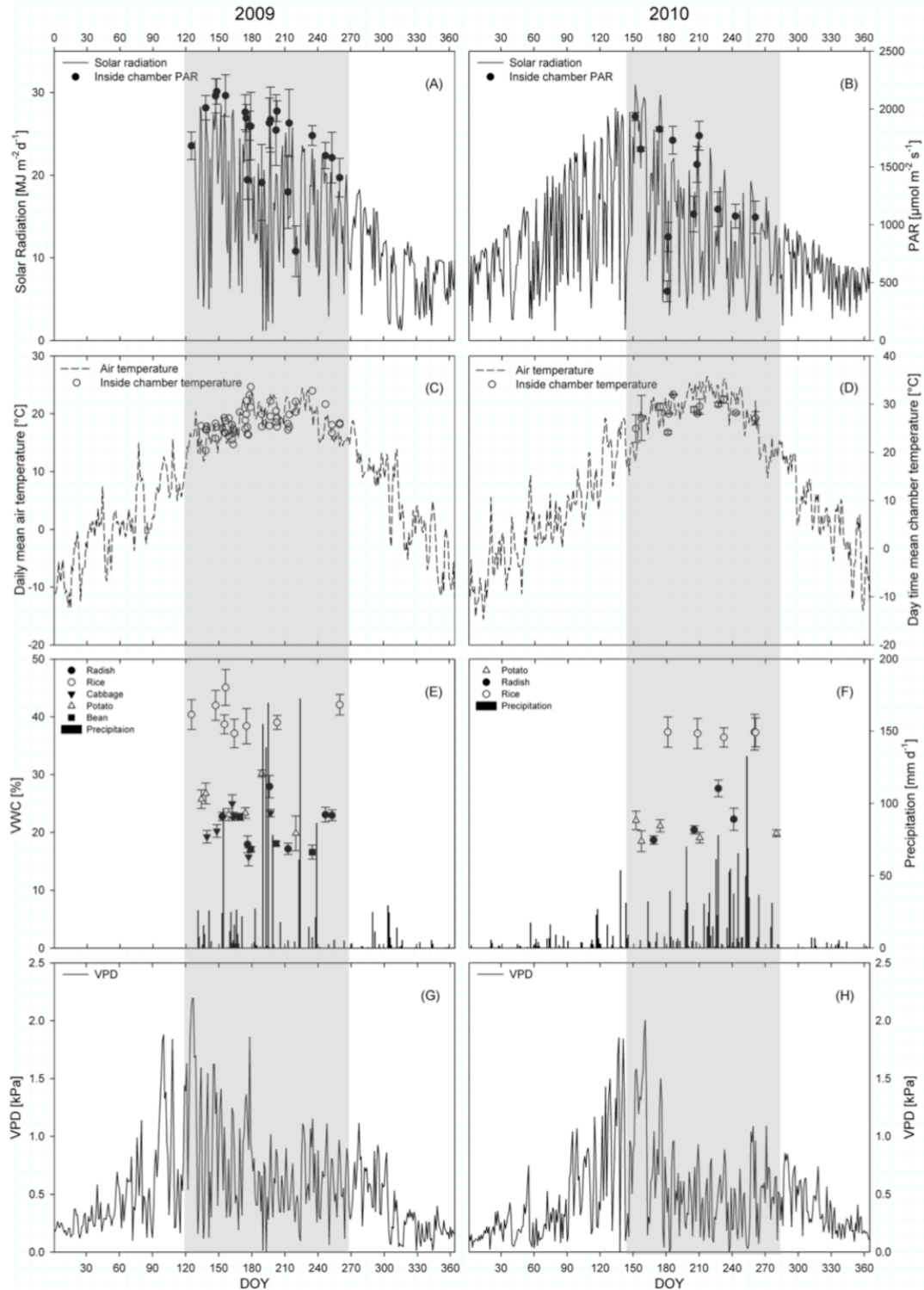
Figure 9: Daily solar radiation measured at 2 m height outside and photosynthetic active radiation (PAR) measured at 50 cm height above the vegetation inside the CO₂ flux chambers during 2009 (A) and 2010 (B). Mean air temperature at 2 m height outside and at 20 cm height inside the CO₂ flux chambers in 2009 (C) and 2010 (D). Volumetric water content (VWC) within 30 cm soil profile and daily precipitation during 2009 (E) and 2010 (F), and mean daily vapor pressure deficit (VPD) in 2009 (G) and 2010 (H). Solar radiation, ambient air temperature and precipitation were measured from a weather station installed in open locations within the study site. Grey shaded area visualizes the period of the measurement campaigns.

2.4.2. Biomass and leaf area development

The maximum leaf biomass in 2009 for radish, cabbage, potato, rice and bean were 0.07 ± 0.01, 0.27 ± 0.05, 0.10 ± 0.03, 0.27 ± 0.05 and 0.35 ± 0.06 kg m^{-2}, respectively, occurring between 49 and 110 days after planting (DAP) (Table 3A). The maximum LAI in 2009 for the respective crops were 2.1, 3.7, 5.0, 6.3, and 6.7 m^2 m^{-2} (Figure 10A & C). In 2009 the total biomass (above plus belowground biomass) for radish, cabbage, potato, rice and bean were 0.48 ± 0.11, 0.55 ± 0.12, 1.44 ± 0.22, 2.54 ± 0.35 and 1.01 ± 0.26 kg m^{-2}, respectively. In 2010, the respective peak leaf biomasses for radish, potato and rice were 0.14 ± 0.02, 0.19 ± 0.00, 0.33 ± 0.04 kg m^{-2}, while their respective total biomasses were 0.53 ± 0.07, 1.85 ± 0.51 and 2.43 ± 0.24 kg m^{-2} (Figure 10B). The maximum LAI in 2010 for the respective crops were 2.8, 6.4 and 5.4 m^2 m^{-2} (Figure 10B/D). Differences in magnitudes and the time when peak values were attained varied among crops and between the years. We compared above- and belowground biomass to the total biomass accumulated, in order to characterize the biomass distribution patterns. For radish, the ratio of biomass allocated to the belowground increased steadily during the development of the plant such that at maturity, almost 73% of total biomass was from belowground. Similar allocation pattern was observed in potato, with 83% of total biomass at maturity coming from belowground tissues. Cabbage had the lowest proportion of biomass allocated belowground, with only 4% of total biomass contributed by roots, at maturity. Both rice and beans showed relatively high biomass allocated to belowground organs (85 and 31%, respectively) during the early stages of growth, but this declined over the season. At the time of maturity, the respective allocations to the roots were only 21 and 7% of the total biomass. Similar patterns of allocation were observed in 2010.
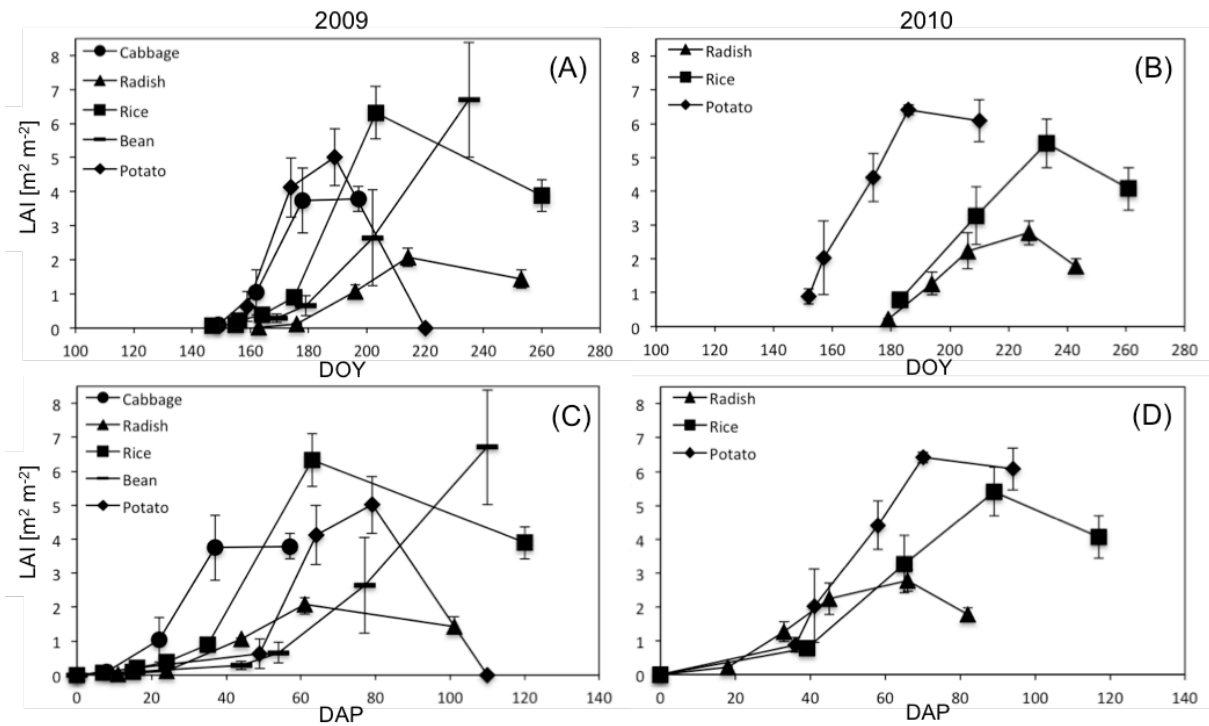
Figure 10: Leaf area index (LAI) development of cabbage, radish, rice, bean and potato. The development of LAI are expressed in day of year (DOY) in 2009 (A) and 2010 (B) and day after planting (DAP) in 2009 (C) and 2010 (D).

Table 3: Dry weight [kg/m^2] of leaves, stems, root, grains and tuber during crop development in 2009 and 2010. Harvest was done after the CO$_2$ plot measurements. DOY is day of year, DAP is days after planting, SD is standard deviation, and BG/Total is the percentage of belowground biomass to total dry weight.

Year	Crop	DOY	DAP	Leaves	SD	Stems	SD	Root	SD	Grains	SD	Tuber	SD	Total	SD	BG/Total [%]
2009	Radish	153	1	<0.01	0	<0.01	0	<0.01	0					<0.01	0	1.7
		163	11	<0.01	0	<0.01	0	<0.01	0					<0.01	0	5.7
		176	24	0.01	0	<0.01	0	<0.01	0					0.01	0	5.3
		196	44	0.04	0	0.02	0	0.03	0					0.08	0.01	34.4
		213	61	0.07	0.01	0.06	0.01	0.24	0.03					0.37	0.05	64.2
		253	101	0.06	0.01	0.07	0.02	0.35	0.07					0.48	0.11	72.9
	Cabbage	148	8	<0.01	0	<0.01	0	<0.01	0					0.01	0	14.8
		162	22	0.04	0.02	0.02	0.01	<0.01	0					0.06	0.04	4.4
		177	37	0.16	0.05	0.11	0.04	0.01	0.01					0.28	0.09	4.5
		197	57	0.27	0.05	0.26	0.06	0.02	0.01					0.55	0.12	3.6
	Potato	138	28	<0.01	0	<0.01	0	<0.01	0			0	0	<0.01	0	-
		159	49	0.10	0.03	0.05	0.02	0.03	0.02			0.09	0.04	0.27	0.09	46.5
		174	64	0.08	0.06	0.07	0.07	0.02	0.01			0.32	0.21	0.49	0.35	68.7
		189	79	0.09	0.03	0.04	0.02	0.03	0.01			0.62	0.19	0.78	0.25	83.3
		220	110									1.44	0.22	1.44	0.22	-
	Rice	147	7	<0.01	0	<0.01	0	0.02	0					0.02	0.01	65.8
		155	15	<0.01	0	<0.01	0	0.03	0.03					0.03	0.03	85.3
		156	16	0.01	0	<0.01	0	0.01	0.01					0.02	0.01	42.8
		164	24	0.02	0	0.01	0.01	0.03	0					0.06	0.02	48.6
		175	35	0.05	0.01	0.01	0.01	0.16	0.11					0.23	0.13	71.1
		203	63	0.27	0.05	0.37	0.12	1.17	0.54					1.81	0.7	64.7
		260	120	0.25	0.02	0.84	0.15	0.54	0.08	0.91	0.1			2.54	0.35	21.2
	Bean	169	44	0.01	0.01	0.01	0	0.01	0					0.03	0.01	31.4
		179	54	0.03	0.01	0.02	0.01	0.01	0					0.05	0.02	19.4
		202	77	0.11	0.06	0.12	0.07	0.03	0.01					0.26	0.14	12.3
		235	110	0.35	0.06	0.49	0.14	0.07	0.02	0.1	0.03			1.01	0.26	7.2
2010	Radish	205	44	0.12	0.01	0.06	0.01	0.13	0.01					0.32	0.03	40.8
		227	66	0.14	0.02	0.08	0.01	0.32	0.04					0.53	0.07	59.8
		243	82	0.08	0.01	0.06	0.01	0.38	0.01					0.5	0.04	36.6
	Potato	152	36	0.05	0.01	0.02	0	0.01	0					0.08	0.02	12.5
		157	41	0.09	0.04	0.06	0.04	0.01	0			0.02	0	0.18	0.08	17.7
		174	58	0.14	0.02	0.13	0.04	0.02	0			0.38	0.01	0.67	0.07	59.4
		186	70	0.19	0	0.18	0.03	0.02	0			0.86	0.06	1.25	0.1	70.4
		210	94	0.18	0.02	0.26	0.03	0.02	0			1.38	0.45	1.85	0.51	76.2
	Rice	181	37	0.04	0.01	0.03	0.01	0.02	0.01					0.09	0.02	23.3
		208	64	0.19	0.03	0.35	0.07	0.11	0.04					0.65	0.14	17.0
		232	88	0.33	0.04	1.13	0.11	0.23	0.05	0.49	0.07			2.17	0.27	10.8
		261	117	0.24	0.04	0.9	0.06	0.21	0.06	1.08	0.08			2.43	0.24	8.5

2.4.3. Diurnal and seasonal patterns of ecosystem CO_2 exchange

Daily courses of R_{eco} for three selected days in 2009 and 2010, representing phenological (early development, full maturity and senescence) stages, when measurements were conducted, are shown in Figure 11. Fluctuations in R_{eco} were minor during the day, with small differences observed among the fields. Daily R_{eco} patterns varied significantly during the season, increasing during crop development and decreasing after crop maturity (Figure 11). Seasonal differences were largest in the cabbage and potato fields (Figure 12A & G). The maximum R_{eco} measured in the cabbage fields was 34.4 ± 4.3 μmol m^{-2} s^{-1} at the end of June 2009 (DOY 177, Figure 12G), while the peak value in the potato fields was 16.6 ± 0.2 μmol m^{-2} s^{-1} at the beginning of July (DOY 186 in 2010). Maximum R_{eco} in the radish and bean fields were 20.2 ± 5.3 μmol m^{-2} s^{-1} and 12.1 ± 0.4 μmol m^{-2} s^{-1}, occurring in late July and early August, respectively (see Figure 12E & H). The maximum R_{eco} in the rice paddies was 3.8 ± 0.5 μmol m^{-2} s^{-1} around DOY 175 in 2009 and 7.4 ± 0.7 μmol m^{-2} s^{-1} around DOY 232 in 2010. The patterns and peak rates were repetitive during the two years.

GPP increased from near-zero values at the beginning of the growth period to peak values between $20.0 - 63.0$ μmol m^{-2} s^{-1} at maturity. Differences among crops were significant and peak GPP rates occurred at different times of the year. The maximum GPP in the cabbage and potato fields were 63.0 ± 7.2 and 39.5 ± 0.6 μmol m^{-2} s^{-1}, occurring in early July and June, respectively. Peak GPP for radish, bean and rice were 32.5 ± 3.1, 27.3 ± 2.5 and 21.8 ± 3.7 μmol m^{-2} s^{-1} observed around DOY 202, 214 and 208, respectively. GPP declined after crop maturity due to leaf senescence. The timing and the magnitude of peak GPP of rice, radish and potato were similar in the two years.

For most crops, the largest NEE amplitude on a day coincided with the peak LAI during the year but the timing varied among crops. The highest NEE during clear days occurred between 10h − 14h (Figure 11, negative NEE indicate net CO_2 uptake from, while positive values

indicate net CO_2 release back into the atmosphere by the ecosystem). Diurnal courses of NEE during three phenological (early development, full maturity, senescence) stages are summarized in Figure 11. Differences in peak NEE on any day between and among plots were correlated with biomass or LAI differences. The maximum NEE measured for potato and cabbage during 2009 were -29.4 ± 0.4 and -38.7 ± 6.6 µmol m^{-2} s^{-1}, recorded around DOY 159 and 162, respectively. Peak NEE for radish, bean and rice were -19.9 ± 3.1, -18.5 ± 2.2 and -15.4 ± 2.2 µmol m^{-2} s^{-1}, respectively, occurring between mid and end of July 2009. The corresponding maximum NEE in 2010 were -17.8 ± 3.4, -20.0 ± 3.1 and -21.0 ± 4.2 µmol m^{-2} s^{-1} for rice, potato and radish, respectively, occurring in July. After crop maturity, NEE declined to near-zero values.
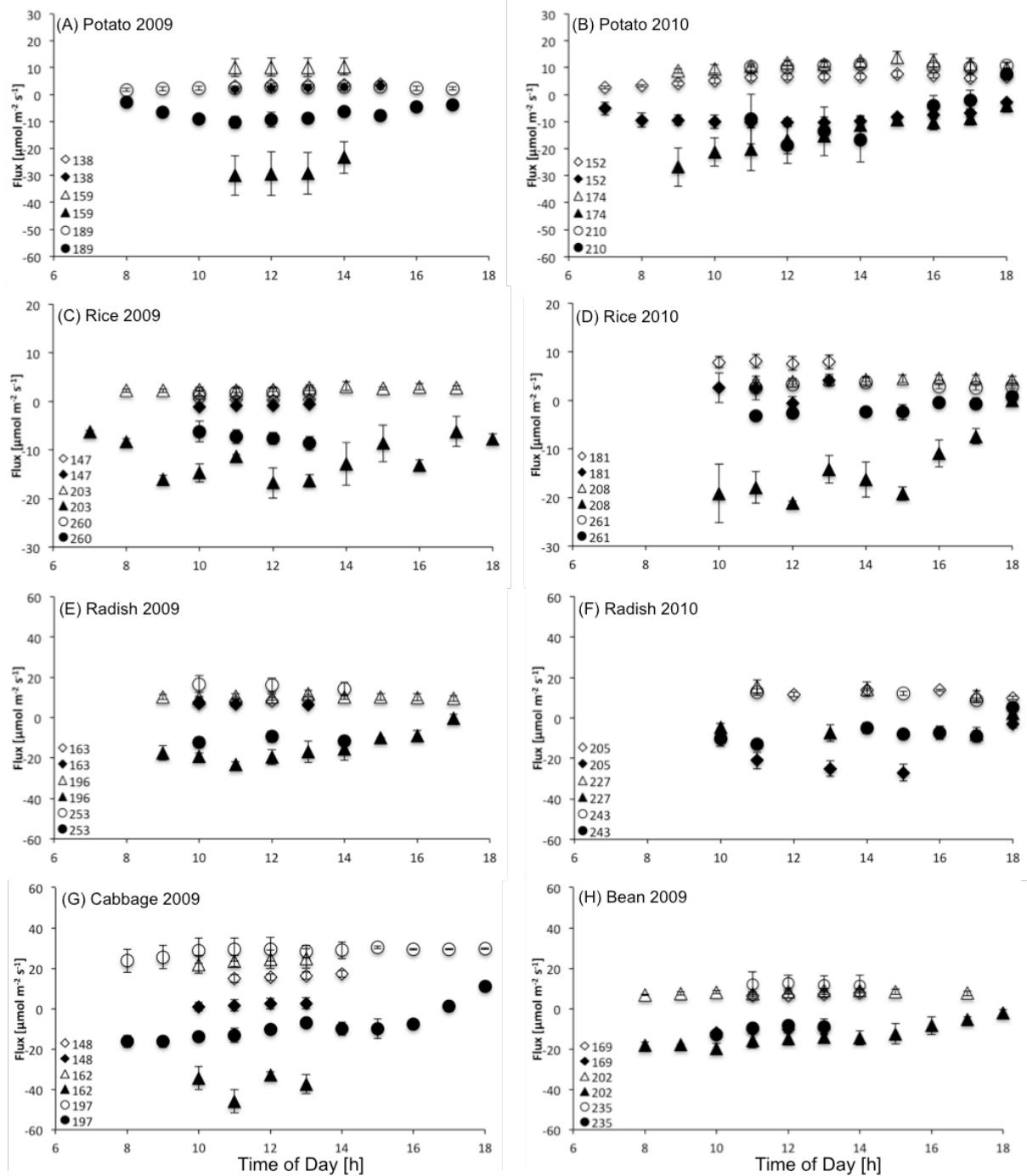
Figure 11: Daily trends of net ecosystem CO$_2$ exchange (NEE, closed symbols) and ecosystem respiration (R$_{eco}$, open symbols) of potato, rice, radish, cabbage, and bean. Data points are means of respective fluxes measured on the four collar plots. None-uniformity of the Y-axes is due to different ranges of NEE magnitudes.
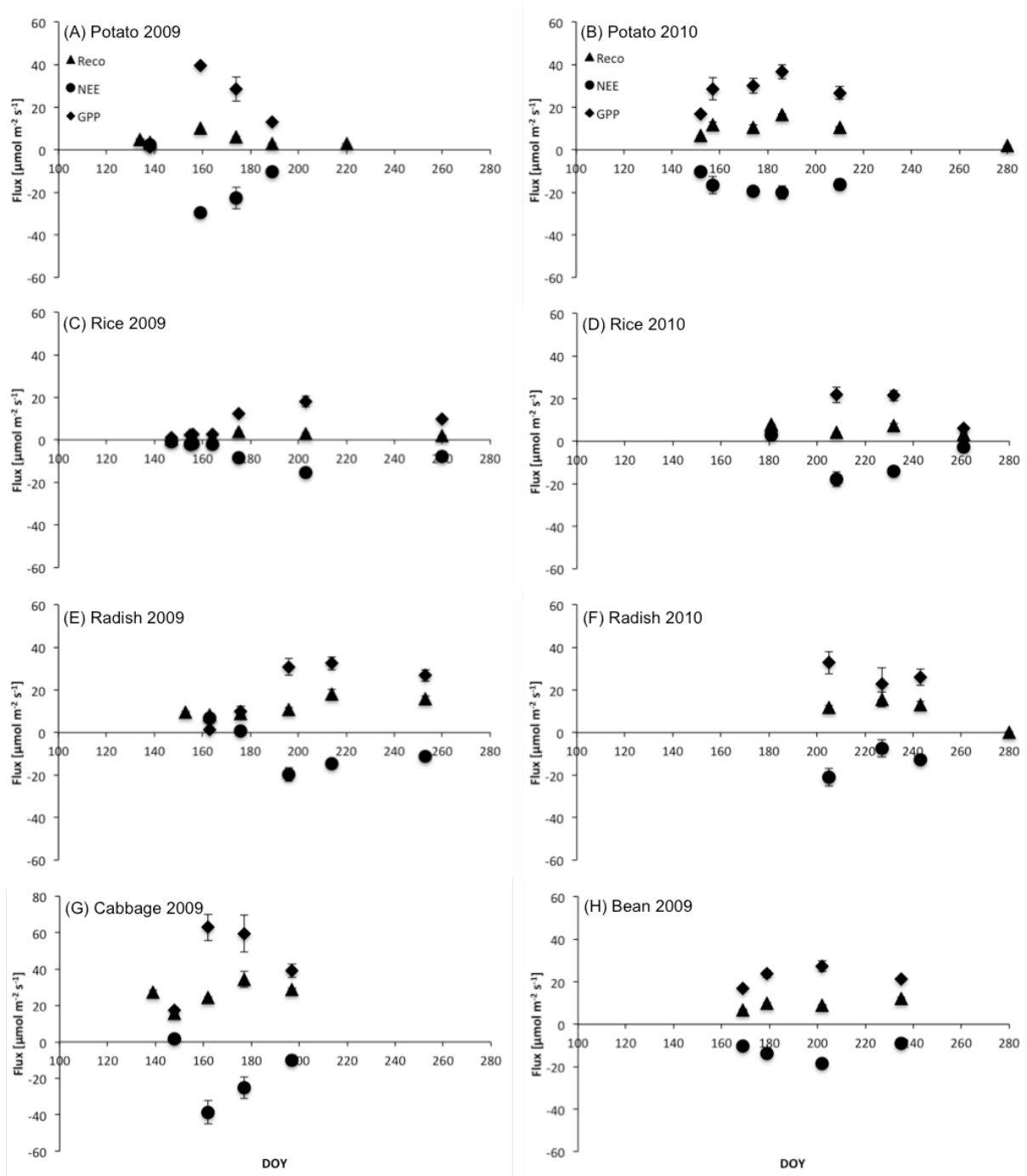
Figure 12: Seasonal trends of net ecosystem CO$_2$ exchange (NEE, circle), ecosystem respiration (R$_{eco}$, triangle), and gross primary production (GPP, diamond) of potato, rice, radish, cabbage, and bean in 2009 and 2010.

2.4.4. Parameterization of ecosystem CO_2 exchange

Physiological parameters derived from the hyperbolic light response model (Equation 6) are shown in Table 4. In all cases, the R^2 values for the respective model fits ranged between 0.91 and 0.99 (Table 4). α, β, $(\beta+\gamma)_{1500}$, and γ varied significantly during the season and also among the crops. The maximum γ values in 2009 were 2.6, 4.9, 10.3, 28.0 and 7.9 $\mu mol\ m^{-2}\ s^{-1}$ in rice, potato, radish, cabbage and bean, while the respective $(\beta+\gamma)_{1500}$ in 2009 were 17.2, 23.0, 32.2, 38.8 and 24.3 $\mu mol\ m^{-2}\ s^{-1}$. In 2010, peak $(\beta+\gamma)_{1500}$ was 33.6 $\mu mol\ m^{-2}\ s^{-1}$ in potato, 23.6 $\mu mol\ m^{-2}\ s^{-1}$ in rice and 40.1 $\mu mol\ m^{-2}\ s^{-1}$ in radish. These values were close to the actual GPP determined directly from measurements (y = 0.944x, $R^2 = 0.84$). Differences among the crops and also during the season were significant. Light use efficiency (α) increased between May and July, associated with the period of crop development, increasing LAI, air temperature and PAR. The maximum α values were different among crops and were attained at different times. This was also the case with β. After full crop maturity, there was a decline in α and β.

Table 4: Parameters and quality of the empirical light-response model in 2009 and 2010 for single day measurements of NEE and R_{eco}. Shown are mean values, standard error for each parameter, and mean R^2. α is the initial slope of the light-response curve and an approximation of the canopy light utilization efficiency ($\mu mol\ m^{-2}\ s^{-1}$), β is the maximum CO_2 uptake rate of the canopy ($\mu mol\ m^{-2}\ s^{-1}$), γ is the average daytime ecosystem respiration ($\mu mol\ m^{-2}\ s^{-1}$) and $(\beta+\gamma)_{1500}$ is the potential maximum GPP at maximum radiation intensities.

Year	DOY	DAP	Crop	γ	S. E.	α	S. E.	β	S. E.	R^2	$(\beta+\gamma)_{1500}$
2009	189	79	Potato	4.87	0.27	-0.08	0.01	-28.43	1.28	0.97	23.03
	196	44	Radish	10.27	0.32	-0.11	0.01	-40.21	1.37	0.98	32.23
	197	57	Cabbage	27.98	0.66	-0.17	0.04	-45.91	2.23	0.97	38.83
	202	77	Bean	7.85	0.47	-0.11	0.02	-28.67	1.25	0.95	24.30
	203	63	Rice	2.64	0.19	-0.06	0.00	-21.50	0.67	0.98	17.16
2010	152	36	Potato	5.77	0.27	-0.05	0.01	-18.66	1.06	0.95	14.82
	157	41	Potato	11.49	0.45	-0.08	0.01	-34.74	1.80	0.97	26.64
	174	58	Potato	11.23	0.37	-0.11	0.01	-28.04	1.08	0.96	24.00
	186	70	Potato	15.13	0.71	-0.10	0.01	-43.84	2.16	0.97	33.59
	210	94	Potato	10.82	0.63	-0.03	0.00	-40.27	6.68	0.91	20.81
	181	37	Rice	8.42	0.50	-0.03	0.01	-11.89	2.09	0.92	9.48
	208	64	Rice	4.31	0.21	-0.07	0.01	-30.37	1.25	0.99	23.63
	232	88	Rice	6.85	0.28	-0.06	0.00	-27.93	1.05	0.97	20.87
	261	117	Rice	3.02	0.12	-0.02	0.00	-5.34	0.53	0.95	4.49
	205	44	Radish	12.42	0.55	-0.13	0.02	-50.24	2.92	0.97	40.07
	227	66	Radish	13.69	0.58	-0.16	0.04	-22.10	1.29	0.93	20.22
	243	82	Radish	11.19	0.34	-0.08	0.01	-27.52	1.38	0.97	22.44

2.4.5. Regulation of CO_2 exchange

Among the micrometeorology variables, only PAR showed a significant ($R^2 \geq 0.9$, $P < 0.05$) influence on daily GPP (Figure 13A), with GPP saturating at PAR < 1000 μmol m^{-2} s^{-1} for most crops. GPP was curvi-linearly correlated with LAI, saturating at LAI > 2, which was unusually low (Figure 13B). Seasonal GPP changes were also positively correlated with α for most crops (Figure 13C). Since LAI and biomass were positively correlated for all the crops (Figure 13D), we anticipated similar relationships between GPP and biomass. There was a positive correlation ($R^2 = 0.67$) between GPP and R_{eco} for all the crops (Figure 14A). The proportionate increase in GPP was however higher compared to R_{eco}, giving a net positive C-balance. Except for cabbage and bean, R_{eco} was positively correlated with soil temperature in the dryland crops (for radish, $R^2 = 0.66$; potato, $R^2 = 0.70$) (Figure 14B). For rice paddy, a stronger correlation existed between air temperature and R_{eco} compared to soil temperature (see Figure 14B, $R^2 = 0.62$).
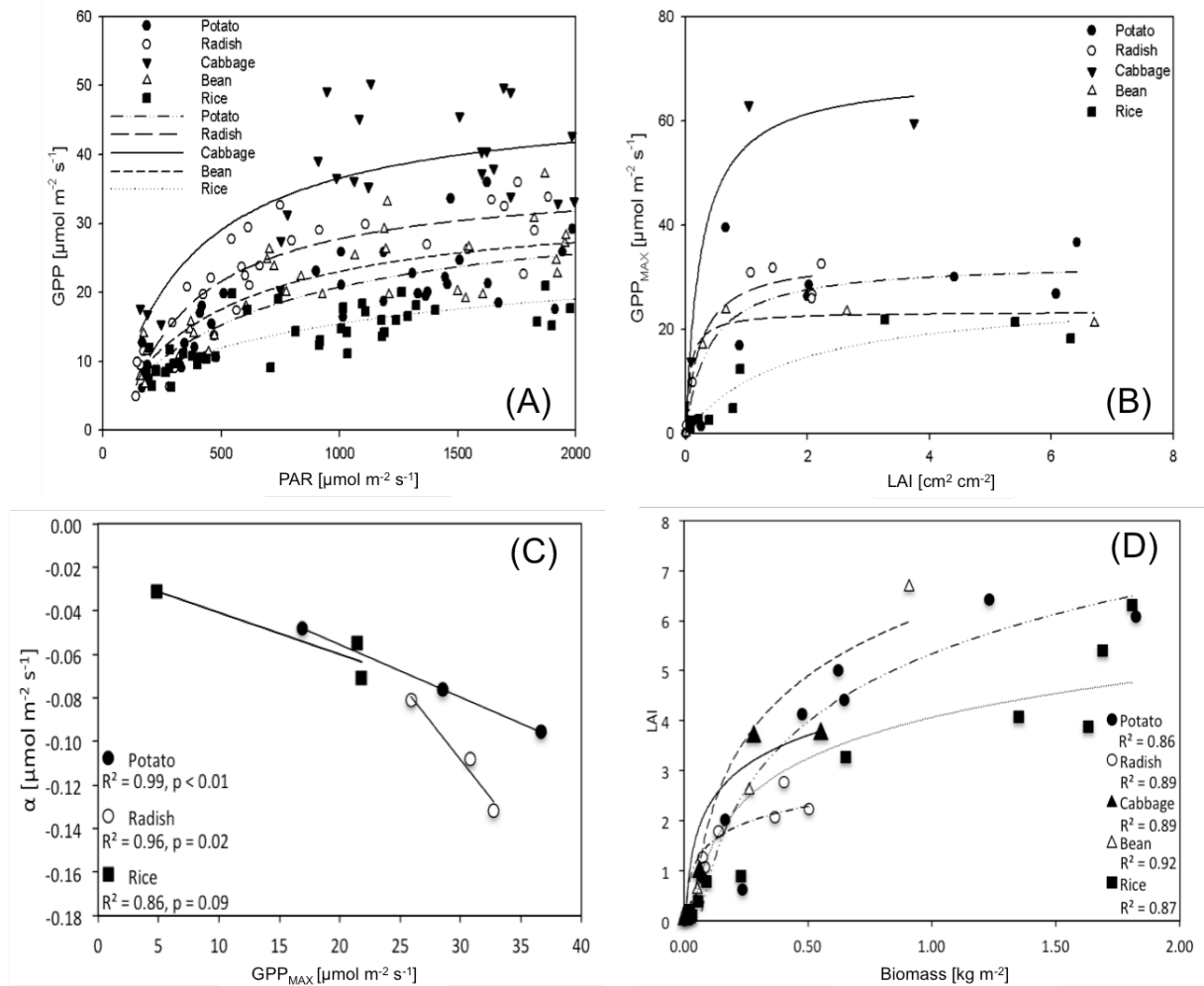
Figure 13: (A) response of GPP to changing light intensities among different crops during 2009; **(B)** changes in the maximum gross primary production (GPP$_{Max}$) in response to changes in leaf area index (LAI) during the growing season in potato, radish, cabbage, bean and rice; **(C)** correlation between light use efficiency (α) and GPP$_{Max}$ (note: data during the senescence are excluded); and **(D)** relationship between total biomass and LAI during development of the respective crops.
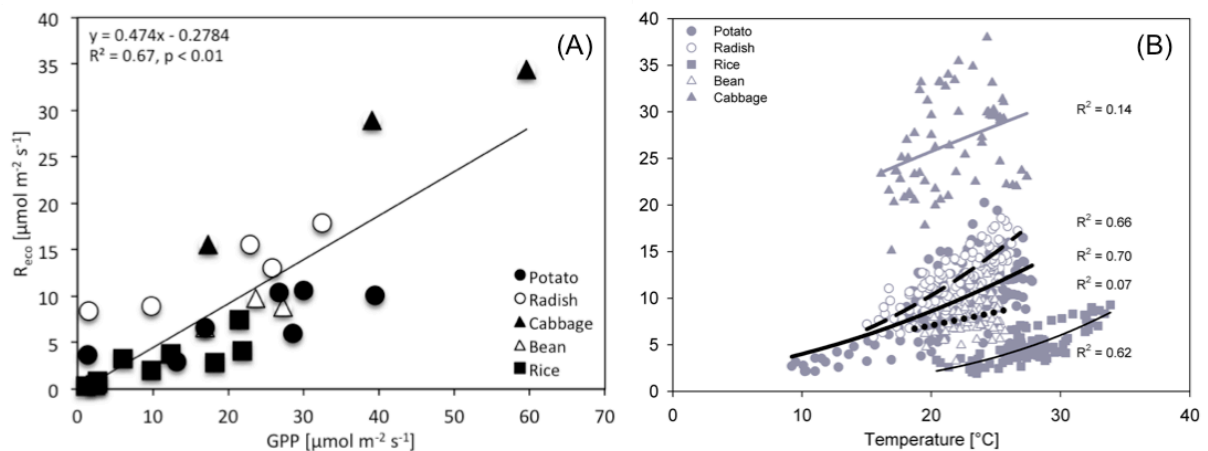
Figure 14: (A) relationship between GPP and R$_{eco}$ in all the studied crops; **(B)** response of ecosystem respiration (R$_{eco}$) for potato (closed circle), radish (open circle), bean (open triangle up), and cabbage (closed triangle up) to soil temperature (T$_{soil}$) and for rice (square) to air temperature (T$_{air}$). Data points in A are means for the respective crops during the entire growth period.

2.5. Discussion

2.5.1. Biomass production and leaf area development

Biomass and LAI development differed among the crops (Table 3, Figure 10) likely as a result of differences in growth patterns, α and carbon allocation patterns. In cabbage, for example, the proportion allocated to the roots was only 4% of the total biomass and the rest was directed to the aboveground biomass, especially for leaf development (Table 3), contributing to rapid growth of its aboveground biomass. On the contrary, crops with higher allocation to the roots throughout their growth period such as radish tended to mature slowly. Carbon allocation patterns influence plant growth rate, with consequences on CO_2 exchange, while the interactions among LAI, α and climate variables, particularly light, determine the CO_2 uptake rates (GPP) of the ecosystem (Baldocchi et al., 1994).

2.5.2. Diurnal and seasonal variations of CO_2 exchange

Variations in seasonal patterns, magnitudes and the timing of maximum NEE, R_{eco} and GPP observed among crops were likely the result of LAI and α differences (Figure 11 & 12). For both years, planting was done at peak radiation intensities and air temperatures during the year (Table 1, Figure 9), conditions that support maximum CO_2 exchange between vegetation and the atmosphere (Mooney, 1972). There was also no water stress recorded during the study. Given that the crops were subjected to similar environmental conditions, we can confidently conclude that weather and soil moisture were not sources of variations among crops. Our GPP rates were in the range reported for monocultures of similar crops elsewhere, e.g. $36.4 - 70.0$ μmol m^{-2} s^{-1} for potatoes (Lawson et. al., 2001; Fleischer et al., 2008), $21.9 - 36.8$ μmol m^{-2} s^{-1} for radish (Jablonski, 1997; Usuda and Shimogawara, 1998), $22.7 - 43.1$ μmol m^{-2} s^{-1} for soybean (Baker et al., 1993; Suyker et al., 2005) and $16.0 - 45.4$ μmol m^{-2} s^{-1} for Asian rice (Saito et al., 2005; Alberto et al., 2009). Compared to the rest of

the crops, GPP of cabbage appeared exceptionally high. It is likely that these high GPP are promoted by the high respiration in cabbage. Zhenxian et al. (1993), Bunce (2000) reported GPP values of $13.0 - 45.0$ μmol m^{-2} s^{-1} for Chinese cabbage (*Barassica rapa*).

In fast growing crops like potato and cabbage, peak GPP occurred in June, whereas for radish, rice and bean, maximum GPP occurred in July/August, with an overlap in their peak GPP (Figure 12). Thus, even though maximum CO_2 uptake in single crops only lasted a couple of weeks, the effect of staggered peak GPP among the different crops resulted in extended period of high CO_2 uptake in this multicultural cropping landscape.

Our R_{eco} measured for most crops fall within the range of R_{eco} rates measured in similar crop fields elsewhere. Compared to the other crops, cabbage exhibited relatively higher R_{eco}. For example Saito et al. (2005), Suyker et al. (2005) and Alberto et al. (2009) reported R_{eco} rates of $3.0 - 7.7$ μmol m^{-2} s^{-1} in rice paddies. Values reported for beans are $11.1 - 12.7$ μmol m^{-2} s^{-1} (Suyker et al., 2005; Hernandez-Ramirez et al., 2011) and $3.5 - 11.2$ μmol m^{-2} s^{-1} for potatoes (Lawson et al., 2001). We observed significant variations in respiration rates among the crops. Since they were grown on similar soils, with no water stress during the growing season, we assume that spatial differences in R_{eco} among the fields were due to differences in GPP. This argument is based upon the observed positive correlation between GPP and R_{eco} (Figure 14A).

The balance between GPP and R_{eco} determines daily and seasonal NEE (Falge et al., 2002b). Except for cabbage and potato, which exhibited peak NEE rates > 20 μmol m^{-2} s^{-1}, most measured crops had their peak NEE between $- 15.4$ and $- 19.7$ μmol m^{-2} s^{-1} in both years. The distribution of daily maximum NEE on both sides of the peak rates was dome-shaped. For most crops, our measured peak rates are comparable to those reported for monocultures of the same crops elsewhere. For example, peak NEE ranged between $- 8.0$ to $- 29.5$ μmol m^{-2} s^{-1} in rice paddies in southern Korea and western Japan (Moon et al., 2003; Saito et al., 2005). Falge et al. (2002b), Suyker et al. (2005), Hernandez-Ramirez et al. (2011),

reported peak NEE of -6.8 to -21.1 $\mu mol\,m^{-2}\,s^{-1}$ in monocultures of bean in Europe and USA. The range for mean NEE reported for soybean was -9.09 to -29.5 $\mu mol\,m^{-2}\,s^{-1}$ (Baker and Griffis, 2005). Values of -8.0 to -35.0 $\mu mol\,m^{-2}\,s^{-1}$ are reported for European croplands (Béziat et al., 2009). Similarities in NEE between our fields and monocultural fields elsewhere likely arise from comparable microclimatic, soil moisture and management conditions. Our NEE rates for potato and cabbage were however higher than -11.4 $\mu mol\,m^{-2}\,s^{-1}$ to -31.6 $\mu mol\,m^{-2}\,s^{-1}$ reported for potato and cabbage, respectively (Sale, 1977; Elsgaard et al., 2012). We speculate that higher fertilization rates in the Korean fields, in comparison, may be the reason for higher NEE for potato and cabbage. In general, peak NEE rates for the respective crops in this multicultural cropping system of Haean seem to compare favorably with monocultures of the same crops elsewhere.

Carbon balance studies investigating seasonal phasing and amplitudes of respiratory and assimilatory processes show significant differences in the seasonal maximum potentials and patterns of maximum diurnal CO_2 exchange of different ecosystems (e.g. C3/C4-crops, grasslands, wetlands, forests, tundra ecosystems) (Falge et al., 2002a; Suyker et al., 2005). Their maximum observed CO_2 uptake values of the year are seen as signatures for the potential carbon sequestration capacity of the ecosystem. Croplands showed highest flux potentials, but the period of maximum (peak) CO_2 exchange is generally limited to only several days (< 31 days) during the vegetation period for most mono-cultural croplands. In a multicultural landscape, different crops attained peak NEE at different times of the year. In some cases, there was an overlap in the period with peak NEE among crops (Figure 12). This means that the period of peak CO_2 uptake was sustained for an extended period of time, than would be the case for monocultures of the same crops. The advantage offered by multicultural cropping system in terms of CO_2 uptake, therefore, lies in the length of time with peak CO_2 uptake as a result of staggered peak GPP of the respective crops as well as the total period when the agricultural landscape is photosynthetically active.

2.5.3. Regulation of CO_2 fluxes among crops

On a daily basis, GPP was a non-linear function of PAR, saturating at PAR > 1000 μmol m^{-2} s^{-1}. Seasonal changes in GPP were also a function of both LAI and α. Similar response patterns have been reported for other crops (Baldocchi, 1994). There was a positive correlation ($R^2 = 0.40 - 0.98$) between α and LAI among different crops, suggesting that light use efficiency increases during the development of a crop (Suyker et al., 2005). This relationship is likely the result of increased chlorophyll quantity arising from increased leaf quantity and size (Kariya and Tsundoda, 1972; Lawlor et al., 1989). On the other hand, α is also controlled by Ribulose 1-5 Bisphosphate Carboxylase/Oxygenase (Rubisco) enzyme, whose function will depend both on its concentration and temperature (Bunce, 2000; Sage and Kubien, 2007; Sharkey et al., 2007). During our study, radiation, soil moisture and nutrients were never limiting plant growth, leaving LAI and α as the main determinants of GPP (Besford et al., 1990; Stitt and Schulze, 1994; Lawson et al., 2001; Parry et al., 2003; Murchie et al., 2008).

In our case, the relationship between GPP and LAI varied strongly among crops. Although this is not unique to our study (Acock et al., 1978; Suyker et al., 2005; Gitelson et al., 2014), in most cases, the relationship is a linear function, unlike in our study, where it saturated at higher LAI. We attribute this to self-shading, which limits further increase in GPP after a given value of LAI is reached (Yoshida, 1981). In our case, this appears to occur at unusually low LAI.

The interplay between carbon uptake and release through respiration is important for the determination of the overall C sink strength of the respective crops (West et al., 2011). We found that GPP significantly ($P < 0.05$, $R^2 = 0.67$) influenced R_{eco} (Figure 14A), which is due to increased maintenance respiration as root biomass increases (Gifford, 1994; Ma et al., 2007). In addition, R_{eco} was also influenced by temperature (Figure 14B). The seasonal trend of R_{eco} observed among the crops may be in response to transport assimilate to the roots

(soil), which traces the pattern of plant growth and increasing air temperatures during the season. Assimilate deliver to the roots and exudation of sugars by roots into the soil stimulate root and soil respiration, respectively. Respiration was also positively correlated with air temperature, in most cases (Figure 14B). Poor correlation between air temperature and cabbage R_{eco} draws from the nature of this crop. A large mass of cabbage tissues is enclosed in a ball of overlapping leaves, which remains wet throughout the year and is very well insulated. A combination of good insulation and water as a poor conductor of heat means that the bulk of internal tissues of cabbage that is actively involved in respiration is decoupled from external environment.

Physiological parameters derived from light response curves accurately characterize the CO_2 exchange of the ecosystem (Gilmanov et al., 2003; 2007), e.g. $(\beta+\gamma)_{2000}$ highly correlates with daily GPP for several ecosystems (Owen et al., 2007). In our study, the model output parameter $(\beta+\gamma)_{1500}$ was highly correlated ($R^2 = 0.84$) with the measured GPP_{max} and in most cases the measured fluxes were well-described by the empirical models. To describe the temperature dependence of R_{eco}, we opted for the Lloyd and Taylor model, which unlike other models that take into account soil moisture as additional variable, is only driven by soil temperature. This decision was arrived at because there was no water stress at the study site during the measurements and soil water was never limiting to crop growth (Suyker et al. 2004; Suyker et al., 2005; Reichstein et al., 2005). The strongest temperature regulation of R_{eco} was from the top 0-10 cm soil profile (Figure 14B).

2.6. Conclusion

We observed strong differences in the diurnal and seasonal trends of CO_2 flux rates (GPP, R_{eco}, NEE) and their magnitudes among radish, potato, cabbage, soybean and rice. While PAR controlled diurnal fluctuations in GPP and NEE, seasonal differences among and within crops were attributed to a changing LAI and α. These differences among crops resulted in a high spatial variability of maximum GPP and different timing of their peak annual CO_2 assimilation. The staggered peak GPP rates, therefore, prolong the period of active CO_2 uptake, unlike in monocultural crops grown under comparable environmental conditions where this peak phase is likely to be shorter. R_{eco} was temperature controlled, but spatial differences in R_{eco} observed among crops were likely the result of variable GPP. Differences among crops were significant, hence modeling approaches need to consider the heterogeneity in ecosystem CO_2 exchange associated with these multicultural agriculture landscapes.

2.7. Acknowledgements

2.8. References

Acock, B., Charles-Edwards, D.A., Fitter, D.J., Hand, D.W., Ludwig, L.J., Warren Wilson, J., Withers, A.C., 1978. The Contribution of leaves from different levels within a tomato crop to canopy net photosynthesis: An experimental examination of two canopy models. J. Exp. Bot. 29, 815–827.

Alberto, M., Wassmann, R., Hirano, T., Miyata, A., Kumar, A., Padre, A., Amante, M., 2009. CO_2/heat fluxes in rice fields: Comparative assessment of flooded and non-flooded fields in the Philippines. Agric. For. Meteorol. 149, 1737–1750.

Aubinet, M., Grelle, A., Ibrom, A., Rannik, Ü., Moncrieff, J., Foken, T., Kowalski, A.S., Martin, P.H., Berbigier, P., Bernhofer, C., Clement, R., Elbers, J., Granier, A., Grünwald, T., Morgenstern, K., Pilegaard, K., Rebmann, C., Snijders, W., Valentini, R., Vesala, T., 1999.

Estimates of the Annual Net Carbon and Water Exchange of Forests: The EUROFLUX. Adv. Ecol. Res. 30, 113-175.

Aubinet, M., Moureaux, C., Bodson, B., Dufranne, D., Heinesch, B., Suleau, M., Vancutsem, F., Vilret, A., 2009. Carbon sequestration by a crop over a 4-year sugar beet/winter wheat/seed potato/winter wheat rotation cycle. Agric. For. Meteorol. 149, 407–418.

Baker, J.T., Allen, L.H.Jr., 1993. Contrasting crop species responses to CO_2 and temperature: rice, soybean and citrus. Vegetatio 104-105, 239-260.

Baker, J.M., Griffis, T.J., 2005. Examining strategies to improve the carbon balance of corn/soybean agriculture using eddy covariance and mass balance techniques. Agric. For. Meterol. 128, 163-177.

Baldocchi, D.D., 1994. A comparative study of mass and energy exchange rates over a closed C3 (wheat) and an open C4 (corn) crop: CO_2 exchange and water use efficiency. Agric. For. Meteorol. 67, 291–321.

Besford, R.T., Ludwig, L.J., Withers, A.C., 1990. The Greenhouse Effect: Acclimation of Tomato Plants Growing in High CO_2, Photosynthesis and Ribulose-1,5-Bisphosphate Carboxylase Protein. J. Exp. Bot. 41, 925–931.

Béziat, P., Ceschia, E., Dedieu, G., 2009. Carbon balance of a three crop succession over two cropland sites in South West France. Agric. For. Meteorol. 149, 1628–1645.

Bunce, J.A., 2000. Acclimation of photosynthesis to temperature in eight cool and warm climate herbaceous C3 species: Temperature dependence of parameters of a biochemical photosynthesis model. Photosyn. Res. 63, 59–67.

Campbell, C.S., Heilman J.L., McInnes, K.J., Wilson, L.T., Medley, J.C., Wu, G., Cobos, D.R., 2001. Diel and seasonal variation in CO_2 flux of irrigated rice. Agric. For. Meterol. 108, 15–27.

Corbin, K.D., Denning, A.S., Lokupitiya, E.Y., Schuh, A.E., Miles, N.L., Davis, K.J., Richardson, S., Baker, I.T., 2010. Assessing the impact of crops on regional CO_2 fluxes and atmospheric concentrations. Tellus 62, 521–532.

Desjardins, R.L., Sivakumar, M.V.K., de Kimpe, C., 2007. The contribution of agriculture to the state of climate: Workshop summary and recommendations. Agric. For. Meterol. 142, 314–324.

Dufranne, D., Moureaux, C., Vancutsem, F., Bodson, B., Aubinet, M., 2011. Comparison of carbon fluxes, growth and productivity of a winter wheat crop in three contrasting growing seasons. Agric. Ecosyst. Environ. 141, 133–142.

Elsgaard, L., Görres, C.M., Hoffmann, C.C., Blicher-Mathiesen, G., Schelde, K., Petersen, S.O., 2012. Net ecosystem exchange of CO_2 and carbon balance for eight temperate organic soils under agricultural management. Agric. Ecosyst. Environ. 162, 52– 67.

Falge, E., Baldocchi, D.D., Tenhunen, J.D., Moureaux, C., Debacq, A., Hoyaux, J., Suleau, M., Tourneur, D., Vancutsem, F., Bodson, B., Aubinet, M., 2002a. Seasonality of ecosystem

respiration and gross primary production as derived from FLUXNET measurements. Agric. For. Meteorol. 113, 53–74.

Falge, E., Tenhunen, J., Baldocchi, D., Aubinet, M., Bakwin, P., Berbigier, P., Bernhofer, Ch., Bonnefond, J. M., Burba, G., Clement, R., Davis, K. J., Elbers, J. A., Falk, M., Goldstein, A. H., Grelle, A., Granier, A., Grünwald, T., Gu, J., Hollinger, D., Janssens, I. A., Keronen, P., Kowalski, A. S., Katul, G., Law, B. E., Malhi, Y., Meyers, T., Monson, R. K., Moors, E., Munger, J.W., Oechel, W., Tha, K., Paw, U., Pilegaard, K., Rannik, Ü., Rebmann, C., Suyker, A., Thorgeirsson, H., Tirone, G., Turnipseed, A., Wilson, K., Wofsy, S., 2002b. Phase and amplitude of ecosystem carbon release and uptake potentials as derived from FLUXNET measurements. Agric. For. Meteorol. 113, 75-95.

FAO. 2006. Guidelines for soil description. 4th ed. Rome, Italy: United Nations FAO.

FAO. 2014. Global Land Cover (GLC-SHARE) Beta-Release 1.0 Database, Land and Water Division. Rome, Italy: United Nations FAO.

Fleisher, D.H., Timlin, D.J., Reddy, V.R., 2008. Elevated carbon dioxide and water stress effects on potato canopy gas exchange, water use, and productivity. Agric. For. Meteorol. 148, 1109–1122.

Gifford, R.M., 1994. The global carbon-cycle - a viewpoint on the missing sink. Aust. J. Plant Physiol. 21, 1–15.

Gilmanov, T.G., Verma, S.B., Sims, P.L., Meyers, T.P., Bradford, J.A., Burba, G.G., Suyker, A.E., 2003. Gross primary production and light response parameters of four Southern Plains

ecosystems estimated using long-term CO_2-flux tower measurements. Global Biogeochem. Cycles 17, 1071.

Gilmanov, T.G., Soussana, J.F., Aires, L., Allard, V., Ammann, C., Balzarolo, M., Barcza, Z., Bernhofer, C., Campbell, C.L., Cernusca, A., Cescatti, A., Clifton-Brown, J., Dirks, B.O.M., Dore, S., Eugster, W., Fuhrer, J., Gimeno, C., Gruenwald, T., Haszpra, L., Hensen, A., Ibrom, A., Jacobs, A.F.G., Jones, M.B., Lanigan, G., Laurila, T., Lohila, A., Marcolla, B., Nagy, Z., Pilegaard, K., Pinter, K., Pio, C., Raschi, A., Rogiers, N., Sanz, M.J., Stefani, P., Sutton, M., Tuba, Z., Valentini, R., Williams, M.L., Wohlfahrt, G., 2007. Partitioning European grassland net ecosystem CO_2 exchange into gross primary productivity and ecosystem respiration using light response function analysis. Agric. Ecosys. and Environ. 121, 93–120.

Gilmanov, T.G., 2010. Productivity, respiration, and light-response parameters of world grassland and agro-ecosystems derived from flux-tower measurements. Rangeland Ecol. Manage. 63, 1–73.

Gitelson, A.A., Peng, Y., Arkebauer, T.J., Schepers, J., 2014. Relationships between gross primary production, green LAI, and canopy chlorophyll content in maize: Implications for remote sensing of primary production. Remote Sens. Environ. 144, 65–72.

Hernandez-Ramirez, G., Hatfield, J.L., Parkin, T.B., Sauer, T.J., Prueger, J.H., 2011. Carbon dioxide fluxes in corn–soybean rotation in the midwestern U.S.: Inter- and intra-annual variations, and biophysical controls. Agric. For. Meteorol. 151, 1831–1842.

Hollinger, S.E., Bernacchi, C.J., Meyers, T.P., 2005. Carbon budget of mature no-till ecosystem in North Central Region of the United States. Agric. For. Meteorol. 130, 59–69.

Hoyaux, J., Moureaux, C., Tourneur, D., Bodson, B., Aubinet, M., 2008. Extrapolating gross primary productivity from leaf to canopy scale in a winter wheat crop. Agric. For. Meteorol. 148, 668–679.

Jablonski, L.M., 1997. Responses of vegetative and reproductive traits to elevated CO_2 and nitrogen in Raphanus varieties. Can. J. Bot. 75, 533-545.

Jans, W.W.P., Jacobs, C.M.J., Kruijt, B., Elbers, J.A., Barendse, S.C.A., Moors, E.J., 2010. Carbon exchange of a maize (*Zea mays* L.) crop: Influence of phenology. Agric. Ecosyst. Environ. 139, 316–324.

Kariya, K., Tsunoda, S., 1972. Relationship of chlorophyll content, chloroplast area index and leaf photosynthesis rate in Brassica. Tohoku J. Agric. Res. 23, 1-15.

Kettering, J., Park, J.H., Lindner, S., Lee, B., Tenhunen, J., Kuzyakov, Y., 2012. N fluxes in an agricultural catchment under monsoon climate: A budget approach at different scales. Agric. Ecosyst. Environ. 161, 101–111.

Kim, T., Kim, G., Kim, S., Choi, E., 2008. Estimating riverine discharge of nitrogen from the South Korea by the mass balance approach. Environ. Monit. Assess. 136, 371–378.

Kwon, Y.S., Lee, H.H., Han, U., Kim, W.H., Kim, D.J., Kim, D.I., Youm, S.J., 1990. Terrain analysis of Haean Basin in terms of earth science. J. Korean Earth Sci. Soc. 11, 236–241.

Lawlor, D.W., Kontturi, M., Young, A.T., 1989. Photosynthesis by flag leaves of wheat in relation to protein, Ribulose bisphosphate carboxylase activity and nitrogen supply. J. Exp. Bot. 40, 43–52.

Lawson, T., Craigon, J., Tulloch, A.M., Black, C.R., Colls, J.J., Landon, G., 2001. Photosynthetic responses to elevated CO_2 and O_3 in field-grown potato (*Solanum tuberosum*). J. Plant Physiol. 158, 309–323.

Lei, H.M., Yang, D.W., 2010. Seasonal and interannual variations in carbon dioxide exchange over a cropland in the North China Plain. Global Change Biol. 16, 2944–2957.

Li, Y.L., Tenhunen, J., Mirzaei, H., Hussain, M.Z., Siebicke, L., Foken, T., Otieno, D., Schmidt, M., Ribeiro, N., Aires, L., Pio, C., Banza, J., Pereira, J., 2008. Assessment and up-scaling of CO_2 exchange by patches of the herbaceous vegetation mosaic in a Portuguese cork oak woodland. Agric. For. Meteorol. 148, 1318–1331.

Lloyd, J., Taylor, J.A., 1994. On the temperature dependence of soil respiration. Funct. Ecol. 8, 315–323.

Ma, S., Baldocchi, D.D., Xu, L., Hehn, T., 2007. Inter-annual variability in carbon dioxide exchange of an oak/grass savanna and open grassland in California. Agric. For. Meteorol. 147, 157–171.

Moon, B.K., Hong, J., Lee, B.-R.,Yun, J.I., Park, E.W., Kim, J., 2003. CO_2 and energy exchange in a rice paddy for the growing season of 2002 in Hari, Korea. Korea J. Agric. Forest Meteorol. 5, 51–60.

Mooney, H.A., 1972. The Carbon Balance of Plants. Annu. Rev. Ecol. Syst. 3, 315-346.

Moors, E.J., Jacobs, C., Jans, W., Supit, I., Kutsch, W.L., Bernhofer, C., Béziat, P., Buchmann, N., Carrara, A., Ceschia, E., Elbers, J., Eugster, W., Kruijt, B., Loubet, B., Magliulo, V., Moureaux, C., Olioso, A., Saunders, M., Soegaard, H., 2010. Variability in carbon exchange of European croplands. Agric. Ecosyst. Environ. 139, 325–335.

Moureaux, C., Debacq, A., Bodson, B., Heinesch, B., Aubinet, M., 2006. Annual net ecosystem carbon exchange by a sugar beet crop. Agric. For. Meteorol. 139, 25–39.

Moureaux, C., Debacq, A., Hoyaux, J., Suleau, M., Tourneur, D., Vancutsem, F., Bodson, B., Aubinet, M., 2008. Carbon balance assessment of a Belgian winter wheat crop (*Triticum aestivum* L.). Global Change Biol. 14, 1353–1366.

Murchie, E.H., Pinto, M., Horton, P., 2008. Agriculture and the new challenges for photosynthesis research. New Phytol. 181, 532–552.

Otieno, D., Lindner, S., Muhr, J., Borken, W., 2012. Sensitivity of peatland herbaceous vegetation to vapor pressure deficit influences net ecosystem CO_2 exchange. Wetlands 32, 895–905.

Owen, K.E., Tenhunen, J., Reichstein, M., Wang, Q., Falge, E., Geyer, R., Xiao, X., Stoy, P., Ammann, C., Arain, A., Aubinet, M., Aurela, M., Bernhofer, C., Chojnicki, B.H., Granier, A., Gruenwald, T., Hadley, J., Heinesch, B., Hollinger, D., Knohl, A., Kutsch, W., Lohila, A., Meyers, T., Moors, E., Moureaux, C., Pilegaard, K., Saigusa, N., Verma, S., Vesala, T.,

Vogel, C., 2007. Linking flux network measurements to continental scale simulations: ecosystem carbon dioxide exchange capacity under non-water-stressed conditions. Global Change Biol. 13, 734–760.

Parry, M.A.J., Andralojc, P.J., Mitchell, R.A.C., Madgwick, P.J., Keys, A.J., 2003. Manipulation of Rubisco: the amount, activity, function and regulation. J. Exp. Bot. 54, 1321–1333.

Pattey, E., Strachan, I.B., Desjardins, R.L., Massheder, J., 2002. Measuring nighttime CO_2 flux over terrestrial ecosystems using eddy covariance and nocturnal boundary layer methods. Agric. For. Meteorol. 113, 145–158.

Pavelka, M., Sedlák, P., Acosta, M., Czerny, R., Taufarová, K., Janous, D., 2007. Chamber techniques versus eddy covariance method during nighttime measurements. International Scientific Conference, Polana nad Detvou, Slovakia.

Pookpakdi, A., 1992. Sustainable Agriculture for Small-Scale Farmers: A Farming Systems Perspective, Extension Bulletin. Food and Fertilizer Technology Center: Taipei.

Qun, D., Huizhi, L., 2013. Seven years of carbon dioxide exchange over a degraded grassland and a cropland with maize ecosystems in a semiarid area of China. Agric. Ecosyst. Environ. 173, 1–12.

Reichstein, M., Falge, E., Baldocchi, D., Papale, D., Aubinet, M., Berbigier, P., Bernhofer, Ch., Buchmann, N., Gilmanov, T., Granier, A., Grunwald, T., Havrankova, K., Ilvesniemi, H., Janous, D., Knohl, A., Laurila, T., Lohila, A., Loustau, D., Matteucci, G., Meyers, T.,

Miglietta, F., Ourcival, J.M., Pumpanen, J., Rambal, S., Rotenberg, E., Sanz, M., Tenhunen, J., Seufert, G., Vaccari, F., Vesala, T., Yakir, D., Valentini, R., 2005. On the separation of net ecosystem exchange into assimilation and ecosystem respiration: review and improved algorithm. Global Change Biol. 11, 1424–1439.

Ren, W., Tian, H.Q., Xu, X.F., Liu, M.L., Lu, C.Q., Chen, G.S., Melillo, J., Reilly, J., Liu, J.Y., 2011. Spatial and temporal patterns of CO_2 and CH_4 fluxes in China's croplands in response to multifactor environmental changes. Tellus 63, 222–240.

Sage, R.F., Kubien, D.S., 2007. The temperature response of C3 and C4 photosynthesis. Plant Cell Environ. 30, 1086–1106.

Saito, M., Miyata, A., Nagai, H., Yamada, T., 2005. Seasonal variation of carbon dioxide exchange in rice paddy field in Japan. Agric. For. Meteorol. 135, 93–109.

Sale, P.J.M., 1977. Net carbon exchange rates of field-grown crops in relation to irradiance and dry weight accumulation. Aust. J. Plant Physiol. 4, 555–569.

Schmidt, M., Reichenau, T.G., Fiener, P., Schneider, K., 2012. The carbon budget of a winter wheat field: An eddy covariance analysis of seasonal and inter-annual variability. Agric. For. Meteorol. 165, 114–126.

Sharkey, T.D., Bernacchi, C.J., Farquhar, G.D., Singsaas, E.L., 2007. Fitting photosynthetic carbon dioxide response curves for C3 leaves. Plant Cell Environ. 30, 1035–1040.

Smith, P., Falloon, P., 2005. Carbon sequestration in European croplands. Soc. Exp. Biol. 47–55.

Smith, P., Jones, M., Osborne, B., Wattenbach, M., 2010. The carbon and greenhouse gas budget of European croplands. Agric. Ecosyst. Environ. 139, 363–383.

Soegaard, H., Jensen, N.O., Boegh, E., Hasager, C.B., Schelde, K., Thomsen, A., 2003. Carbon dioxide exchange over agricultural landscape using eddy correlation and footprint modelling. Agric. For. Meterol. 114, 153–173.

Stitt M., Schulze D., 1994. Does Rubisco control the rate of photosynthesis and plant growth? An exercise in molecular ecophysiology. Plant Cell Environ. 17, 465–487.

Sus, O., Williams, M., Bernhofer, C., Béziat, P., Buchmann, N., Ceschia, E., Doherty, R., Eugster, W., Grünwald, T., Kutsch, W., Smith, P., Wattenbach, M., 2010. A linked carbon cycle and crop developmental model: Description and evaluation against measurements of carbon fluxes and carbon stocks at several European agricultural sites. Agric. Ecosyst. Environ. 139, 402–418.

Suyker, A.E., Verma, S.B., Burba, G.G., Arkebauer, T.J., Walters, D.T., Hubbard, K.G., 2004. Growing season carbon dioxide exchange in irrigated and rainfed maize. Agric. For. Meteorol. 124, 1–13.

Suyker, A.E., Verma, S.B., Burba, G.G., Arkebauer, T.J., 2005. Gross primary production and ecosystem respiration of irrigated maize and irrigated soybean during a growing season. Agric. For. Meteorol. 131, 180–90.

Usuda, H., Shimogawara, K., 1998. The effects of increased atmospheric carbon dioxide on growth, carbohydrates, and photosynthesis in radish, *Raphanus sativus*. Plant Cell Physiol. 39, 1–7.

West, T.O., Bandaru, V., Brandt, C. C., Schuh, A. E., Ogle, S. M., 2011. Regional uptake and release of crop carbon in the United States. Biogeosciences Discuss. 8, 631–654.

Wohlfahrt, G., Anfang, C., Bahn, M., Haslwanter, A., Newesely, C., Schmitt, M., Droesler M., Pfadenhauer, J., Cernusca, A., 2005. Quantifying ecosystem respiration of a medow using eddy covariance, chambers and modelling. Agric. For. Meteorol. 128, 141–162.

Yanggu County Office annual report (Ed.), 2010. Yanggu Statistical Yearbook 2009, Yanggu.

Yoshida, S., 1981. Fundamentals of Rice Crop Science. IRRI, P.O. Box 933, Manila, Philippines.

Zhenxian, Z., Xianehang, Y., Liping, C., Jinyu, S., Shuhua L., 1993. Effect of water conditions on photosynthesis in Chinese cabbage. Acta Hortic. Sin. 20, 358-362.

Chapter 3

3. Canopy scale CO_2 exchange and productivity of transplanted paddy and direct seeded rainfed rice production systems in S. Korea

Lindner, Steve[1]; Xue, Wei[1]; Nay-Htoon, Bhone[2]; Choi, Jinsil[3]; Ege, Yannic[1]; Lichtenwald, Nikolas[1]; Fischer, Fabian[1]; Ko, Jonghan[3]; Tenhunen, John[1] and Otieno, Dennis[1]

(1) Plant Ecology, BayCEER, University of Bayreuth, Universitätsstraße 30, 95447 Bayreuth, Germany.

(2) Agro-ecosystem Research, BayCEER, University of Bayreuth, Universitätsstraße 30, 95447 Bayreuth, Germany.

(3) Applied Plant Science, Chonnam National University, 77 Yongbong-ro, Buk-gu, Gwangju 500-757, Republic of Korea.

3.1. Abstract:

Rice (*Oryza sativa* L.) is a primary food crop that supports more than half the world population. Paddy rice accounts for more than 75% of the total global rice production but requires large amounts of water for irrigation. Increasing water scarcity, however, raises concerns regarding the sustainability of paddy rice production and highlights the need for alternative approaches. Improved rice varieties that require less water, are drought tolerant and which can be directly seeded offer promising alternatives. In this study, we evaluated the performance of an improved rice variety (*Oryza sativa* subsp. Japonica cv. Unkwang) grown under direct seeding and rainfed (RF) cultivation. Aboveground biomass and leaf area development were measured every month by destructive harvesting. Canopy net ecosystem CO_2 exchange (NEE) and ecosystem respiration (R_{eco}) were measured using chambers. Gross primary production (GPP) was calculated from NEE and R_{eco}. The maximum green leaf area index (GLAI) attained under rainfed agriculture was 4.9 ± 0.5 $m^2 m^{-2}$ compared to 5.4 ± 1.1 $m^2 m^{-2}$ in the conventional paddy rice (PR) production system. The respective peak total aboveground biomasses were 2.16 ± 0.28 and 1.85 ± 0.27 kg m^{-2} while the corresponding grain weights were 1.16 ± 0.09 and 1.19 ± 0.10 kg m^{-2}, amounting to total yields of 6.61 ± 0.22 and 5.99 ± 0.68 t/ha^{-1} for PR and RF, respectively. The maximum daily cumulative GPP were 11.1 and 12.0 gC m^{-2} d^{-1}, respectively, occurring at peak season, corresponding to maximum photosynthetic active radiation (PAR) and GLAI. On a daily basis, PAR explained >82% of the daily fluctuations in GPP while >90% of the seasonal changes in GPP were due to changes in GLAI and light use efficiency (α). Higher α in RF was attributed to higher leaf nitrogen (N) content. With adequate soil moisture supply, the Unkwang variety demonstrated the potential to grow under rainfed agriculture with comparatively good amount of yield. Since direct seeding, as in rainfed agriculture, eliminates the need for prior flooding of plots, it maximizes the use of early rainfall, which could be a

water saving strategy and a reason to promote the introduction of Unkwang variety in the paddy rice-dominated Asian farming system.

3.2. Introduction

Rice (*Oryza sativa* L.) is a primary food crop supporting more than half the world's population and covers about 150 million hectares of land (Bouman, 2007). Worldwide, most rice production is done through flooding or paddy cultivation (Barker et al., 1999). Increasing water scarcity due to droughts and competing demands for water resources (IPCC, 2008) from growing domestic and industrial uses however, threaten the current production practices, raising the need for alternative production approaches. In this regard, the development of improved varieties that require less water or are more drought tolerant has been promoted (Barker et al., 1999). The culture of direct-seeded rice grown in unsaturated soils is another promising way to reduce irrigation requirements by more than half, compared to the conventional paddy rice (IRRI, 2002; Kato et al., 2006a; Okami et al., 2013).

In paddy rice (PR) fields, the amount of water that directly supports production is the transpired water since it is directly linked to CO_2 uptake, plant growth and yield. The bulk of the water in the flooded field is not directly related to production and is either re-directed back to the streams, percolated or evaporated. Thus, production systems that only supply the evapotranspiration demands could be a big saving on water resources and are environmentally friendlier (Toung and Bouman, 2003). Dry-seeded, rainfed rice (RF) offers an alternative to rice farmers, especially in Asia, where PR production is more or less cultural and does not accommodate alternative crops as a means of ensuring food security. RF production is already being experimented in some parts of Asia as an alternative to the traditional PR (Kato et al., 2006a). Although most results from these trials show yield losses of between 20 – 30% caused by drought (Okami et al., 2013), there are indications that yields of up to 8 – 11 t ha^{-1} (typical of paddy rice) are tenable with proper management (Okami et al., 2013). The dry-seeded RF technology may thus offer an opportunity for rice production through efficient use of ambient rainfall.

The main challenge to RF production however, is to supply adequate water that replaces daily evapo-transpiration and ensuring that photosynthesis proceeds uninterrupted. High transpirational water demand that occurs almost on a daily basis during midday, when vapor pressure deficit (VPD) is high, potentially lowers production, since plants close their stomata in order to check runaway cavitation at the expense of CO_2 fixation (Sperry, 2000). On an annual basis, this could lead to a significant reduction in yield. RF may improve water uptake through increased root biomass, or physiological adjustments by re-directing assimilates to the roots to increase the root osmoticum (Munns, 1988; Kato et al., 2007; Wada et al., 2014). In such cases however, resources that could be used in grain production are re-directed in order to increase the plant's water uptake capacity, potentially lowering yield.

While PR may be spared such a reduction in productivity because it stands in saturated soil, it faces a different challenge that may also effectively reduce shoot water supply and result in water stress during the day. Flooding of paddy fields limits oxygen diffusion into the soil, creating an anoxic soil substrate. Plant roots must, therefore, rely on oxygen supply from the surface, transported by the aerenchyma to the root apex (Moog and Brüggemann, 1998; Busch, 2001; McDonald et al., 2002; Colmer et al., 2003). To minimize radial oxygen losses during transport, large sections of the roots are often suberized (i.e. deposition of suberin, a hydrophobic plant polymer, on the cell walls and in the intercellular space), effectively blocking water flow through the apoplast, such that the roots can no longer take part in water uptake. In this case, water uptake is restricted to the short, narrow portions near the root apex of the deep roots, which remain unsuberized (Ranathunge et al., 2004; Kotula et al., 2009). This must effectively lower the efficiency of water uptake in PR and could result in transient water stress and stomatal closure during midday, when light conditions and temperature are most conducive for plant production. In this case, flooding may not offer any advantage to PR, unless through the dampening the VPD above the canopy. Incorporating cultivars with

efficient water and nutrient uptake and transport into the RF production offers an opportunity to respond to the challenges associated with rice production (Kato et al., 2006a).

In this study, we experimented on a new rice cultivar (*Oryza sativa* L. subsp. Japonica cv. Unkwang) that has been developed from a high yielding, cold tolerant and early maturing variety to accommodate the demands of the northern plains and mountainous areas of South Korea (Kim et al., 2006). The Unkwang rice variety was grown under both the rainfed and conventional paddy production systems for comparison. Our hypotheses were that under adequate soil moisture supply, the Unkwang rice grown in a rainfed system: a) maintains similar rates of CO_2 uptake and light use efficiencies compared to that in a paddy system, and b) does not alter C allocation patterns in comparison to the paddy condition. Under such circumstances we anticipated similarities in crop development and yield between RF and PR.

3.3. Materials and Methods

3.3.1. Study site

The study was conducted during the growing period of 2013 at the Chonnam National University's research farm (35° 10' N, 126° 53' E, alt. 33m) in Gwangju, Chonnam province, South Korea. Chonnam province is one of the major rice growing regions of S. Korea, with a typical East Asian monsoon climate, a mean annual temperature of 13.8°C and precipitation of between 1391 and 1520 mm/yr (1981–2010). More than 60% of precipitation occurs during the summer monsoon season (July to August). The top soil layer (0 – 30 cm) is categorized as loam (Sand 388 g kg^{-1}, Silt 378 g kg^{-1}, Clay 234 g kg^{-1}), with a pH 6.5, C_{org} 12.3 C g kg^{-1}, available P 13.1 mg P_2O_5 kg^{-1}, CEC 14.4 c mol_c kg^{-1}, and total N before fertilization of 1.0 g N kg^{-1}.

3.3.2. Experimental design/Description of the experimental plots

An improved rice variety, *Oryza sativa* subsp. Japonica cv. Unkwang (Iksan 435 x Cheolweon 54) was cultivated as flooded paddy crop (PR) and as rainfed crop (RF) in two adjacent (separated by 100 m) experimental rice fields. PR was planted in 3 replicate blocks measuring 73.0 m x 19.5 m, with a perimeter cement wall. Sampling was confined to 8 m by 8 m sub-plots at the center of the blocks to minimize edge effects. In the RF field, we demarcated 3 replicate plots measuring 37.5 m x 28.0 m for our measurements. These plots were randomly selected, but at the middle of the field to avoid edge effects too. In both PR and RF, the sample plots were accessed using footbridges to minimize disturbances of the soil and canopy.

3.3.3. Field management

Measurements were conducted during the 2013 growing season. The rice seedlings were grown for 4 weeks as seedling mats in the greenhouse, before being transplanted into the PR field, whereas in RF the rice was directly seeded. Management practices and planting dates, including rice transplanting and harvesting days are summarized in Table 5. Fertilization rate of 115 kg N/ha (80% as basal dosage and 20% during the tillering stage) for PR and RF were done before transplanting and at seeding stages, respectively, at a ratio of 11 : 6 : 5 (N : P : K), following the recommendations of the Korean Ministry of Agriculture, Food and Rural Affairs (MAFRA). Rice in RF and PR were planted at a distance of 10 cm and a line spacing of 30 cm at a seed-density of 50.48 kg/ha. The PR field was kept flooded from 5 days before transplanting until the heading stage (late July). Irrigation water in PR was applied when the water level decreased below 5 cm above the soil surface. The RF field was never irrigated and relied entirely on the ambient rainfall. Weeds and insects were controlled with herbicides and insecticides, respectively.

Table 5: Field management of the study site in 2013 in Gwangju.

Event	Date Paddy Rice	Date Rainfed Rice
Plowing	10.05.13	17.04.13
Flooding	14.05.13	–
Herbicides application	16.05.13	–
Basal fertilization	19.05.13	22.04.13
Transplanting / Planting	20.05.13	22.04.13
Pesticides application	20.05.13	26.04.13
Herbicides application	–	06.05.13
Manual weeding	–	22.05.13
Herbicides application	–	25.05.13
Manual weeding	–	20.06.13
Supplemental fertilization	07.06.13	09.06.13
Harvest	07.10.13	10.10.13

3.3.4. Microclimate

Meteorological variables, including air temperature, humidity, precipitation and global radiation were continuously measured with a 2 m high automatic weather station (AWS, WS-GP1, Delta-T Devices Ltd., UK). Data were recorded every 5 minutes, averaged and logged half-hourly. Additionally, discontinuous records of photosynthetic photon flux density (PPFD, LI−190, LI−COR, USA) within the transparent CO_2 measurement chambers (approx. 50 cm above ground surface), air temperature (T_{air}) at 20 cm height inside and outside the CO_2 chambers (Digital thermometer, Conrad, Hirschau, Germany) and soil temperature (T_{soil}) at 10 cm soil depth (Soil thermometer, Conrad, Hirschau, Germany) within the soil frames were taken during the CO_2 flux measurements. Data were recorded every 15 s alongside CO_2 fluxes. This allowed closer monitoring of the internal chamber microclimate, in order to relate the CO_2 fluxes to the actual conditions within the chambers during measurements.

3.3.5. Soil water content

Volumetric soil water content (VWC) at 30 cm depth was measured at several locations close to the collars using $EC-5$ soil moisture sensors (Decagon, WA, USA). The sensors were installed 1 week before the onset of CO_2 flux measurements and kept in the field throughout the season. Data were logged every 30 min using EM50 data-logger (Decagon, WA, USA).

3.3.6. CO_2 flux measurement with chambers

In each treatment block, 4 soil frames (collars) enclosing healthy, representative crops (crop plots) and 3 bare plots (soil plots) were established in June 2013, several days before the commencement of CO_2 flux measurements. Each collar enclosed an area measuring 39.5 cm by 39.5 cm, providing a base for the removable CO_2 chambers. Repeated measurements were conducted on the same collars on selected days during the growing season (Table 6). Measurements were carried out between $06-18h$ (12 cycles per day), at least once every 2 weeks between June and September 2013. Most CO_2 flux measurements were performed on sunny days, when peak (midday) light intensity was >1300 µmol m^{-2} s^{-1}. Net ecosystem CO_2 exchange (NEE), ecosystem respiration (R$_{eco}$) and soil respiration (R$_{soil}$) were sequentially observed with a systematic rotation over all plots using climate-controlled, manually operated, transparent and opaque chambers, respectively as described by Otieno et al. (2012), Lindner et al. (2014). The chambers measured 40 x 40 x 54 cm^3. Change in chamber CO_2 concentration over time was assessed with a portable, battery operated infrared gas analyzer (LI–820, LI–COR, USA).

CO_2 fluxes were calculated from a linear regression describing the time dependent change in CO_2 concentration within the chamber. Influence of the CO_2 concentration change on plant physiological response was ignored. Internal chamber temperature during the measurements was maintained within 1 °C relative to ambient, using dry ice packs mounted at the back of the chamber.

Gross primary production (GPP) was determined as:

$$\text{GPP} = \text{-NEE} + R_{eco}$$ **Equation 8**

where R_{eco} is Ecosystem respiration = the sum of plant respiration (R_P) and soil respiration (R_{soil}).

3.3.7. Empirical description of canopy responses

Empirical description of the measured NEE was performed with a non-linear least squares fit of the data to a hyperbolic light response model using Equation 9, also known as the Michaelis-Menten or rectangular hyperbola model (Owen et al., 2007)

$$NEE = -\frac{\alpha * \beta * PAR}{\alpha * PAR + \beta} + \gamma$$ **Equation 9**

where α is the initial slope of the curve and an approximation of the canopy light utilization efficiency (μmol CO_2 m^{-2} s^{-1}/ μmol photons m^{-2} s^{-1}), β is the maximum NEE of the ecosystem (μmol CO_2 m^{-2} s^{-1}), PAR is photosynthetic photon flux density (μmol photon m^{-2} s^{-1}), γ is an estimate of the average ecosystem respiration occurring during the observation period (μmol CO_2 m^{-2} s^{-1}). Since the rectangular hyperbola may saturate very slowly in terms of light, we used the value calculated from $\alpha\beta$*PAR/(α*PAR+β) for high light intensity levels (PAR = 1500 μmol m^{-2} s^{-1}) in this study. This value approximates the potential maximum GPP and can be thought of as the average maximum canopy uptake capacity during each observation period (noted here as (β+γ)$_{1500}$). The parameters (β+γ)$_{1500}$ (e.g. NEE at PAR = 1500 μmol m^{-2} s^{-1}) and γ were estimated for each day using NEE data from the four measurement plots per day.

Statistical analysis and best fits for light and curves were performed using Sigma Plot version 11.0.

3.3.8. Calculation of net-primary-production (NPP)

Net primary production equivalent to canopy net assimilation rate (NPP) is defined as:

NPP = GPP - R$_p$ **Equation 10**

Replacing GPP with Equation 8 leads to Equation 11:

NPP= -NEE + R$_{eco}$ − R$_P$ **Equation 11**

I.e.,

NPP = -NEE + R$_{soil}$ **Equation 12**

where soil respiration was described as being dependent on soil temperature (T$_{soil}$) by the function of Lloyd and Taylor (Lloyd and Taylor, 1994), normalized to 15°C,

$$R_{soil} = R_{soilref}e^{E_0\left(\frac{1}{T_{ref}-T_0}-\frac{1}{T_{soil}-T_0}\right)}$$ **Equation 13**

where T$_{ref}$ and T$_o$ are fixed to 15 and -46°C, respectively. E$_0$ depicting increasing amplitude of T$_{soil}$-temperature curve was considered to be a free parameter and was fitted to each data set. R$_{soilref}$ is reference soil respiration. Daily integrated NPP (NPP$_{int}$) was interpolated based on the hourly measurements using the parameterized light curves and PAR data recorded at the automatic weather station.

3.3.9. Biomass sampling

After CO_2 flux measurements, aboveground biomass enclosed by the 39.5 cm x 39.5 cm soil frame (for CO_2 flux measurements) was harvested at 3 randomly chosen locations (representing 3 replicates) in RF and PR. The aboveground biomass was sorted into leaves, grains, culms and dead material. Green leaf area (GLA) was determined with leaf area meter

(LI−3000A, LI−COR, USA) from the sampled leaves. All the biomass was oven-dried to a constant weight at 85°C for at least 48 hours. Green leaf area index (GLAI) was determined from total GLA within the 39.5 cm by 39.5 cm ground area and expressed per unit square meter.

3.3.10. Plant carbon and nitrogen determination

Sub-samples from the dried biomass of the respective collars (for CO_2 flux measurements) were ball-milled into fine powder, re-dried at 80°C and kept in a desiccator for further analysis. A small fraction of the dried samples (< 1 g) was analyzed for total carbon/ nitrogen (C/N) content (%) using C:N Analyzer 1500 (Carlo Erba Instruments, Milan, Italy).

3.3.11. Statistical analyses

Statistical analysis was performed using R (R Core Team, 2012). Significance level was set to $P \leq 0.05$. All variables were tested for normal distribution (Shapiro–Wilk-test) and homogeneity of variance (Levene-test). The sample sizes were the same for both RF and PR; hence we performed student t-test. Factor interactions were examined through regression analyses using the Pearson correlation test.

3.4. Results

3.4.1. Microclimate

Weather conditions during the growing season are summarized in Figure 15. The daily mean maximum solar radiation during the measurement period occurred in July and was 25 ± 1 MJ m^{-2} d^{-1} (Figure 15A). During NEE measurements using the transparent chambers, the light environments inside and outside the chambers were not significantly different. Inside the transparent chambers, the maximum PAR recorded during the measurements ranged between 1500 and 1800 µmol m^{-2} s^{-1}. Daily average air temperature increased steadily from 8°C in spring, to a maximum of 31°C in August (Figure 15B). Leaf temperatures were significantly different ($p < 0.01$) between PR and RF, but in each case the maximum temperatures of around 36°C in PR and 38°C in RF, were attained in August. The total amount of rainfall between May and September was 1028 mm (Figure 15C). Most of the rainfall occurred during late June to July, associated with the summer monsoon, and in September. VWC in the RF field ranged between 37.2 and 54.8% (Figure 15D), whereas the soils in PR were water-logged throughout the growing season. Relative humidity (rH) was significantly higher ($p < 0.01$) in PR then RF. The lowest rH occurred in August. Noon time average of rH was $78 \pm 1.4\%$ in PR and $53 \pm 2.3\%$ in RF. Consequently, the mean daily vapor pressure deficit (VPD) was significantly lower ($p < 0.01$) in PR then RF. The highest averaged day-time VPD values during our measurements occurred in July with 1.62 ± 0.58 kPa for PR and in August with 2.83 ± 0.93 kPa for RF (Figure 15D).
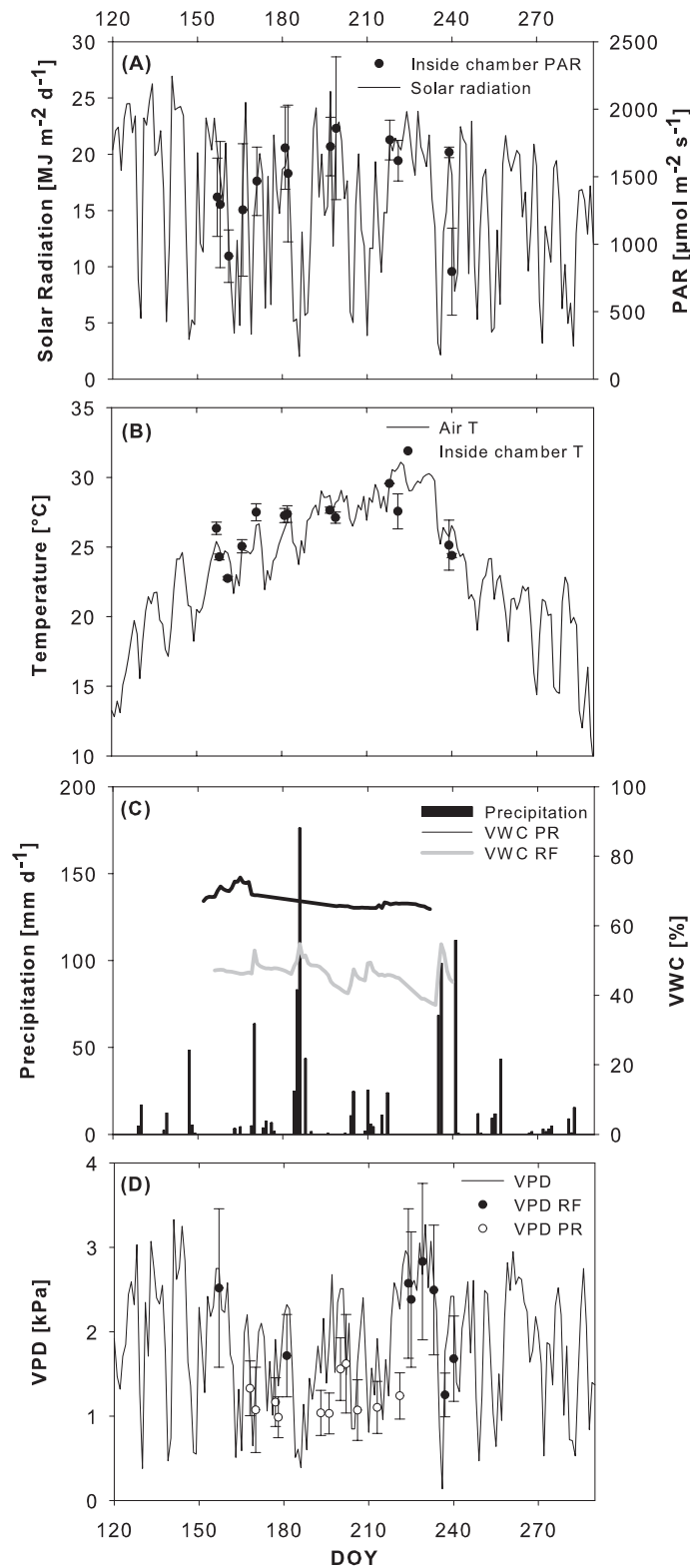
Figure 15: **(A) Daily solar radiation measured at 2 m height and photosynthetic active radiation (PAR) measured at 50 cm height above the vegetation inside the transparent CO_2 flux chambers, respectively, (B) mean air temperature at 2 m height outside and at 20 cm height inside the chambers, (C) volumetric water content (VWC) within 30 cm soil profile and daily precipitation, and (D) mean daily vapor pressure deficit (VPD) at 2 m height in the open location, at 1 m above the paddy rice (VPD PR) and rainfed rice (VPD RF), respectively.**

3.4.2. Daily and seasonal patterns of ecosystem CO_2 uptake

Examples of daily patterns of NEE and R_{eco} for three selected days corresponding to early (DOY 181/182), mid (DOY 218/221) and mature (DOY 240/239) growth stages in paddy/rainfed rice, respectively, are shown in Figure 16. On clear, sunny days, the maximum NEE during the day were recorded between 10h − 14h, with lower rates recorded during the earlier or later part of the day. R_{eco}, however, remained relatively constant during the day.

The mean maximum NEE rates during the vegetative period were -19.9±0.1 and -15.0±3.2 $\mu mol\, m^{-2}\, s^{-1}$ for PR and RF, respectively (Figure 16), while the respective maximum R_{eco} rates during the same period were 5.9 ± 0.1 and 28.6 ± 0.8 $\mu mol\, m^{-2}\, s^{-1}$. In both treatments, the timing of the peak NEE and R_{eco} coincided with the maximum green leaf area index (GLAI), occurring in July and August for PR and RF, respectively. The maximum integrated NEE (NEE_{int}) were -8.0 and -3.3 $gC\, m^{-2}\, d^{-1}$ in PR and RF, respectively. NEE_{int} was consistently, significantly higher in PR than in RF (Figure 17B). The daily integrated GPP (GPP_{int}) increased during the growing period, attaining its maximum rates of 11.1 $gC\, m^{-2}\, d^{-1}$ in PR and 12.0 $gC\, m^{-2}\, d^{-1}$ in RF, in July and August, respectively (Figure 17A).

Unlike NEE, the NPP (a measure of net plant C exchange) of PR and RF were not significantly different and the seasonal patterns were relatively similar, except for the one month delay in peak NPP in the RF compared to PR (Figure 17C). The maximum integrated NPP (NPP_{int}) were 8.2 $gC\, m^{-2}\, d^{-1}$ in PR and in 10.3 $gC\, m^{-2}\, d^{-1}$ in RF (Figure 17C).
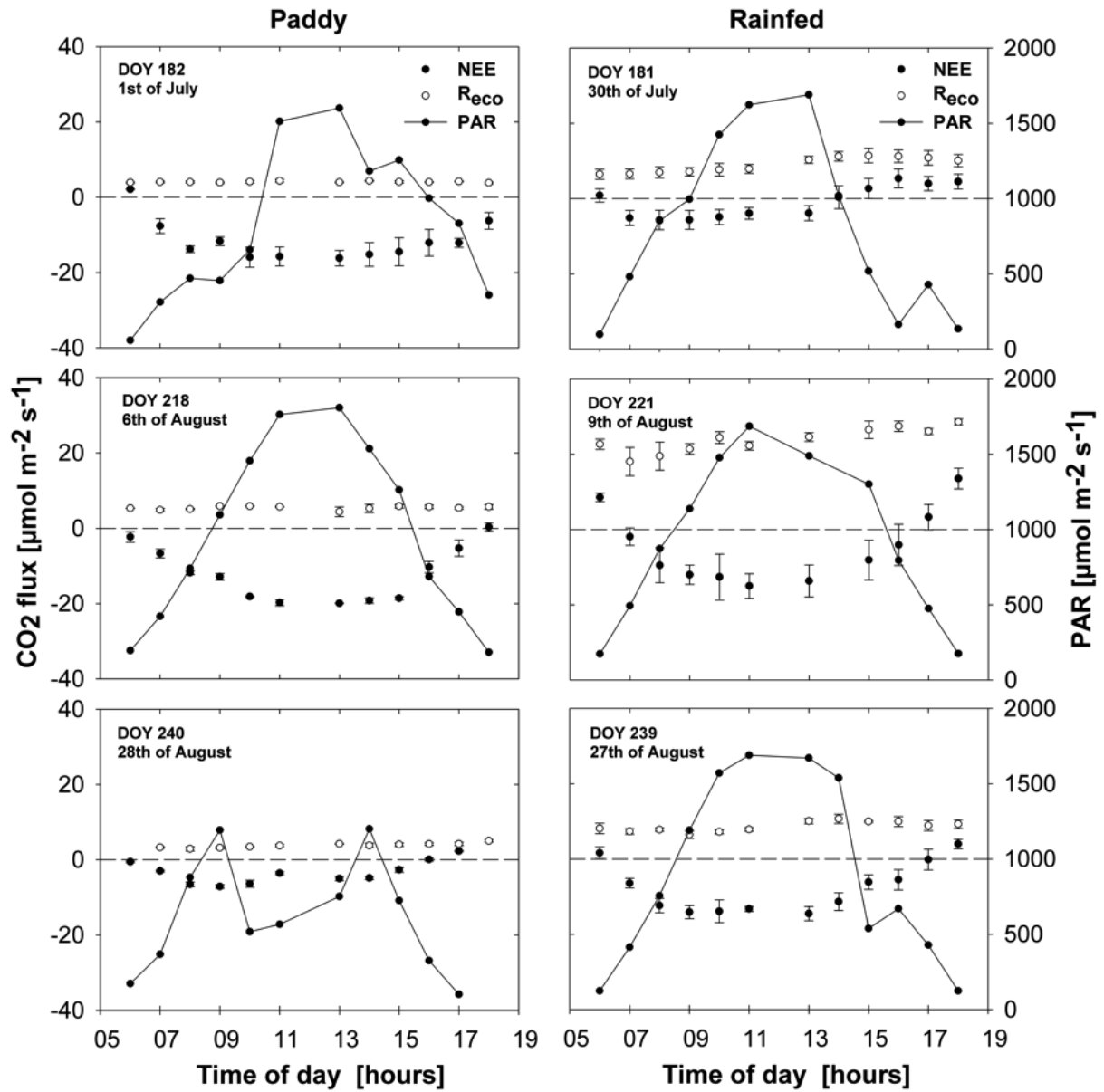
Figure 16: Daily trends of NEE and R$_{eco}$ in paddy rice (left panel) and rainfed rice (right panel), with light intensities (PAR, black line) on selected days during the development period. Data points are means of respective fluxes measured on the four collar plots.
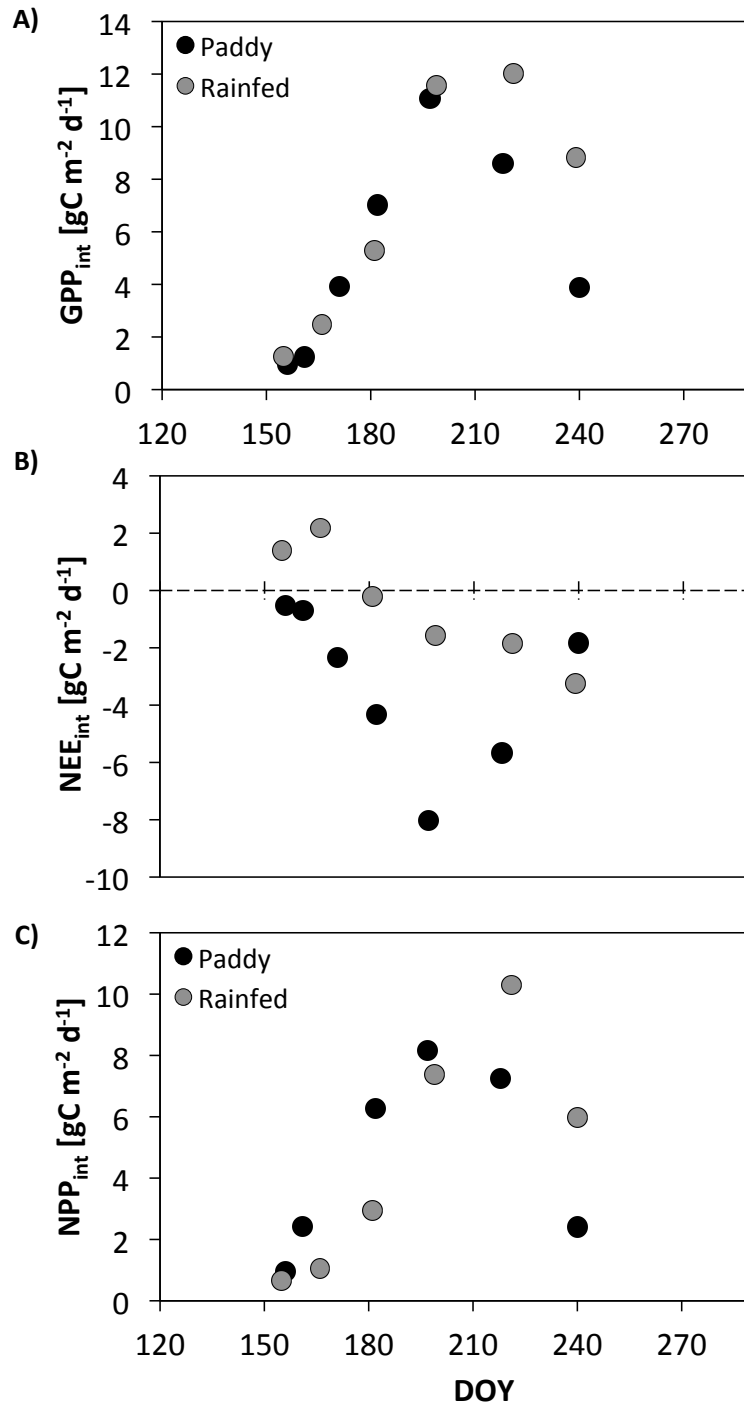
Figure 17: Seasonal changes in (A) daily gross primary production (GPP$_{int}$), (B) daily net ecosystem exchange (NEE$_{int}$) and (C) net primary production (NPP$_{int}$) of paddy (black circles) and rainfed rice (grey circles) derived from α and β of the hyperbolic light response curve (Table 6).

More than 80% of the daily fluctuations in GPP, both in the PR and RF (Figure 18), were explained by PAR. The functional relationship between GPP and PAR was, therefore, used to derive canopy physiological parameters for describing canopy physiology at different stages

of crop developmental (Table 6). Simulated potential maximum canopy GPP at near-saturating PAR (= 1500 μmol m^{-2} s^{-1}), i.e. $((\beta+\gamma)_{1500})$ were 25.3 and 27.4 μmol m^{-2} s^{-1} in PR and RF, while the respective maximum quantum yields (or light use efficiency, α) were -0.047 and -0.098 (μmol CO_2 m^{-2} s^{-1}/ μmol photons m^{-2} s^{-1}).
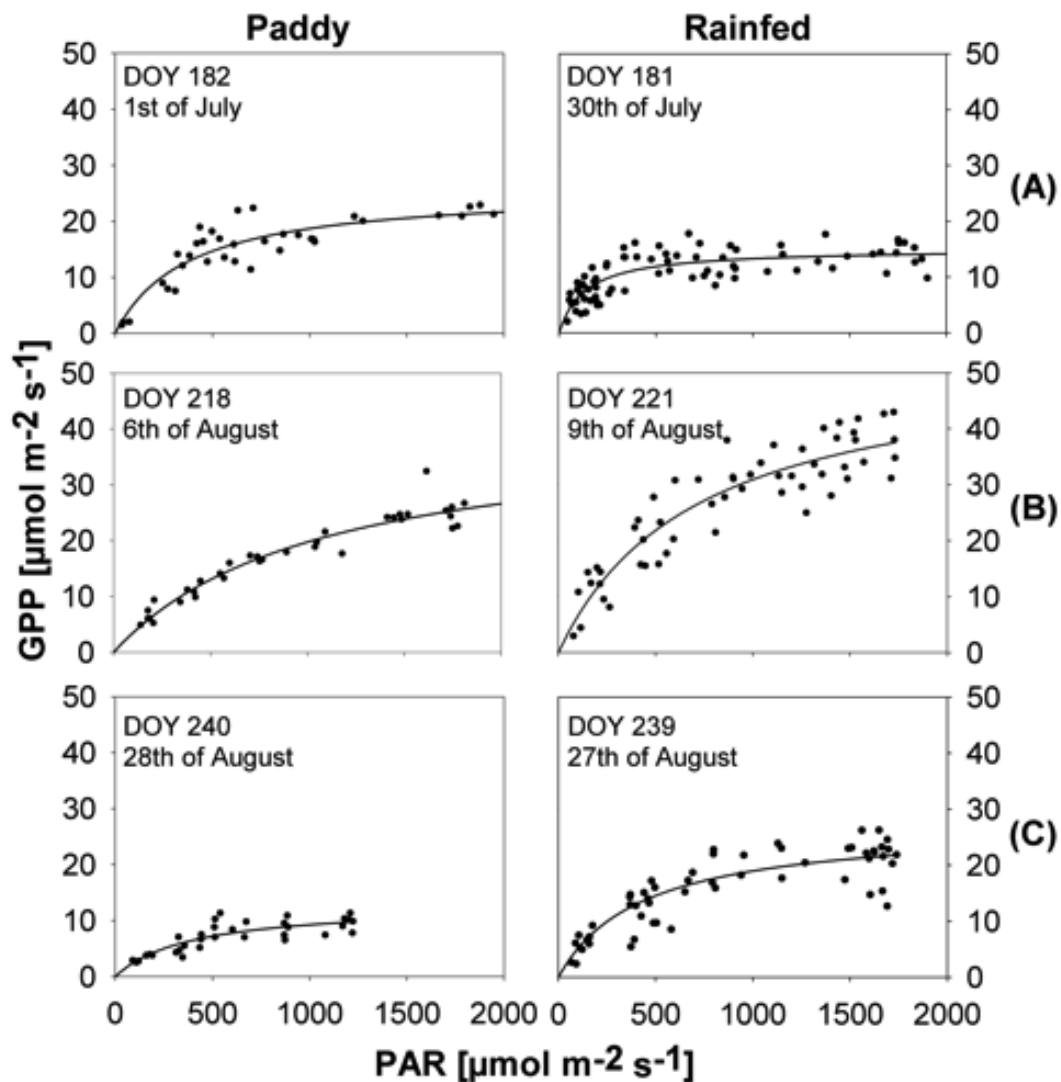
Figure 18: Response of CO_2-Assimilation to changing light intensities of paddy (left panels) and rainfed (right panels) rice representing three distinct phenological stages (Top panels – initial growth season, middle panels – mid season, lower panels – maturity) during the development of the rice crop.

Table 6: Quantum yield (α), Potential maximum GPP and the coefficient of determination (R^2) of the relation between NEE and PAR in A) paddy (PR) and B) rainfed rice (RF) in 2013.

DOY		γ	S. E.	α	S. E.	β	S. E.	R^2	$(β+γ)_{1500}$
A) PR	158	0.66	0.04	-0.006	0.001	-3.51	0.22	0.96	2.56
	161	0.83	0.04	-0.007	0.001	-8.71	1.32	0.89	4.70
	171	2.45	0.26	-0.019	0.002	-18.32	6.53	0.96	11.17
	182	4.15	0.28	-0.036	0.008	-25.27	1.16	0.97	17.20
	197	4.70	0.40	-0.047	0.007	-39.59	3.43	0.95	25.31
	218	4.50	0.23	-0.035	0.003	-39.50	2.74	0.97	22.40
	240	3.15	0.23	-0.025	0.005	-13.53	1.90	0.85	9.95
B) RF	157	4.06	1.04	-0.009	0.010	-3.47	0.70	0.86	2.77
	166	7.16	0.47	-0.011	0.002	-14.24	1.71	0.93	7.51
	181	7.85	0.16	-0.047	0.005	-15.21	0.56	0.97	12.52
	199	15.40	0.29	-0.098	0.012	-29.79	1.19	0.99	24.76
	221	15.69	0.36	-0.090	0.012	-34.34	0.53	0.97	27.38
	239	8.62	0.28	-0.055	0.006	-30.04	1.55	0.95	21.98

3.4.3. Biomass, leaf area and leaf N content

The total aboveground biomass (leaves, stems and grain) was 1.85 ± 0.27 and 2.16 ± 0.28 kg m^{-2} of which 0.24 ± 0.06 and 0.31 ± 0.05 kg m^{-2} was apportioned to the leaves in PR and RF, respectively. Peak biomass was attained in July in the PR fields, while it occurred a month later in RF, coinciding with the respective peak green leaf area index (GLAI) of 5.4 ± 1.1 and 4.9 ± 0.5 $m^2 m^{-2}$ (Figure 19A & B). Total crop yield (harvested grain) was 1.19 ± 0.10 and 1.16 ± 0.09 kg m^{-2}, which was equivalent to 6.61 ± 0.22 and 5.99 ± 0.68 t ha^{-1} in PR and RF, respectively. While RF fields had 0.62 t ha^{-1} more yield than PR, the two were not significantly different. We however, observed significant differences between PR and RF in their C allocation patterns (i.e. allocation to the leaf, stem and grain) (see Table 7). During the early stages of growth, a large proportion of carbon was directed to leaf development both in the PR and RF. At maturity, grains accounted for 64.4 and 53.9% of the total aboveground biomass in PR and RF, respectively. Leaf N content was significantly higher in RF than PR and leaf N content declined with age (Table 7).

Table 7: Percentage of carbon allocated in the aboveground biomass for the respective crop organ and leaf nitrogen content in paddy and rainfed rice.

DOY		Leaf-C [%]	Culm-C [%]	Grain-C [%]	Leaf-N [%]
A) Paddy Rice	158	65.52	34.48		4.41
	161	59.96	40.04		4.64
	171	45.66	54.34		2.88
	182	48.94	51.06		3.12
	197	28.93	71.07		2.77
	218	15.28	39.39	45.33	2.58
	240	6.34	29.27	64.39	1.42
B) Rainfed Rice	157	62.50	37.50		5.24
	166	65.00	35.00		4.79
	181	32.54	67.46		4.39
	199	36.03	63.97		3.72
	221	22.07	58.20	19.74	3.58
	239	10.96	35.10	53.89	3.05
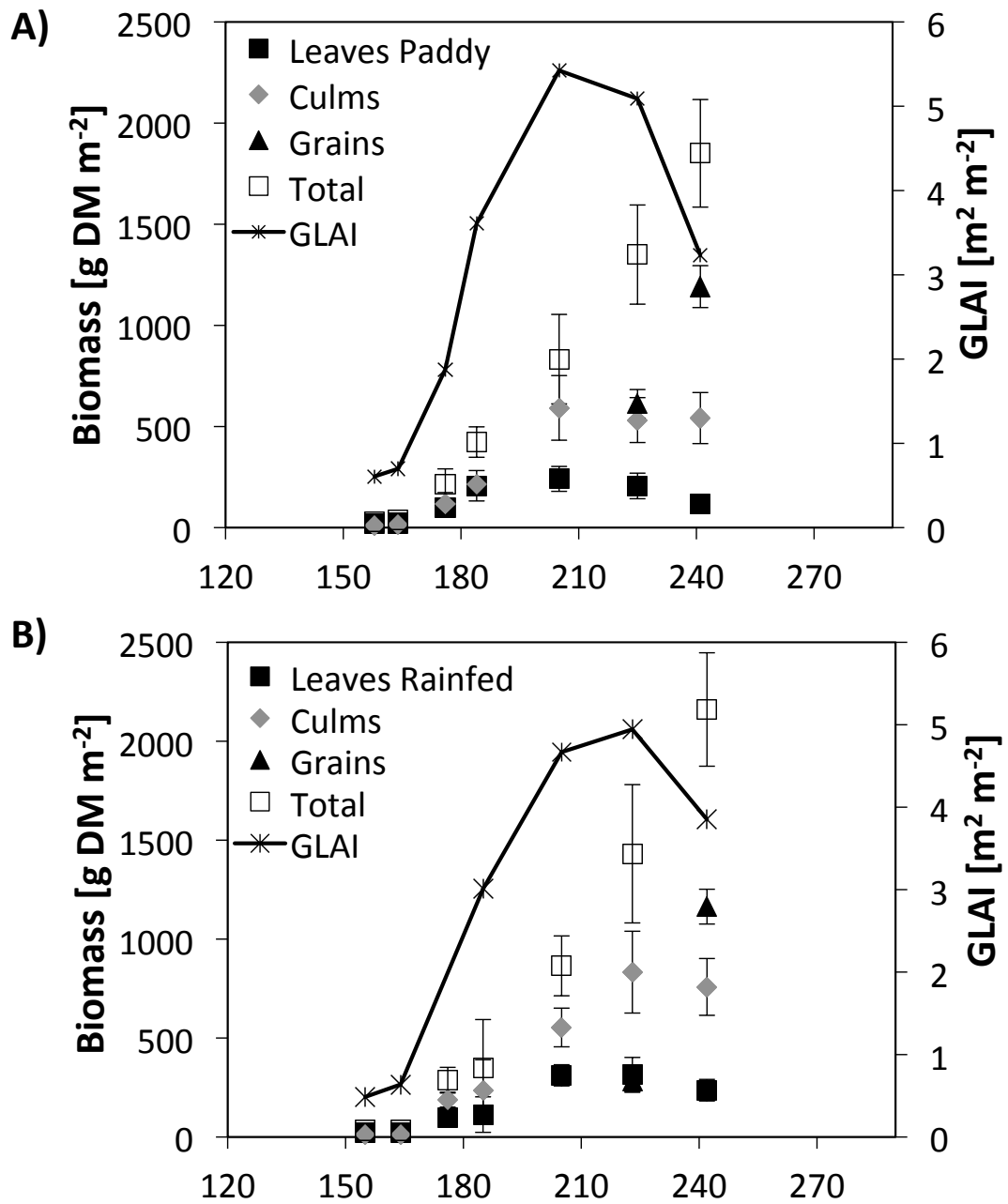
Figure 19: Dry weight [g DM m^{-2}] of leaves, culms, grains and green leaf area (GLAI) of the CO$_2$-measurement chambers during crop development in A) paddy and B) rainfed rice. Harvest was done after the CO$_2$ plot measurements.

3.4.4. Regulation of CO_2 uptake

At any time during the growing period, the maximum GPP rates (GPP_{max}) on a clear sunny day were linearly correlated ($R^2 = 0.87$ and 0.98, for PR and RF, respectively) with GLAI (Figure 20A) and α ($R^2 = 0.89$ and 0.96) (Figure 20B). Also, α was positively correlated ($R^2 = 0.93$ and 0.94) with GLAI (Figure 20C). Compared to PR, RF demonstrated higher light use efficiency at higher GLAI. In both PR and RF, α was also sensitive to leaf N content and increased at higher leaf N content ($R^2 = 0.86$ and 0.99, Figure 20D).
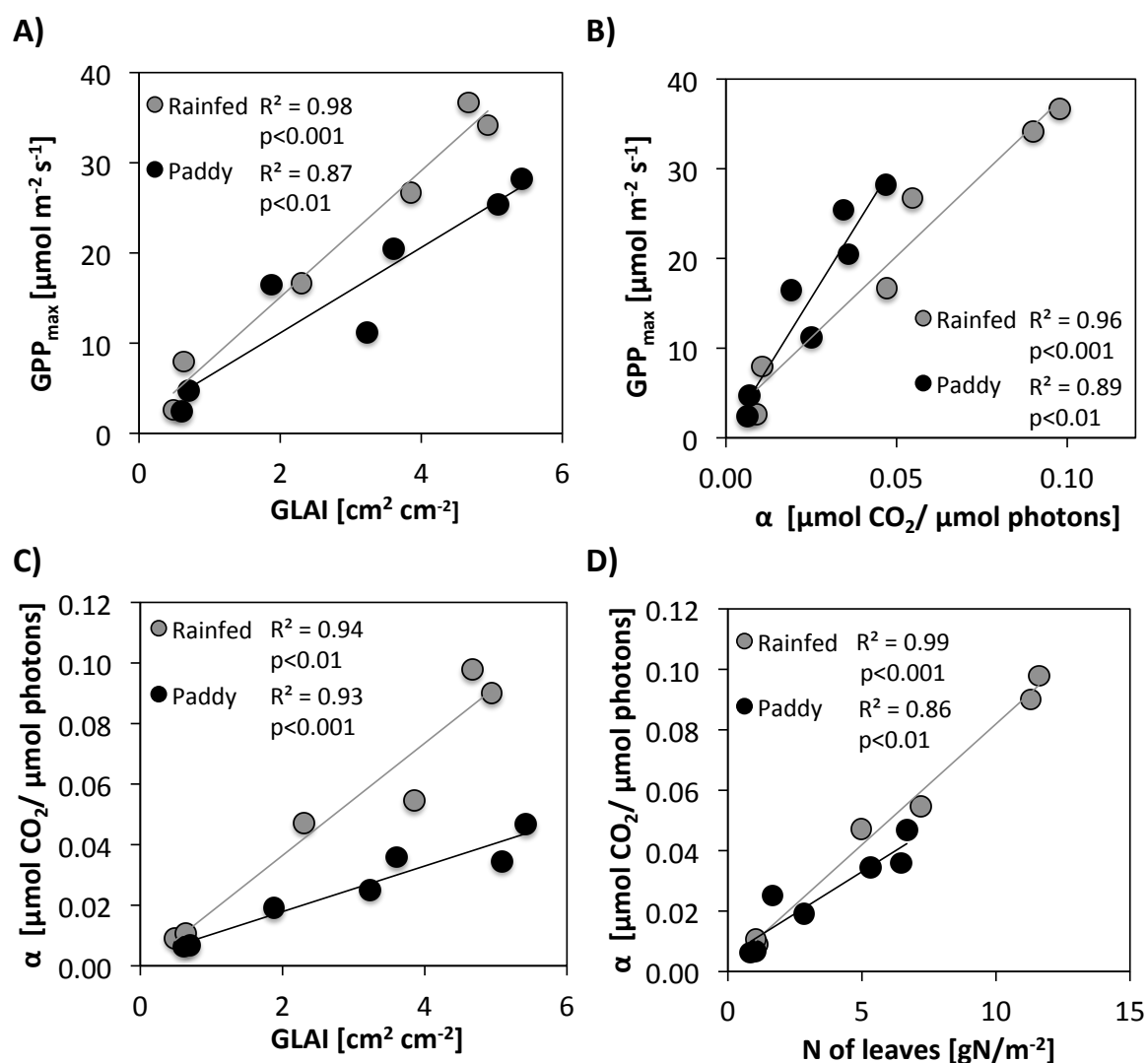
Figure 20: GPP_{max} response to (A) green leaf area index (GLAI) and (B) light use efficiency (α), while (C) describes the changes in α in response to changing GLAI and (D) the influence of leaf nitrogen (N) on light use efficiency (α) in the rainfed and paddy rice.

3.5. Discussion

In paddy rice production, the common practice is to raise seedlings in seedbeds before transplanting them into flooded fields, a process which requires 3 – 4 weeks (Cabangon et al., 2002). In the meantime, the prepared fields are flooded with water, awaiting seedling transplantation. Water loss through seepage and percolation during this period is estimated at 25 mm d^{-1}, while evaporation accounts for 2 mm d^{-1} (Tuong and Bouman, 2003). Direct seeding as in RF removes the need for irrigation and the idle period during land preparation (Bhuiyan et al., 1995), but the growing period is longer compared to PR (see Table 5). The amount of saved water, therefore, will depend on the balance between the reduction in water use caused by shortened land preparation and the increase in water use caused by the long vegetation period (Cabangon et al., 2002). Our study was, however, limited in capacity and could not provide these details. On the other hand, direct-seeded rice was planted earlier in the field compared to paddy rice. The amount of rainfall received between the two out-planting periods was 63.9 mm. Given an evapotranspiration rate of 1.2 mm d^{-1} for a young RF field (Nay-Htoon et al., in prep.), we deduce that 52.6% of this rainwater was put to productive use. Early establishment of rice, therefore, promotes better use of early season rainfall, and may be associated with improved yield and reliability.

A characteristic of paddy rice fields is the prevailing high humidity and low VPD above the rice canopy (Alberto et al., 2009), which supports full stomatal opening during midday, when radiation is at its peak. This ensures maximum CO_2 assimilation and GPP rates at a time when transient water stress due to high VPD negatively affects CO_2 uptake by the vegetation as a result of stomatal closure in most terrestrial plants (Wopereis et al., 1996; Alberto et al., 2009). The mean maximum VPD measured in the PR field was 1.62 kPa compared to 2.83 kPa in the RF field. VPD differences between the two fields, however, had no significant influence on leaf photosynthesis (Xue et al., subm.) and canopy GPP (Figure 16). Instead, canopy GPP (Figure 17A) in both PR and RF attained and sustained saturation rates during

most of the bright sunny days. In both cases, more than 80% of the daily GPP fluctuations were explained by PAR (Figure 18). Thus, we can speculate that, despite growing on non-saturated soils, root water uptake by RF is potentially adequate to sustain the maximum photosynthesis, under environmental conditions similar to ours. This is demonstrated by similar NPP between PR and RF during the growing period (Figure 17C). It is however not clear why development stops and maturity attained earlier in the RF crops.

While significant declines in VWC within the top 30 cm soil profile were recorded in RF during periods without rainfall (Figure 15C), the plants did not show signs of water stress. Possible reasons include 1) extensive rooting system that access stable soil moisture below 30 cm depth (Kato et al., 2006b; Kato et al., 2007), 2) large root biomass (Kato et al., 2006a) and 3) osmotic adjustment that facilitate effective water uptake from the drying soil (Munns, 1988). Such adjustments, which promote improved soil water uptake, however, shift C from the aboveground organs and were likely to lower yield in RF (Munns et al., 1988). Alberto et al. (2013) reported maximum GPP rates of 30 μmol m^{-2} s^{-1} under moderate VPD, while GPP was not sensitive to declining VWC within the top 10 cm soil profile, as long as SWC in deeper soil layers (>15 cm) was >21%. They attributed such responses to large root biomass located in the soil layers deeper than >15 cm. In our case, the maximum GPP recorded for PR was 26.7 μmol m^{-2} s^{-1} compared to 43.1 μmol m^{-2} s^{-1} in RF (Figure 18). GPP rates reported previously for Asian paddy rice range between 10 and 56 μmol m^{-2} s^{-1} (Miyata et al., 2000; Campbell, 2001; Saito et al., 2005), while the rates reported for rainfed rice in Asia range from 4 – 40 μmol m^{-2} s^{-1} (Alberto et al., 2009, 2013; Centritto et al., 2009). Given that NPP was not significantly different between PR and RF, lower GPP in the PR compared to RF in our study was partly due to lower R_{eco} measured in the PR field (ref. Equation 8). It is likely that a significant amount of CO_2 generated from root and soil respiration was lost in the water column and was not registered by the analyzer. Diffusion rate of gases in the flooded

compared to dry soils is 100 times lower, leading to reduced gas exchange between root tissues and the atmosphere (Armstrong and Drew, 2002).

In paddy rice, GPP is positively correlated with the aboveground biomass until maturity (Campbell et al., 2001; Alberto et al., 2013). This implies that the bulk of the NPP is allocated in the aboveground biomass (Smith et al., 2010), unlike in RF, where root development is also critical. Surprisingly, the maximum aboveground biomass recorded in RF was 2400 g m^{-2} compared to 1800 g m^{-2} in PR (Figure 19). The need for structural support in RF could be one reason for higher C allocation to the culms compared to PR, which partially relies on hydrostatic support of the standing water. Approximately 13% of the total aboveground biomass was allocated to the leaves in PR compared to 29% in RF. The higher leaf mass in RF was predominantly due to increased leaf thickness as opposed to leaf area (higher specific leaf weight), since GLAI were not significantly different between them (Figure 19). This could be a strategy in RF to increase photosynthetic efficiency, while checking on run-away transpiration. Due to this high leaf biomass, RF potentially could perform higher productivity, contributing to the observed higher GPP. It is likely that a large portion of this productivity is invested in securing sufficient soil water uptake (Munns et al., 1988). Higher GPP in RF is supported by the higher specific leaf weight, higher leaf N content (Table 7) and higher quantum yield. That the total yield between PR and RF were not significantly different, despite significant differences in GPP was not surprising. We speculate that in addition to investing proportionately larger amounts of C in structural support of the erect stems, RF invested a significant amount of carbon in order to improve root water uptake through increased root biomass and osmotic adjustment. This needs further investigations and we recommend more studies along these lines.

The yield in rain fed rice currently stands at 2.3 t ha^{-1} (Toung and Bouman, 2003), but drought-resistant cultivars produced yield levels of $5-6$ t ha^{-1}. Bouman et al. (2007) calculated that the country-average paddy rice yields in Asia ranges between 3 and 9 t ha^{-1},

with an overall average of about 5 t ha^{-1}. Alberto et al. (2009), Frageria and Baligar (2001) reported an average grain yield of 5.2 – 6.3 t ha^{-1} for paddy rice. Peng et al. (2006) found minor reduction in yields in RF compared to PR, with 6.32 and 7.78 t ha^{-1}, respectively, and no significant differences in yield (7.22 t ha^{-1} for RF and 7.84 t ha^{-1} for PR) of a variety that was adapted to both flooded and aerobic conditions. These values are comparable to our results. The results demonstrate that under ample soil moisture supply both PR and RF develop relatively similar canopies and comparable yield.

3.6. Conclusion

We conclude that with adequate rainfall, the new hybrid Unkwang rice variety has the potential to grow as direct seeded, rainfed rice, attaining yields that are comparable to paddy conditions. When grown as rainfed rice, Unkwang exhibits higher GPP, but it is likely that a significant portion of this GPP is apportioned to the roots to ensure improved water uptake. Improved leaf N and higher specific leaf weight result into higher quantum yield, contributing to improved productivity in RF. On a daily basis, PAR determined the daily fluctuations in GPP while seasonal GPP differences were due to GLAI and α differences. While direct seeding as in the RF eliminates the need for irrigation, maximizes the use of early rain events and is likely to require less water, it extends the production period. This study demonstrates the potential of Unkwang as a high yielding variety suitable for promoting rice production under rainfed conditions without extended soil drying. We recommend further studies to determine the amount of water that can be saved through using Unkwang cropped under rainfed conditions.

3.7. Acknowledgements

3.8. References

Alberto, M.C.R., Wassmann, R., Hirano, T., Miyata, A., Kumar, A., Padre, A., Amante, M., 2009. CO_2/heat fluxes in rice fields: Comparative assessment of flooded and non-flooded fields in the Philippines. Agric. For. Meteorol. 149, 1737–1750.

Alberto, M.C.R., Buresh, R.J., Hirano, T., Miyata, A., Wassmann, R., Quilty, J.R., Correa, T.Q., Sandro, J., 2013. Carbon uptake and water productivity for dry-seeded rice and hybrid maize grown with overhead sprinkler irrigation. F. Crop. Res. 146, 51–65.

Armstrong, W., Drew, M.C., 2002. Root growth and metabolism under oxygen deficiency. In: Waisel, Y., Eshel, A., Kafkafi, U. (Eds.), Plant Roots: The Hidden Half. , 3rd ed. Marcel Dekker, New York, pp. 729–761.

Barker, R., Dawe, D., Tuong, T.P., Bhuiyan, S.I. and Guerra, L.C. 1999. The outlook for water resources in the year 2020 : challenges for research on water management in rice

production. In: Assessment and Orientation towards the 21st Century. Proceedings of 19th session of the International Rice Commission, Cairo, Egypt, 7-9 September 1998. Rome, Italy : FAO. 96-109.

Bouman, B.A.M., Lampayan, R.M., Tuong, T.P., 2007. Water management in irrigated rice: coping with water scarcity. Los Baños (Philippines): International Rice Research Institute. 54 p.

Busch, J., 2001. Characteristic values of key ecophysiological parameters in the genus Carex. Flora 196, 405–430.

Bhuiyan, S.I., Sattar, M.A., Khan, M.A.K., 1995. Improving water use efficiency in rice irrigation through wet seeding. Irri. Sci. 16, 1–8.

Cabangon, R.J., Tuong, T.P., Abdullah N.B., 2002. Comparing water input and water productivity of transplanted and direct-seeded rice production systems. Agric. Water Manage. 57, 11–31.

Campbell, C.S., Heilman, J.L., McInnesa, K.J., Wilson, L.T., Medley, J.C., Wu, G., Cobos, D.R., 2001. Diel and seasonal variation in CO_2 flux of irrigated rice Colin Agric. For. Meteorol. 108, 15–27.

Centritto, M., Lauteri, M., Monteverdi, C.M., Serraj, R., 2009. Leaf gas exchange, carbon isotope discrimination, and grain yield in contrasting rice genotypes subjected to water deficits during the reproductive stage. J. Exp. Bot. 60, 2325–2339.

Colmer, T.D., Gibberd, M.R., Wiengweera, A., Tinh, T.K., 2003. The barrier to radial oxygen loss from roots of rice (*Oryza sativa* L.) is induced by growth in stagnant solution. J. Exp. Bot. 49, 1431–1436.

Fageria, N.K., Baligar, V.C., 2001. Lowland rice response to nitrogen fertilization. Soil Sci. Plant Analysis 32, 1405-1429.

IPCC, 2008. Appendix A to the Principles Governing IPCC Work. Geneva: Intergovernmental Panel on Climate Change, first edition 1999, last amended 2008 (http://ipcc.ch/pdf/ipcc-principles/ipcc-principles-appendix-a.pdf)

IRRI, 2002. Progress toward developing resilient crops for drought-prone areas- Abstracts of the workshop May 27-30, 2002. Los Banos, Philippines http://www.irri.org/publications/limited/pdfs/ResilientCrops.pdf

Kato, Y., Kamoshita, A., Yamagishi, J., Abe, J., 2006a. Growth of three rice (Oryza sativa L.) cultivars under upland conditions with different levels of water supply. I. Nitrogen content and dry matter production. Plant Prod. Sci. 9, 422–434.

Kato, Y., Abe, J., Kamoshita, A., Yamagishi, J., 2006b. Genotypic variation in root growth angle in rice (Oryza sativa L.) and its association with deep root development in upland fields with different water regimes . Plant Soil 287, 117–129.

Kato, Y., Kamoshita, A., Yamagishi, J., Imoto, H., Abe, J., 2007. Growth of Rice (Oryza sativa L.) Cultivars under Upland Conditions with Different Levels of Water Supply 3. Root

System Development, Soil Moisture Change and Plant Water Status. Plant Prod. Sci. 10, 3-13.

Kim, K.Y., Ha, K.Y., Ko, J.C., Choung, J.I., Lee, J.K., Ko, J.K., Kim, B.K., Nam, J.K., Shin, S.S., Choi, Y.H., Kim, Y.D., Oh, M.K., Kim, Y.K., Kim, C.K., Jung, K.Y., 2006. A new early maturity rice cultivar, "Unkwang" with high grain quality and cold tolerance. Korean J. Breed. 38, 261-262.

Kotula, L., Ranathunge, K., Steudle, E., 2009. Apoplastic barriers effectively block oxygen permeability across outer cell layers of rice roots under deoxygenated conditions: roles of apoplastic pores and of respiration. New Phytol. 184, 909-917.

Lindner, S., Otieno, D., Lee, B., Xue, W., Arnhold, S., Kwon, H., Huwe, B., Tenhunen, J., 2014. Carbon dioxide exchange and its regulation in the main agro-ecosystems of Haean catchment in South Korea. Agric. Ecosyst. Environ. 199, 132-145.

Lloyd, J., Taylor, J.A., 1994. On the temperature dependence of soil respiration. Funct. Ecol. 8, 315–323.

McDonald, M.P., Galwey, N.W., Colmer, T.D., 2002. Similarity and diversity in adventitious root anatomy as related to root aeration among a range of wetland and dryland grass species. Plant Cell Environ. 25, 441–451.

Miyata, A., Leuning, R., Denmead, O.T., Kim, J., Harazono, Y., 2000. Carbon dioxide and methane fluxes from an intermittently flooded paddy field. Agric. For. Meteorol. 102, 287–303.

Moog ,P.R., Brüggemann, W., 1998. Flooding tolerance of Carex species. II. Root gas-exchange capacity. Planta 207, 199–206.

Munns, R., 1988. Why Measure Osmotic Adjustment? Australian Journal of Plant Physiology 15, 717–726.

Nay-Htoon, B., Xue, W, Dubbert, M., Lindner, S., Jeong, S., Fu, T., Kim, M., Cuntz, M., Ko, J., Tenhunen, J., Werner, Ch., in prep. Water use efficiency of rainfed and paddy rice (*Oryza sativa*): Is flux partitioning crucial to understand water use efficiency?

Okami, M., Kato, Y., Yamagishi, J., 2013. Grain yield and leaf area growth of direct-seeded rice on flooded and aerobic soils in Japan. Plant Prod. Sci. 16, 276-279.

Otieno, D., Lindner, S., Muhr, J., Borken, W., 2012. Sensitivity of peatland herbaceous vegetation to vapor pressure deficit influences net ecosystem CO_2 exchange. Wetlands 32, 895–905.

Owen, K.E., Tenhunen, J., Reichstein, M., Wang, Q., Falge, E., Geyer, R., Xiao, X., Stoy, P., Ammann, C., Arain, A., Aubinet, M., Aurela, M., Bernhofer, C., Chojnicki, B.H., Granier, A., Gruenwald, T., Hadley, J., Heinesch, B., Hollinger, D., Knohl, A., Kutsch, W., Lohila, A., Meyers, T., Moors, E., Moureaux, C., Pilegaard, K., Saigusa, N., Verma, S., Vesala, T., Vogel, C., 2007. Linking flux network measurements to continental scale simulations: ecosystem carbon dioxide exchange capacity under non-water-stressed conditions. Global Change Biol. 13, 734–760.

Peng, S., Bouman, B., Visperas, R.M., Castañeda, A., Nie, L., Park, H.K., 2006. Comparison between aerobic and flooded rice in the tropics: Agronomic performance in an eight-season experiment. Field Crops Res. 96, 252-259.

R Core Team, 2012. R: a language and environment for statistical computing. R Foundation for Statistical Computing, Vienna. URL http://www.R-project.org/. ISBN 3-900051-07-0.

Ranathunge, K., Kotula, L., Steudle, E., Lafitte, R., 2004. Water permeability and reflection coefficient of the outer part of young rice roots are differently affected by closure of water channels (aquaporins) or blockage of apoplastic pores. J. Exp. Bot. 55, 433–447.

Saito, M., Miyata, A., Nagai, H., Yamada, T., 2005. Seasonal variation of carbon dioxide exchange in rice paddy field in Japan. Agric. For. Meteorol. 135, 93–109.

Smith, P., Lanigan, G., Kutsch, W.L., Buchmann, N., Eugster, W., Aubinet, M., Ceschia, E., Béziat, P., Yeluripati, J.B., Osborne, B., Moors, E.J., Brut, A., Wattenbach, M., Saunders, M., Jones, M., 2010. Measurements necessary for assessing the net ecosystem carbon budget of croplands. Agric. Ecosyst. Environ. 139, 302–315.

Sperry, J.S., 2000. Hydraulic constraints on plant gas exchange. Agric. For. Meteorol. 104, 13–23.

Tuong, T.P., Bouman, B.A.M., 2003. Rice Production in Water-scarce Environments. IRRI, Manila, Philippines. ISBN 0851996698

Wada, H., Masumoto-Kubo, C., Gholipour, Y., Nonami, H., Tanaka, F., Erra-Balsells, R., Tsutsumi, K., Hiraoka, K., Morita, S., 2014. Rice chalky ring formation caused by temporal reduction in starch biosynthesis during osmotic adjustment under foehn-induced dry wind. PLoS One 9(10).

Wopereis, M.C.S., Kropff, M.J., Maligaya, A.R., Tuong, T.P., 1996. Drought-stress responses of two lowland rice cultivars to soil water status. Field Crops Res. 46, 21–39.

Xue, W., Nay-Htoon, B., Lindner, S., Dubbert, M., Ko, J., Werner, Ch., Tenhunen, J., subm. Regulations of efficient carbon gain and water use in rice from leaf to canopy scale: role of resource distribution and CO_2 diffusion conductance.

Chapter 4

4. Nutritional and developmental influences on components of rice crop light use efficiency

Wei Xue[1,2]; Steve Lindner[1]; Bhone Nay-Htoon[3]; Maren Dubbert[3,6]; Dennis Otieno[1], Jonghan Ko[4]; Hiroyuki Muraoka[5]; Christiane Werner[3,6]; John Tenhunen[1]; Peter Harley[1]

(1) Department of Plant Ecology, BayCEER, University of Bayreuth, 95440 Bayreuth, Germany

(2) State Key Laboratory of Desert and Oasis Ecology, Xinjiang Institute of Ecology and Geography, Chinese Academy of Sciences, 830011 Urumqi, China

(3) Department of Agroecosystem Research, BayCEER, University of Bayreuth, 95440 Bayreuth, Germany

(4) Department of Applied Plant Science, Chonnam National University, 500757 Gwangju, South Korea

(5) River Basin Research Center, Gifu University, 1-1 Yanagido, Gifu, 501-1193 Japan

(6) Department of Ecosystem Physiology, University of Freiburg, 79085 Freiburg, Germany

4.1. Abstract

Light use efficiency (LUE) plays a vital role in determination of crop biomass and yield. Important components of LUE, i.e. canopy structure, nitrogen distribution, photosynthetic capacity and CO_2 diffusion conductance were investigated in paddy rice grown under low, normal and high supplemental nitrogen (0, 115, and 180 kg N ha^{-1}). Photosynthetic characteristics varied linearly with leaf nitrogen content (N_a), independent of treatment and canopy position, so differences in photosynthesis were due to differences in N allocation. CO_2 diffusion resistances were significant and constrained LUE (more during late season), but there were no differences between treatments. Early in the season (tillering stage) leaves in the fertilized treatments had higher photosynthetic rates due to higher leaf N content leading to larger amounts of rate-limiting photosynthetic proteins, which gave them an early head start and boost in productivity and leaf area index, bringing increases in canopy light absorption. Later during the growth season, differences in leaf N_a and photosynthetic characteristics between treatments were slight. Enhanced LAI in fertilized plots throughout the growing season was related to greater leaf number and leaf area per planted bundle and a larger leaf area in the upper canopy (LAUC). Fertilized treatments had a higher LAUC with high leaf nitrogen concentration and reduced mesophyll diffusion limitation but greater exposure to full sunlight that led to improved nitrogen use efficiency and efficient carbon gain. In conclusion, differences in carbon gain and biomass accumulation under differing N fertilization were associated primarily with resource allocation associated with canopy leaf area development rather than leaf morphological or physiological properties. The results provide new insights with respect to the multi-dimensional coordinated structural and physiological adjustments governing LUE over the course of rice crop development.

4.2. Introduction

As proposed by Monteith (1972, 1977) ecosystem or crop productivity is largely determined by the amount of solar radiation intercepted and the efficiency with which that absorbed energy is converted to carbohydrates in the process of photosynthesis. The percentage of incident photosynthetically active radiation that is absorbed by a plant canopy (APAR) is largely determined by canopy architecture (leaf area index, leaf angle distribution) and leaf pigments, while the efficiency of energy conversion is a function of leaf physiological processes. Although light use efficiency (LUE) has been equated with quantum use efficiency in the plant physiology literature (Ehleringer and Pearcy, 1983), in the remote sensing and crop production communities, LUE is defined as total carbon uptake (Gitelson and Gamon, 2015), integrated over some period of time divided by the total irradiance incident on or absorbed by the vegetation.

LUE of developing crops therefore depends on canopy leaf area and leaf angle distribution which determine light interception, on the distribution of nitrogen in the canopy as it relates to the profile of photosynthetic capacity, and on diffusional limitations which restrict delivery of CO_2 to the site of fixation (Parry et al., 2011). Until recently, the only diffusional limitations considered were boundary layer and stomatal conductances. Recent progress in the analysis of leaf gas exchange, however, has elucidated an additional component of leaf structure and function that significantly affects crop photosynthesis, namely the mesophyll conductance of the leaves, g_m (Ethier and Livingston, 2004; Niinemets et al., 2009A).

Depending on the magnitude of g_m, the CO_2 gradient between substomatal cavities and the chloroplast stroma varies, which impacts the physiology of photosynthesis and, over the long-term, influences natural selection along ecological gradients (Muir et al. 2014; Flexas et al., 2012; Niinemets et al., 2009B), and g_m has been identified as an important factor in regulation of crop primary production (Adachi et al., 2013; Parry et al., 2011). Mesophyll conductance is positively correlated with and essentially linearly related to photosynthetic capacity

(Bernacchi et al., 2002; Evans and Loreto, 2000) when considering a broad spectrum of leaf types with varying leaf density (Niinemets, 2009B). However, based on existing data from herbaceous species, the relationship is relatively scattered (Flexas et al., 2012; Niinemets et al., 2009B; Warren and Adams, 2006), indicating that additional factors influence carbon uptake of crop species to a different degree and in different ways. For example, nitrogen allocation rather than leaf structural modifications may primarily mediate changes in g_m and A_{max} (the maximum net photosynthesis rate at saturating light, optimal temperature and normal atmospheric CO_2 concentration) in species with herbaceous-type leaves (Niinemets, 2007).

While mesophyll conductance has gained much attention recently, comprehensive studies of nutritional influences on leaf area index development and allocation, canopy nitrogen distribution, stomatal conductance (g_s) limitations, time-dependent changes in A_{max} and canopy GPP, and the ecophysiological regulation of g_m are lacking (Niinemets, 2009B) and needed as they are fundamental physiological concepts in sustainable crop production (Foulkes and Reynolds, 2015). To gain greater insight, several studies concerning the relationships among leaf N, g_m, g_s and photosynthesis in crops have been implemented, but these have been carried out in controlled environments or over short time periods. Longer-term studies of crop production over the seasonal cycle and in natural field environments are needed in order to better understand the multiple influences that regulate LUE and production. In this study, gas exchange and chlorophyll fluorescence measurements were made on leaves of rice to determine CO_2 uptake, transpiration, g_s and g_m. These measurements were carried out simultaneously with observations of crop development and canopy CO_2 exchange in experimental fields of Chonnam National University, Gwangju, South Korea under three nutrient treatment levels. We examine the extent to which increased nutrient supply leads to increases in canopy leaf area, altered nitrogen investments, as well as changes in leaf gas exchange and biomass production (Yoshida, 1981).

We address the following hypotheses:

1. Seasonal development of rice is characterized by a LUE optimization-oriented coordination in LAI, canopy N distribution, and leaf conductance (g_s and g_m) limitations on carbon gain.

2. Increasing nutrient supply to the rice crop leads to an acceleration in the rate of canopy development (rate of increase in LAI) and overall carbon gain, but not to the basic way in which coordination of the process relevant to LUE occurs.

3. Variation in leaf function in rice grown with different nutrient supply and under varying light environments within the crop canopy is largely explained by variations in leaf nitrogen allocation and nitrogen-driven gas exchange.

4.3. Materials and Methods

4.3.1. Study site

The experimental site is located at the agricultural fields of Chonnam National University, Gwangju, South Korea (126°53′ E, 35°10′ N, altitude 33 m). Rice (*Oryza sativa* L. cv. Unkwang) seedlings cultivated in a nursery were transplanted to a flooded field using a four-row rice transplanting machine on May 20th, 2013 (day of year – DOY - 140), with a row-line spacing of 12×30 cm. On average, each planted bundle contained five seedlings. A mass ratio of N:P:K of 11:5:6 was used in the paddy rice plots for three fertilization treatments: 0 kg N ha^{-1} (no supplemental fertilization as a control referred to as low; plot size ~511 m^2), 115 kg N ha^{-1} (the agricultural agency recommended amount, referred to as normal, plot size ~1387 m^2) and 180 kg N ha^{-1} (referred to as high, plot size ~511 m^2). Nitrogen was applied in two dosages, 80% as basal dosage two days prior to transplanting and 20% during the tillering stage, 19 Days After Transplanting (DAT). P fertilizer (62 kg ha^{-1}) was applied as a 100% basal dosage, and K fertilizer (60 kg ha^{-1}) was applied as 65% basal dosage and 35% during tillering. All field management practices of paddy rice and fertilizer dosages reflected the practices of farmers in the region. Fertilizer migration between nutrient treatments and

potential losses via runoff were minimized by cement walls 35 cm wide, inserted to a depth of one meter in the soil. Excess water drained out of the field during the summer monsoon in July and August when heavy rainfall occurred. The time periods during which rice under these field conditions grew in different agronomic developmental stages after transplanting were unaffected by fertilization treatment, and are shown in Table 8.

Table 8: Time periods during which paddy rice cultivar Unkwang grew in different agronomic stages.

Growth stage	Day After Transplanting	Day Of Year
Recovery from transplanting	0 – 10	142 - 152
Active tillering	10 – 30	152 - 172
Elongation	30 – 64	172 - 206
Flowering	64 – 70	206 - 212
Grain-filling	71 – harvest	212 - harvest

To underpin several physiological assumptions, the same rice variety was planted in September 2014 in a greenhouse at the University of Bayreuth, Germany (11°34′ E, 49°56′ N). Seedlings were transplanted at 10 cm height into plastic containers (top diameter 25.4 cm and height 25 cm) with similar plant spacing as in the 2013 field experiment. The equivalent to the 115 kg N ha^{-1} field treatment was applied again two times, before transplanting and at the tillering stage as nutrient liquid from 100g N/l Wuxal super (Agrarvers and Oberland Inc., Schongau, Germany). For gas exchange experiments, the plants were then acclimated in a growth chamber to daytime air temperature 30°C, relative humidity 60% and light intensity of 900 μmol m^{-2} s^{-1}. Air temperature during nighttime was constant at 25°C.

4.3.2. Field measurements of diurnal courses of canopy and leaf CO_2 exchange

Four plots were established in the middle of the paddy fields for each nutrient treatment to monitor diurnal canopy CO_2 gas exchange, using a custom-built set of one transparent and one opaque chamber (L 39.5 × W 39.5 × H 50.5 cm; detailed information on chamber construction and measurement protocols are given in Li et al. (2008) and Lindner et al. (2015). Three frames, each enclosing three bundles of healthy plants, and a fourth frame without plants were deployed. Diurnal gas exchange courses of net ecosystem CO_2 exchange (NEE − with transparent chamber) and ecosystem respiration (R_{eco} − with opaque darkened chamber) per square meter ground surface were monitored at hourly intervals from sunrise to sunset. Incident PAR in the transparent chamber was measured with a quantum sensor (LI−190, LI−COR, Lincoln, Nebraska, USA). A hyperbolic light response model was fit to estimate gross primary production (GPP; sum of NEE and R_{eco}) as a function of incident PAR, generating instantaneous canopy light use efficiency (LUE_{ins}) defined as the initial slope of the response, and an estimate of potential maximum GPP rate at PAR of 1500 μmol m^{-2} s^{-1} (GPP_{max}) (Li et al., 2008; Lindner et al., 2015). Canopy LUE_{inc}, defined as daytime integrated GPP divided by daytime total incident above-canopy PAR, was calculated for each day of measurement.

Diurnal gas exchange and chlorophyll fluorescence measurements in the sunlit (uppermost), second, third and fourth mature leaves of the high fertilization group were conducted using a portable gas-exchange and chlorophyll fluorescence system (GFS−3000 and PAM Flourometer 3050−F, Heinz Walz GmbH, Effeltrich, Germany) on 57 and 73 DAT to track ambient environmental conditions external to leaf cuvette. The measurement dates of diurnal courses of the sunlit (uppermost) leaves in the low and normal groups were 31 and 72 DAT, and 25 and 77 DAT, respectively. Middle parts of two or three intact and healthy leaves were enclosed from sunrise to sunset. Microenvironmental factors such as incident light intensity, air/leaf temperature, air humidity, and CO_2 concentration were recorded simultaneously.

Leaf-level light use efficiency was determined from a linear estimation of photosynthesis response to light when incident PAR was less than 200 μmol m^{-2} s^{-1}.

4.3.3. Measurements of CO_2 response curves of net assimilation rate

The Walz GFS−3000 was used to measure net assimilation CO_2 response curves at different leaf temperatures. CO_2 response curves of uppermost canopy leaves were measured twice for the low and normal fertilization treatments, on around 28 DAT (tillering stage) and around 74 DAT (beginning of grain-filling stage: subsequently termed grain-filling). CO_2 curves were commenced after leaves had acclimated to the cuvette microenvironment (CO_2 concentration of 400 μmol mol^{-1} and saturating PAR of 1500 μmol m^{-2} s^{-1}) after which CO_2 concentration was changed progressively according to the sequence 1500, 900, 600, 400, 200, 100 to 50 μmol mol^{-1}. Relative humidity was controlled to ca. 60%. Assimilation rate and stomatal conductance data were recorded after new steady-state readings were obtained. At least three replicate CO_2 curves were obtained at each leaf temperature, which was varied in 5°C steps from 20 to 35°C at the tillering stage and from 25 to 35°C at the grain-filling stage. For each CO_2 response curve, the protocol described by Sharkey et al. (2007) was used to estimate values for the parameters V_{cmax} and J_{max}.

A_{max} (photosynthesis rate at 400 μmol CO_2 mol^{-1}, saturating PAR of 1500 μmol m^{-2} s^{-1} and 30°C) in leaves at different depths in the canopy were measured on around 54 DAT (low, normal and high fertilization treatments) and around 72 DAT (low and high fertilization treatments) using the GFS-3000. On 90 DAT similar photosynthetic capacity determinations were conducted, but only on the uppermost leaves in the canopy.

4.3.4. Measurement of canopy reflectance

Radiometric measurements were carried out intensively in three nutrient groups over growth season by a portable instrument equipped by multispectral radiometers (MSR, Cropscan Inc, MN, USA). The MRS-5 was positioned facing vertically downward at 2 m above crop canopies, and measurements were taken at solar noon to minimize the effect of diurnal changes in solar zenith angle. 6 replications surrounding plots for canopy gas exchange measurements were conducted, and reflectance measurements were then averaged. Normalized difference vegetation indices (NDVI) was calculated from the spectral bands obtained in the channel 3 and 4 of the MSR5, corresponding to the red (630-690 nm) and near infra red wavelength (760-900 nm) respectively by following formula,

$$NDVI = \frac{\rho_{nir} - \rho_{red}}{\rho_{nir} + \rho_{red}}$$

Equation 14

To get the NDVI on those days when measurements of canopy gas exchange were implemented and on other days that were clear and sunny at solar noon, the time series function was fit to measured NDVI,

$$NDVI = a \cdot t^{b} \cdot e^{c \cdot t}$$

Equation 15

where a, b and c are coefficients and t is time (day after transplanting).

4.3.5. Characterization of leaf nitrogen content, leaf area, leaf angle, and biomass

After conducting gas exchange measurements, leaf samples were collected to estimate leaf area, dry mass and nitrogen content. On 26, 33, 54, 72 and 86 DAT, three planted bundles consisting of fifteen plants (five seedlings comprising one planted bundle) from each treatment were harvested, and total plant area (leaf and stem) of each was determined with an LI-3100 leaf area meter (LI-COR Inc, Lincoln, Nebraska, USA). On 54 and 72 DAT a portion of the standing canopy in each fertilization treatment was stratified into vertical layers, each layer 15 cm in thickness. Leaf and stem area and biomass in each stratified layer were measured. After chamber gas exchange measurement, the green biomass overlying one half square meter of ground in each nutrient group was harvested. All samples were dried at 60°C in a ventilated oven for at least 48 hours before determination of dry mass. Leaf nitrogen content was measured by C:N analyzer (Model 1500, Carlo Erba Instruments, Milan, Italy). On 43 DAT, three typical bundles from each treatment were randomly selected to record individual leaf laminar area. Grain yield determinations were obtained at four sampling plots (0.5 × 0.5 m) at the end of the growing season at 113 DAT (253 DOY), and were weighed after air-drying. Seasonal changes of leaf area index were measured using a plant canopy analyzer (LAI-2000, LI-COR, Lincoln, Nebraska, USA). Measurements were taken across the rows and above the water surface using a cover with small view of 45$^°$ at early growth stages and one with large view of 270$^°$ at later growth stages. All measurements were made when there was no direct beam of sunlight, either in the late afternoon or during periods of uniform cloudiness.

4.3.6. Characterization of canopy light and nitrogen distribution profiles

Vertical profiles of incident light were determined either the day before or on the day of plant sampling with light data loggers (HOBO, Onset Computer Corporation, Bourne, MA) mounted on thin rods with vertical spacing of 15 cm from base 0 cm to top of the canopy, and where multiple rods were placed along a transect diagonal to the planted rows. Data was logged every 15 min on two consecutive days when the measurements of stratified leaf area were made for nutrient groups. The HOBO logger light values were periodically compared to PAR measured with a LI-COR quantum sensor to develop a calibration curve and to estimate the PAR profiles. A trapezoidal integration was conducted to obtain daily integrated PAR. Close correspondence between daily integrated PAR from the quantum sensor of the GFS-3000 and those from HOBO loggers indicated that the computation method was reliable. PAR was assumed to be attenuated through the canopy according to the Lambert-Beer law, where Q, the daily integrated PAR at a given canopy height is calculated as:

$$Q = Q_o \exp\left(- K_l f\right),$$ **Equation 16**

where Q_o is the daily integrated PAR above the canopy, K_L the canopy light attenuation coefficient, and f is the plant area index (PAI) from the top of canopy to the measurement level. There were few leaves in the 15-30 cm layer and no leaves in the 0-15 cm layer during late growth stages. Substantial presence of stems at lower layers, nevertheless, caused light attenuation, and plant area index showed a better correlation with measured light intensity at each layer than LAI. An exponential equation analogous to Equation 16, substituting an N extinction coefficient K_N for K_L, was used to describe leaf nitrogen distribution. When K_L or K_N is equal to 0, uniform distributions of light or N resources occur in the profiles. Increasing coefficients indicate a steeper gradient in resource distribution.

Light use efficiency based on absorbed PAR (LUE_{abs}) was defined as the ratio of daily integrated canopy GPP at each measuring date to integrated PAR intercepted by the canopy.

Intercepted radiation, Q_{int}, was estimated by two methods, one using Equation 17, derived from Equation 16 (Hui et al., 2001).

$$Q_{int} = Q_o \left(1 - \exp\left(-K_l \cdot f\right)\right)$$ **Equation 17**

The other is from NDVI-fPAR correlation (fPAR is fraction of incident to Q_{int}). The relationship between vegetation index NDVI and fPAR is generally found to be curvilinear (Choudhury, 1987; Goward and Huemmrich, 1992; Inoue et al., 2008). Linear correlation between those two biophysical variants in paddy rice before ripening stage was structured by Inoue (2008), while their data integrated with those in cereal crops grown under different ecological conditions from Choudhury (1987) actually followed exponential trend which is formulated by,

$$fPAR = fPAR_{max} \left[1 - \left(\frac{NDVI_{max} - NDVI}{NDVI_{max} - NDVI_{min}} \right)^{\varepsilon} \right]$$ **Equation 18**

For determination of fPAR two types of variant need to be priori quantified based on field grown rice at specific nutrient manipulation condition: canopy geometry property (ε) which is the ratio of dampening factor K_p and factor K_{vi}, maximum and minimum NDVI values. K_p is coefficiency controlling correlation between canopy light interception and LAI, K_{vi} being coefficiency controlling relationship between NDVI and LAI. $fPAR_{max}$ in rice is 0.95 recommended by Atwell et al. (1999). Max. NDVI in fertilization group and low group were 0.92 and 0.84 which were field observations, respectively. K_p and K_{vi} at 0.48 and 0.8 in rice suggested by Nay-Htoon (2015) were adopted, generating ε of 0.6, which compares favorably to modeling outputted ε of 0.58 via apply Equation 18 to integrated data group in Fig. 21a. Min. NDVI (x-intercept) is 0.11 when fPAR is zero. The model simulation was tested against field observations at three nutrient groups. Striking correspondence between prediction by Equation 18 and field observations (calculated from Equation 17) documented that values of independent variants in Equation 18 are representative proxy reflecting rice growth and

development and can be used for estimation of fPAR and thereby LUE_{abs} at the days when canopy gas exchange were collected.
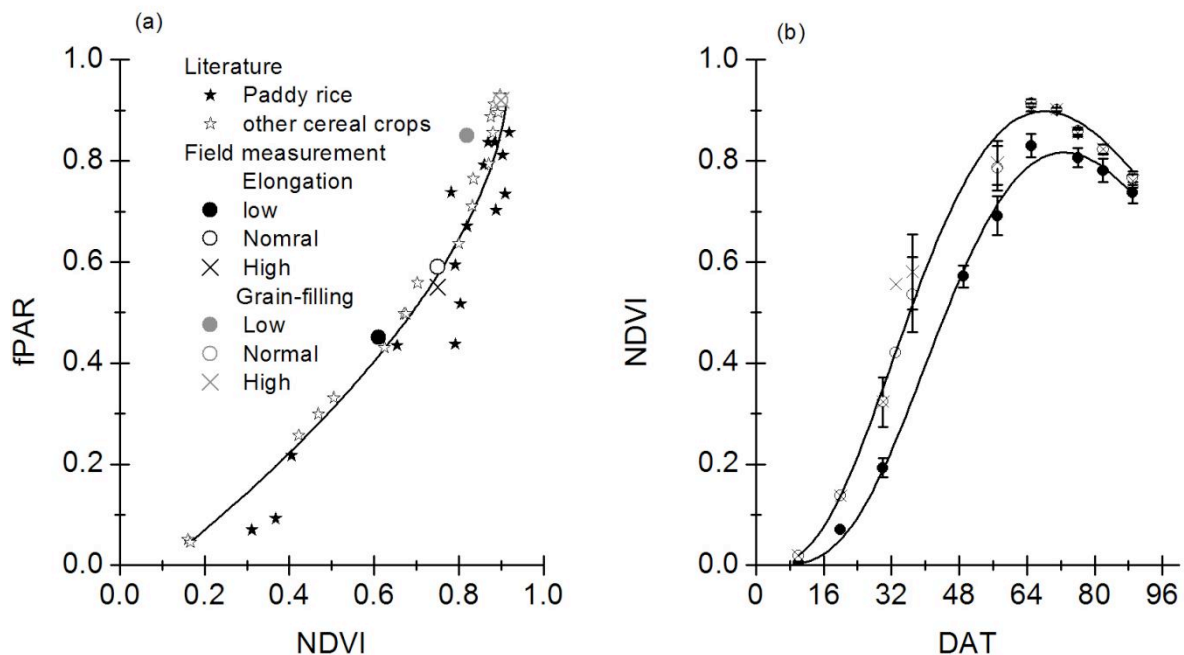
Figure 21: (A) Exponential correlation between normalized difference vegetation indices (NDVI) and fraction of incident PAR to absorbed PAR in cereal crops. Filled stars represent data in paddy rice from Inoue et al. (2008) and open stars in other cereal crops from Choudhury (1987). (B) Seasonal development of NDVI in paddy rice grown under three nutrient treatments: low (filled circles, 0 kg N ha^{-1}), normal (open circles, 115 kg N ha^{-1}) and high (cross symbols, 180 kg N ha^{-1}).

The amount of sunlit leaf area (leaves exposed to full sunlight) in each canopy layer at the low and normal groups during grain-filling stage was estimated based on the classical gap probability function in canopies (see Caldwell et al. (1986) for detailed description), in which sunlit leaf area is a function of solar position in the sky and the surface area and leaf geometry of each layer. For these calculations, a weighted average method considering the proportion of individual leaf area to total leaf area at each layer was used to generate average leaf angle of each layer. Leaf absorptance of PAR was assumed to be 0.84, and the leaf clumping factor used was 0.8, representative values for grain crops. Tight correlation between predications in light intensity at each layer by radiation transfer model and measurements y=0.82x+1.2 ($R^2 =$ 0.90, p < 0.01) meant the pragmatic implementation of classical gap probability function to mimic canopy dynamics with respect to light distribution and sunlit leaf area.

4.3.7. Estimation of the mesophyll diffusion conductance (g_m)

The variable J_P method of Harley et al. (1992) for estimating mesophyll conductance was applied to data on the ETR-limited portions of CO_2 response curves. The proportion of generated electron transport rate that is used by CO_2 fixation process was quantified (Appendix A, Figure 29A). In general, ETR, inferred from fluorescence measurements, became stable when C_i was higher than ca. 240 µmol mol^{-1}. Assimilation rate and ETR in the region from 240 to 600 µmol mol^{-1} were used, because i) g_m estimates over this range of C_i values are reliable, since photosynthesis is limited by regeneration of RuBP and limitations by triose phosphate utilization usually occur only at higher CO_2 concentrations (Flexas et al., 2007; Harley et al., 1992; Sharkey et al., 2007); and ii) the determinations are appropriate for the values observed for C_i under natural field conditions (ca. 250 µmol mol^{-1}). Thus,

$$g_m = A/(C_i - ((\Gamma^*(J_P + 8A + 8R_{day}))/(J_P - 4A - 4R_{day}))) , \qquad \textbf{Equation 19}$$

where A, C_i and J_p are measured directly. Chloroplast CO_2 compensation point (Γ^*), the intercellular CO_2 concentration at which carboxylation rate equals photorespiration rate in the light was determined for our rice cultivars to be 44.4 ± 1.3 µmol mol^{-1} (Appendix A, Figure 29B), which is consistent with values reported for cultivars as tobacco (Bernacchi et al., 2002). R_{day}, non-photorespiratory CO_2 evolution in the light, was approximately 60% of dark respiration as measured by gas exchange.

Using values of V_{cmax} and J_{max} determined from CO_2 response measurements, rates of net assimilation were predicted assuming different values of C_c, the CO_2 partial pressure at the site of fixation, which is jointly determined by fixation rate, stomatal and mesophyll conductances. The limitations on photosynthetic capacity resulting from finite stomatal and mesophyll conductance were evaluated by comparing measured A_{400} at $C_a = 400$ with rates predicted assuming infinite stomatal and/or mesophyll conductance by Equations 20-22 (Harley et al., 1986; Monteith, 1972):

$$L_{gm} = 100 \frac{A_{cc=ci} - A_{400}}{A_{cc=ci}}$$ **Equation 20**

$$L_{gs} = 100 \frac{A_{ci=400} - A_{400}}{A_{ci=400}}$$ **Equation 21**

$$L_{total} = 100 \frac{A_{cc=400} - A_{400}}{A_{cc=400}}$$ **Equation 22**

where L_{gm} is the percent limitation due to mesophyll conductance, L_{gs} that due to stomatal conductance, and L_{total} the total percent limitation of the conductance pathway on photosynthesis.

4.4. Results

4.4.1. Seasonal changes in canopy reflectance, biomass production, canopy LUE, and leaf area in response to fertilizer treatments

Time series functions connecting measured NDVI at solar noon during sunny days were indicated in Figure 21 that NDVI value at fertilization group during vegetative growth stage before flowering and ripening stage were significant higher than control group (Friedman ANOVA, $p = 0.045$). Green biomass accumulation in all three nutrient groups exhibited similar seasonal trends. Biomass increased rapidly after ca. 30 DAT, reached a maximum on ca. 64 DAT, and subsequently declined (Figure 22A). Peak aboveground biomass was significantly higher in the normal and high fertilization treatment groups by 62% and 56%, respectively, compared to the low group. Similar to biomass production, grain yields in normal and high fertilization treatments were similar but markedly higher than in the control group by 58% and 73%. The seasonal change in measured rates of GPP$_{max}$ is shown in Figure 22B. During tillering (16 DAT) GPP$_{max}$ was low in all treatments (ca. 2 μmol m^{-2} s^{-1}; no significant difference, $p > 0.05$) and increased rapidly with increasing LAI. GPP$_{max}$ increased throughout the elongation period, but plants in the normal and high fertilization treatments

155

showed increased carbon gain relative to the low fertilization after 30 DAT (p = 0.05). The highest GPP_{max} (~28 μmol m^{-2} s^{-1}) occurred in fertilized plots at approx. 60 DAT, just before commencement of the grain-filling stage, at which time GPP_{max} in unfertilized plots averaged ~21 μmol m^{-2} s^{-1}. Subsequently, GPP_{max} in low N plots leveled off and GPP_{max} in fertilized treatments declined to ~23 μmol m^{-2} s^{-1}, so that 20 days later, during grain-filling (78 DAT), GPP_{max} in fertilized groups was only 10% higher. GPP_{int} exhibited similar seasonal trends across the three groups, reaching a maximum of 11.3 g C d^{-1} in the fertilized group and 9.4 g C d^{-1} in the plots receiving no additional nitrogen (Figure 22B).

Seasonal time courses for daily LUE_{inc} (Figure 22C) based on incident light were similar to those for GPP_{max} and GPP_{int}. On an incident radiation basis, differences among treatments were found as expected with higher LUE_{inc} in fertilized plots after 16 DAT, and the difference increasing over time. At approx. 60 DAT, the differences were statistically significant (p = 0.039).

LAI in all treatments increased rapidly through the elongation stage, and substantial differences in LAI among treatments occurred after 34 DAT (p < 0.01; Figure 22D) as LAI increased much more rapidly in the fertilized plots. These differences in LAI between treatments had multiple causes. Early in the elongation stage at 43 DAT, both leaf number and leaf mass per planted bundle were much higher in the normal and high plots than in the low treatment (Table 9). There were no significant differences in leaf biomass per bundle between the normal and high treatments, but the differences between non-fertilized and fertilized plots increased dramatically throughout the elongation stage (p < 0.05). Furthermore, plants in the fertilized treatments exhibited significantly greater amounts of leaf area in the upper levels of the growing canopy. At 43 DAT, early in the elongation stage, the mean area of individual leaves whose height of petiolar insertion was more than 20 cm above ground surface was significantly greater in the fertilized treatments than in the low N plots (the normal and high treatments greater by 33% and 22%, respectively; Table 9). Similar

differences were found later in the elongation stage, at 53 DAT, with fertilized plots accumulating a greater amount of leaf area in leaves originating in upper portions of the canopy, between 45 and 60 cm and between 60 and 75 cm above ground. By the grain-filling stage, however, leaf area in the upper levels of the canopy (above 60 cm insertion height) were 21.6, 23.0, and 23.0 cm^2 in the low, normal and high nutrient groups, and were no longer significantly different (Table 9).
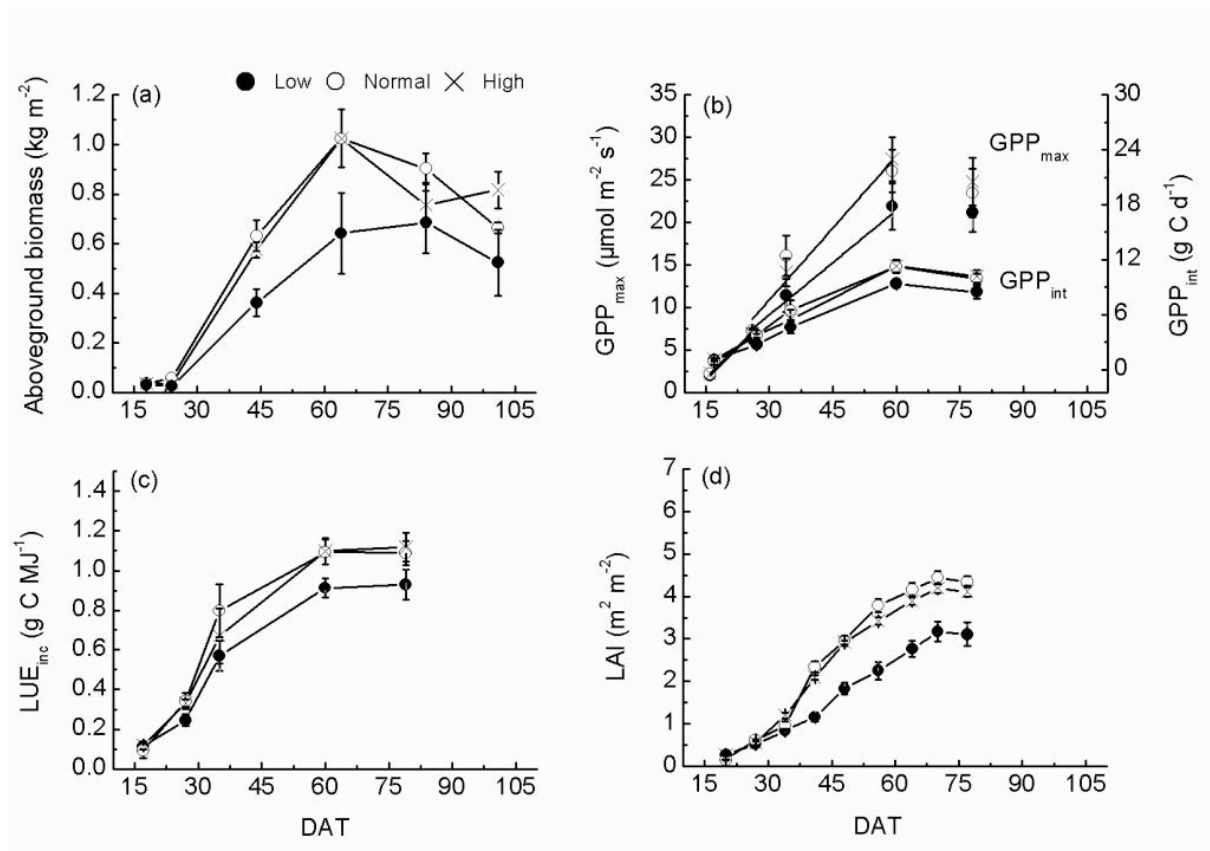
Figure 22: **Seasonal courses for (A) aboveground biomass production, (B) observed maximum rates in gross primary production (GPP_{max}) during daily measurement cycles, integral daytime GPP (GPP_{int}), (C) canopy light use efficiency (LUE_{inc}), and (D) leaf area index for paddy rice grown at three levels of fertilization. Low = no fertilizer addition; normal = 115 kg N ha^{-1}; high = 180 kg N ha^{-1} as described in the methods. Bars indicate S.E.; n = 2 to 12.**

Table 9: Leaf dry mass per planted bundle (g) and mean leaf laminar area (cm^2) at different developmental stages and in different canopy layers in paddy rice grown at low (0 kg N ha^{-1}), normal (115 kg N ha^{-1}) and high (180 kg N ha^{-1}) fertilizer levels. S.E. is given in parentheses.

Growth stage	Nutrient treatment	Leaf dry mass per bundle (g)	Number of leaves per bundle	Mean leaf area in a given canopy height range (cm^2)			
Canopy height above ground				**> 20 cm**	**45-60 cm**	**60-75 cm**	**75-90 cm**
Early-elongation 43 DAT (184 DOY)	Low	2.1	57 (4)	22.1 (2.2)			
	Normal	3.1	101 (4)	29.4 (1.1)			
	High	3.4		26.9 (1.3)			
Mid-elongation 53 DAT (194 DOY)	Low	4.6 (0.5)			9.3 (0.6)	3.7 (0.9)	
	Normal	7.2 (1.1)			13.10 (0.8)	7.2 (0.8)	
	High	6.8 (0.4)			12.0 (0.8)	4.2 (1.0)	
Grain-filling 73 DAT (214 DOY)	Low	4.2 (0.4)			9.9 (1.0)	12.8 (1.4)	8.9 (1.0)
	Normal	8.7 (0.7)			13.8 (0.7)	13.4 (1.0)	9.6 (1.2)
	High	9.6 (1.1)			13.0 (0.6)	12.2 (0.9)	10.8 (1.4)

4.4.2. Seasonal changes in leaf morphology and physiology in response to fertilizer treatments and canopy position

During the course of development, average specific leaf area (SLA) of top of canopy leaves decreased by approx. 33% (Figure 23A), but SLA values for sunlit leaves in the three fertilization groups were not significantly different ($p > 0.05$). Despite this presumed increase in leaf thickness over the growing season, leaf nitrogen per unit area (N_a) decreased strongly, by approx. 40% in all treatments (Figure 23A). The decrease occurred more rapidly during the elongation stage when the crop canopy was closing rapidly, than during the flowering and grain-filling stages. Although no significant differences in N_a between leaves of the normal and high fertilization treatments were observed over the entire growing season, leaf nitrogen in both was significantly greater than in the low fertilizer treatment during leaf elongation. No significant differences in N_a were observed between the three groups at grain-filling stage (after 60 DAT, $p < 0.05$).
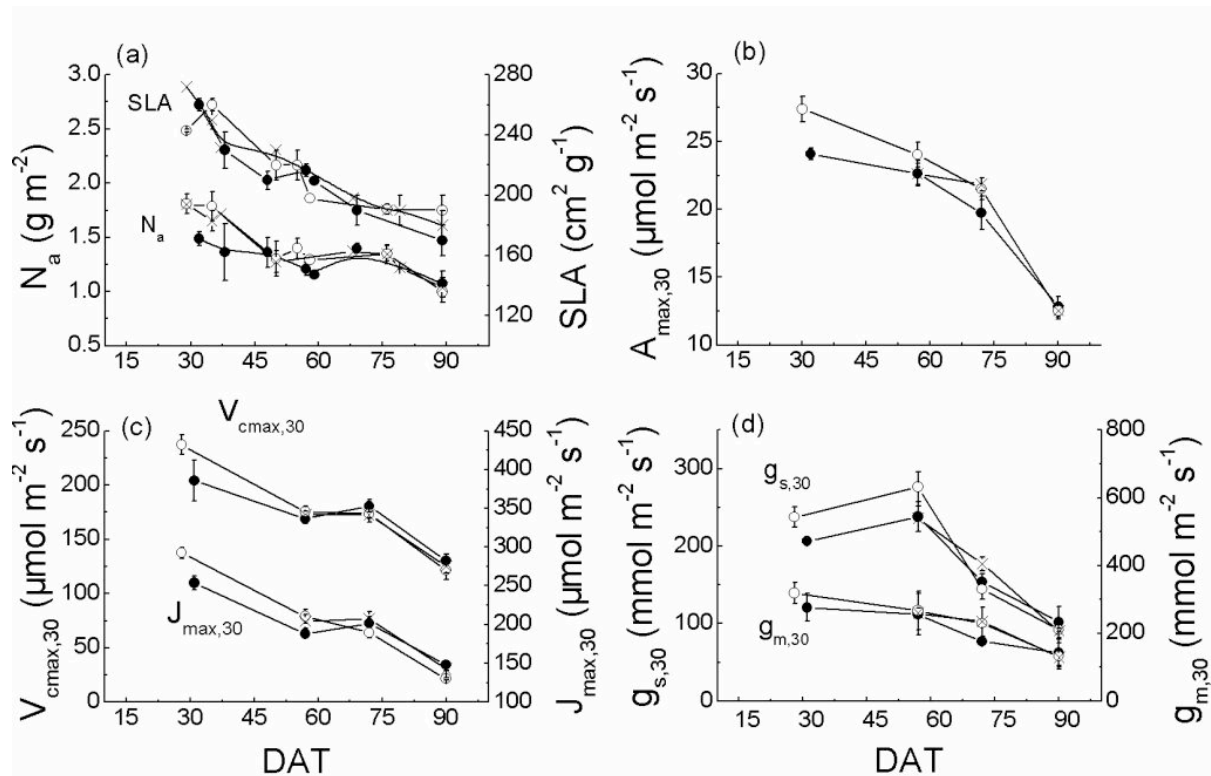
Figure 23: (A) Seasonal changes in sunlit mature leaves at top of canopy for leaf nitrogen content (N_a), specific leaf area (SLA), (B) photosynthesis capacity ($A_{max,30}$), and (C) maximum Rubisco carboxylation rate ($V_{cmax,30}$), maximum electron transport rate ($J_{max,30}$), (D) stomatal conductance ($g_{s,30}$), and mesophyll conductance ($g_{m,30}$) under the same environmental conditions. Bars indicate S.E., n = 3 to 6.

The seasonal decreases and differences among treatments in N_a were reflected in concurrent changes in photosynthetic activity, measured at saturating PAR and 30°C ($A_{max,30}$). Thus, $A_{max,30}$ was 14% lower in the low fertilization treatment during early growth (p = 0.02; Figure 23B), but the differences were relatively small (~7%) during the grain-filling stage (ca. DAT 72). Carboxylation ($V_{cmax,30}$) and electron transport ($J_{max,30}$) capacities (Figure 23C) were greater in the normal and high fertilization treatments at tillering stage (prior to 60 DAT; p = 0.05 and p = 0.04, respectively), consistent with observed differences in A_{max} and N_a. Parallel decreases in mesophyll and stomatal conductance also occurred over the course of the season (Figure 23D), but differences among treatments were not apparent. The limitations on carbon gain due to mesophyll conductance (L_{gm}) and stomatal conductance (L_{gs}) were of similar magnitude in all treatments and did not differ significantly at comparable phenological stages (Table 10). As conductances decreased from the elongation stage to grain-filling stage,

159

however, the limitations by both g_m and g_s increased dramatically, by between 22 and 49%. The total limitation of carbon gain due to transport from the external air to the site of fixation was substantial, ranging from 28 to 37%, with the highest value occurring in the low fertilization plants at the grain-filling stage, when the lowest leaf N_a was also observed.

Table 10: Comparisons among nutrient treatments in plant area index (PAI, m^2 m^{-2}), leaf area index (LAI, m^2 m^{-2}), daytime integral GPP (GPP$_{int}$, g C d^{-1}), average overall CO_2 diffusive limitation (L$_{total}$, %), stomatal limitation (L$_{gs}$, %) and mesophyll limitation (L$_{gm}$, %), canopy light attenuation coefficient (K$_L$), and canopy nitrogen attenuation coefficient (K$_N$) at elongation (ca. 54) and grain-filling stages (ca. 73) at low (0 kg N ha^{-1}), normal (115 kg N ha^{-1}) and high (180 kg N ha^{-1}) fertilizer levels. Grain yields (g m^{-2}) in three groups is indicated. S.E. is given in parentheses, n = 3 to 6.

	Low		Normal		High	
	Elongation	Grain-filling	Elongation	Grain-filling	Elongation	Grain-filling
PAI	3.54 (0.66)	4.45 (0.53)	5.56 (0.50)	6.38 (0.51)	5.30 (0.55)	6.40 (0.69)
LAI	2.04 (0.17)	3.2 (0.23)	3.36 (0.13)	4.53 (0.16)	3.15 (0.07)	4.29 (0.13)
GPP$_{int}$	9.39 (0.48)	8.67 (0.70)	11.25 (0.25)	9.94 (0.55)	11.31 (0.68)	10.20 (0.65)
L$_{total}$	29.6 (4.1)	37.1 (5.1)	29.1 (5.5)	--	27.6 (3.2)	35.3 (4.8)
L$_{gm}$	16.9 (4.0)	24.3 (2.1)	15.6 (1.24)	--	16.1 (1.51)	24.2 (2.4)
L$_{gs}$	18.3 (1.16)	23.7 (3.7)	20.6 (5.4)	--	21.6 (1.31)	26.4 (2.6)
K$_L$	0.19 (0.04)	0.42 (0.04)	0.18 (0.03)	0.40 (0.05)	0.16 (0.04)	0.39 (0.04)
K$_N$	0.14 (0.02)	0.28 (0.02)	0.06 (0.005)	0.14 (0.01)	0.06 (0.01)	0.12 (0.01)
Yield	717 (110.5)		1135 (131.2)		1243 (22.94)	

Changes in leaf physiological function with depth in the canopy were investigated during the elongation and grain-filling stages (Figure 24). Leaf N_a decreased with depth in the canopy for all treatments during the elongation phase, but the decline was particularly pronounced in the low fertilization treatment (Figure 24A). Thus, significantly higher levels of N_a were observed in second and third leaves in the higher nitrogen treatments at the elongation stage (Figure 24A; p = 0.003), which may be related to initial N investments during tillering (ca. 30 DAT) (cf. Figure 23A). During grain-filling, when canopy closure was more complete, N_a declined even more rapidly with depth in canopy, but the N_a profiles were similar (p > 0.05) for all treatments (Figure 24B). In general, leaf nitrogen profiles were reflected in similar declines in physiological variables related to photosynthetic activity, such as $A_{max,30}$, $V_{cmax,30}$, $J_{max,30}$, $g_{m,30}$, and $g_{s,30}$ (Figure 24C-L). Despite observed differences in N_a profiles during the

elongation phase, canopy profiles of these physiological variables showed no striking treatment differences during either period of growth ($p > 0.05$).

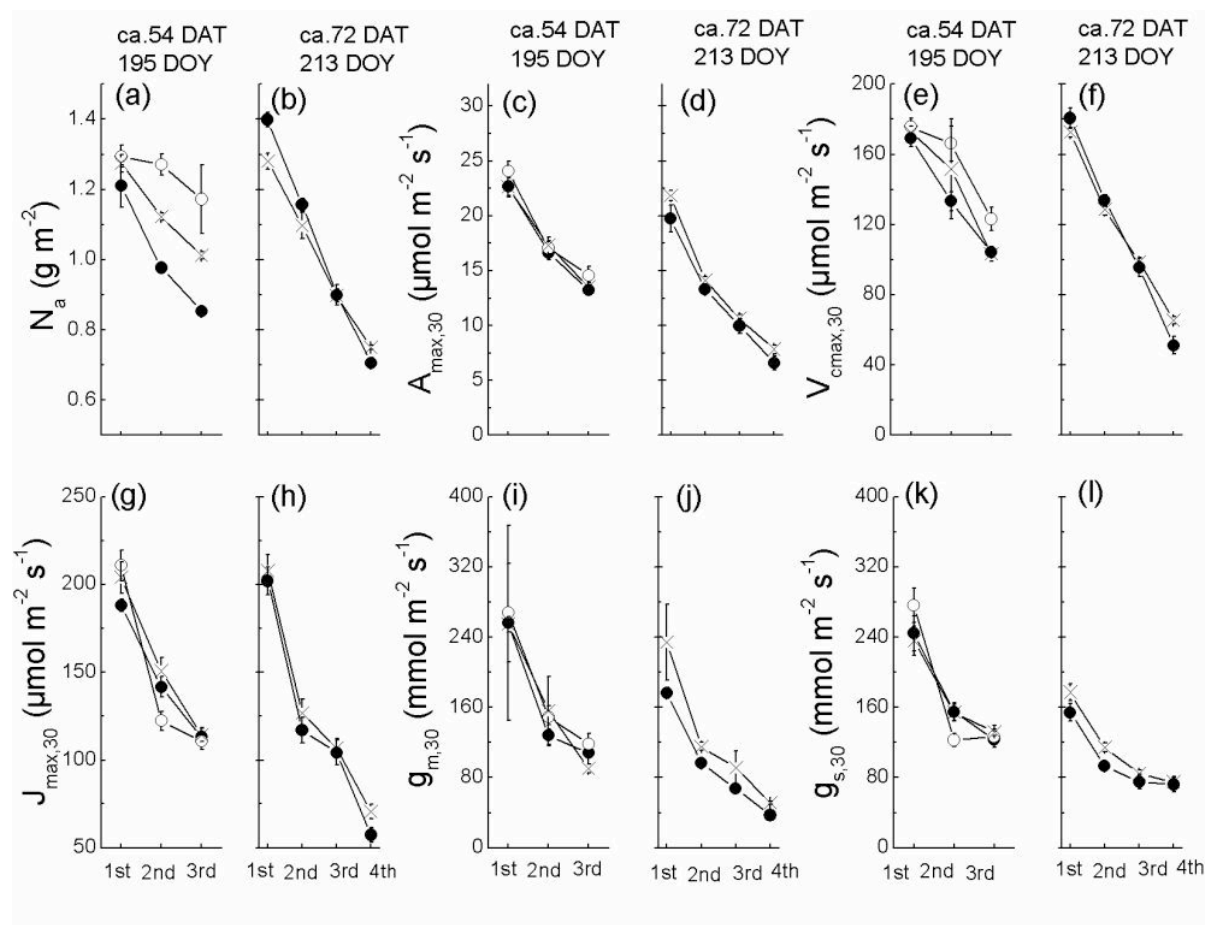**Figure 24: Dependence on leaf position in crop canopy of paddy rice for leaf nitrogen content N_a (A, B), photosynthetic capacity $A_{max,30}$ (C, D), maximum Rubisco carboxylation rate $V_{cmax,30}$ (E, F), maximum electron transport rate $J_{max,30}$ (G, H), mesophyll conductance $g_{m,30}$ (I, J), and stomatal conductance $g_{s,30}$ (K, L) at elongation and grain-filling stages. Bars indicate S.E., n = 3 to 6.**
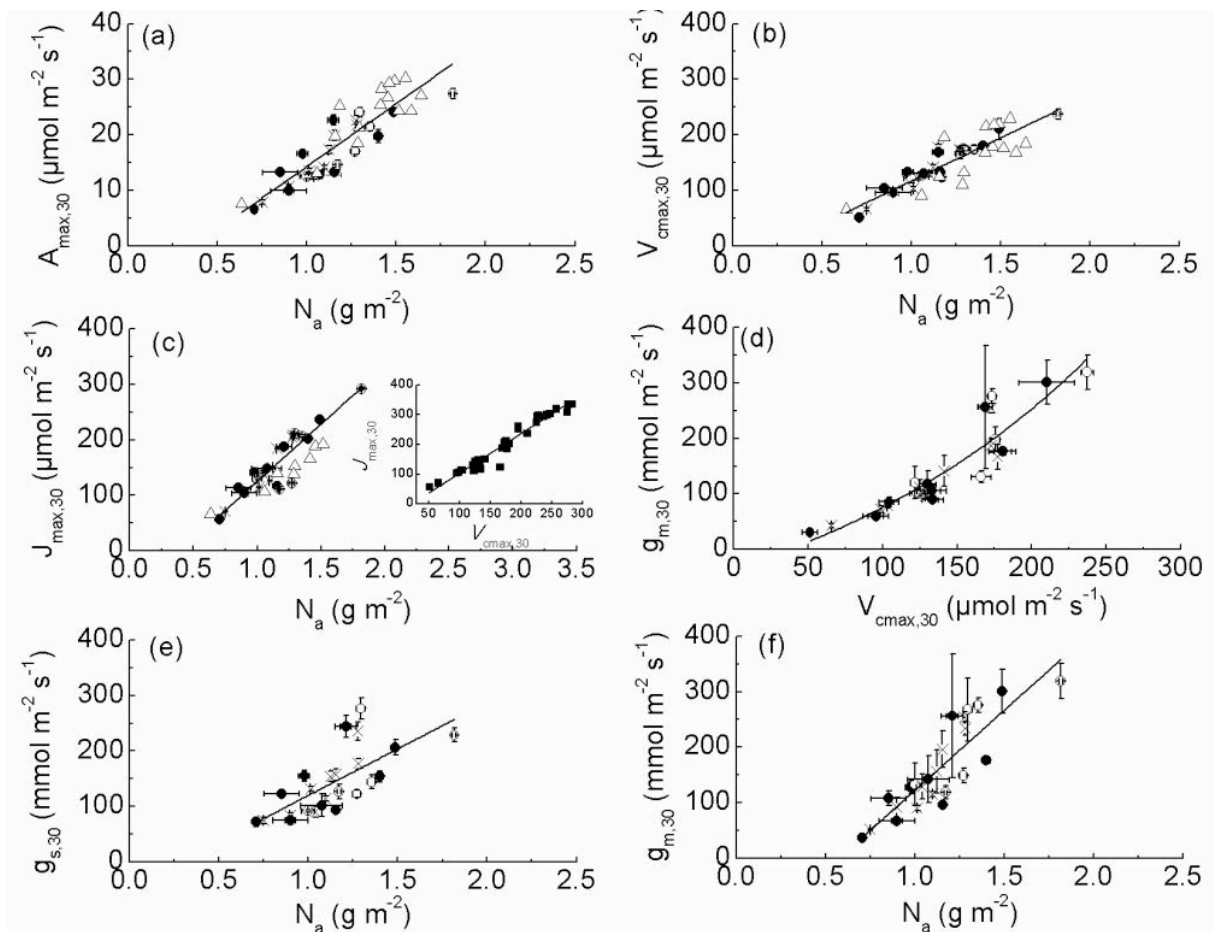
Figure 25: (A) Dependence of photosynthetic capacity ($A_{max,30}$) on leaf nitrogen content (N_a); (B) relationship of maximum carboxylation rate ($V_{cmax,30}$) to N_a; (C) correlation between maximum electron transport rate ($J_{max,30}$) and N_a; (C) correlation of mesophyll conductance ($g_{m,30}$) and $V_{cmax,30}$, (E) stomatal conductance ($g_{s,30}$) and N_a, and (F) $g_{m,30}$ and N_a pooling data from both sunlit and within-canopy leaves grown in the field and from growth chamber experiments (open triangle). Inset in plot c indicated correlation between $J_{max,30}$ and $V_{cmax,30}$.

The conservative nature of leaf function in dependence on N_a is shown in Figure 25. When measured data on leaf gas exchange traits were pooled across all treatments, a tight linear correlation between N_a and $A_{max,30}$ is evident ($R^2 = 0.78$, $p < 0.01$; Figure 25A). Reflecting the dependence of A_{max} on Rubisco capacity and light harvesting, strong linear correlations between $V_{cmax,30}$ and N_a, and between $J_{max,30}$ and N_a were also found across all treatments ($R^2 > 0.80$, $p < 0.01$; Figure 25B and C). $V_{cmax,30}$ linearly scaled to $J_{max,30}$ with a constant ratio of 1.3, independent of growth environment (inset in Figure 25C). A strong but curvilinear relationship was observed between $V_{cmax,30}$ and $g_{m,30}$ ($R^2 = 0.76$, $p < 0.01$). V_{cmax} appears to be an important determinant of mesophyll conductance, although the curvilinearity suggests that

some additional physiological factors play a role. Both $g_{m,30}$ ($R^2 = 0.78$, $p < 0.01$) and $g_{s,30}$ ($R^2 = 0.47$, $p < 0.01$) increased linearly with N_a, but the slope was significantly higher for $g_{m,30}$ (Figure 25E and F). As a result, we observed a negative correlation between N_a and ratio of $g_{s,30}$ to $g_{m,30}$ ($R^2 = 0.61$, $p < 0.001$) (Figure 26D).
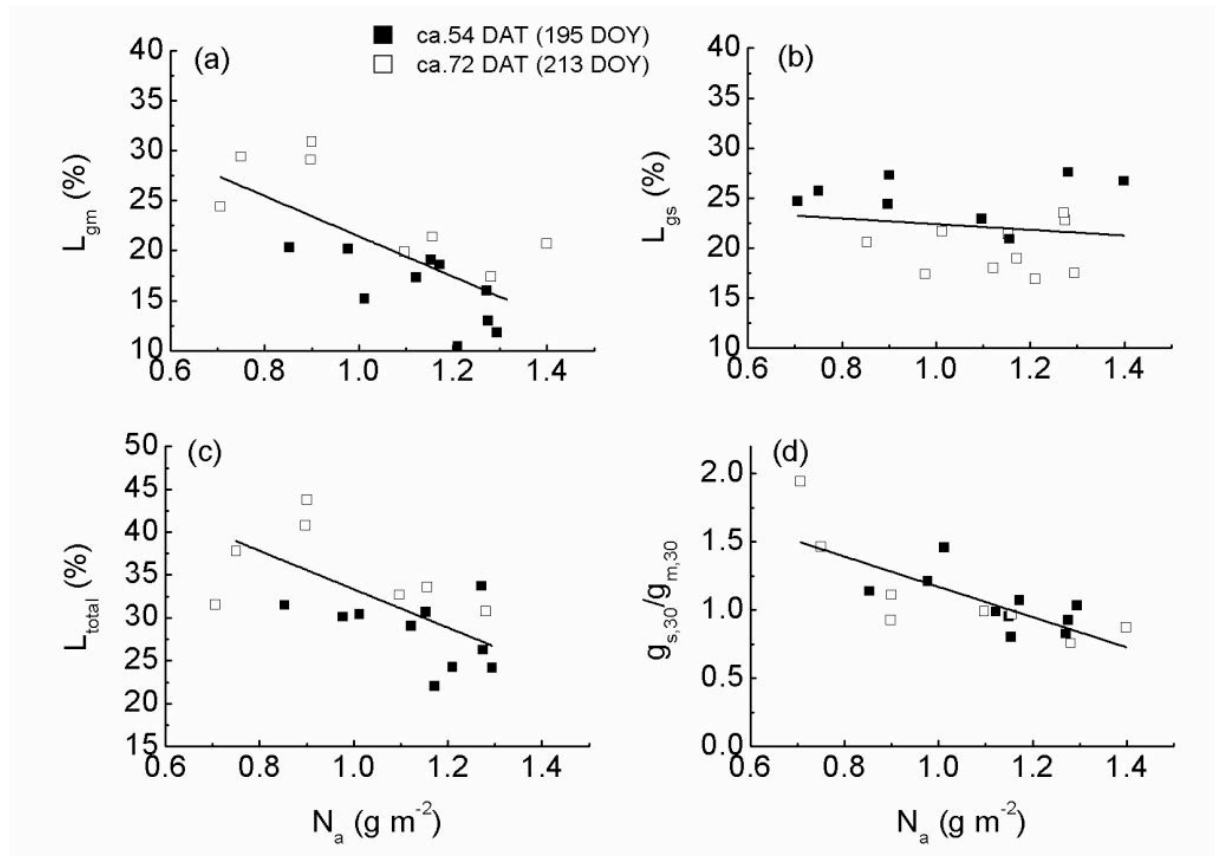
Figure 26: Photosynthetic limitation by (A) mesophyll conductance (L_{gm}) and by (B) stomatal limitation (L_{gs}) in canopy profiles against leaf nitrogen content (N_a) at the low, normal and high fertilization treatments in sunlit leaves during elongation and grain-filling stages, whereas (C) shows the the total percent limitation of the conductance pathway on photosynthesis in relation to N_a, and (D) the ratio of $g_{s,30}$:$g_{m,30}$ in dependence of N_a.

There was a strong negative correlation between L_{gm} and N_a in canopy profiles (Figure 26A) ($R^2 = 0.50$, $p = 0.014$), but only a slight, non-significant ($R^2 = 0.04$, $p = 0.51$) decline in L_{gs} with increasing N_a (Figure 26B). Due to the N_a dependency of L_{gm}, L_{total} also declined with increasing N_a ($R^2 = 0.50$, $p = 0.006$) (Figure 26C). The varying trend for mesophyll and stomatal limitation respectively corresponded to the CO_2 drawdown i.e. concentration gradient between leaf surface and intercellular airspace, between intercellular airspace and chloroplast carboxylation site, respectively (not shown).

4.4.3. Seasonal changes in canopy structure in responses to nutrient additions and effects on canopy LUE

LUE_{inc} increases with increasing canopy LAI (Figure 27A) and the relationship applies to all fertilization treatments, but as canopy closure increases, the effect of additional increases in LAI lessens. The result is a hyperbolic response of LUE_{inc} to developing LAI which approaches a saturation value of ca. 1.1 g C MJ^{-1} at LAI values above 3 m^2 m^{-2}. Differences among nutrient groups in light use efficiency on an absorbed radiation basis (LUE_{abs}) during the active tillering (p = 0.46 between low and normal group) and grain-filling stages (p = 0.49 between low and normal group) were not statistically significant (Figure 27B). Overall, LUE_{abs} in all treatments increased after seedlings transplanting and approached observed maximum level 3.2 g C MJ^{-1} at the low group at the end of active tillering stage, after that decreased, which changes in parallel with leaf nitrogen content (Figure 23A).

Total LAI differed between treatments (Figure 22D) but there were also treatment differences in the vertical distribution of leaf area within the canopy. When leaf area in each of five canopy layers (each 15 cm thick) is expressed as a percentage of the total canopy leaf area (Figure 27C and D), it is clear that during both elongation and grain-filling stages, an increasing percentage of total leaf area is allocated to upper levels of the canopy as N fertilization is increased. A tight correlation between LUE_{inc} and total leaf N (N_{total}) during both elongation and grain-filling stages were achieved. Fertilized plots had high LUE_{inc} accompanied by higher N_{total}. These differences must be related to enhanced LAI since leaf N values were similar or higher in the unfertilized group (Figure 24A and B). Thus, it seems that canopy leaf area development and allocation were important determinants of canopy carbon gain.

When LUE_{inc} for all treatments is plotted against the percentage of total leaf area which is found above 45 cm (termed as leaf area of upper canopy, LAUC), a linear relationship is obtained at both elongation ($R^2 = 0.84$, p = 0.056) (Figure 27E) and grain-filling stages ($R^2 = 0.99$, p = 0.002) (Figure 27F). At elongation stage, enlargement of LAUC by 75% promoted LUE_{inc} up to 21%, and enhancement of LUE_{inc} during grain-filling stage was 23.1% compared to 32% enlargement of LAUC (Figure 27F). Similar linear relationship between LUE_{ins} and LAUC at elongation and grain-filling phases was evidenced, giving increment of LUE_{ins} by 19.5% and 25.7%, respectively for a 75% and 32% increase in LAUC (Figure 27E). At both development stages, increasing LAUC could be one growth strategy for the plant canopy to improve carbon gain, since there was a tight correlation between leaf nitrogen content on a mass basis and leaf LUE ($R^2 = 0.62$; p < 0.01, data not shown). Another advantage due to enlargement of the upper canopy was that a higher proportion of leaf area was exposed to full sunlight, especially during midday (Figure 28C and D). Compared to the low nutrient group, over the course of the day, the total amount of sunlit leaf area of the upper canopy in the normal group was significantly larger, by 44%. To examine the effect of changing the vertical distribution of leaf area, we reversed the vertical distribution patterns found in the two fertilization treatments and recalculated sunlit leaf area (gray lines in Figure 28C and D) (i.e., the vertical distribution of leaf area in the low treatment (Figure 27D) was used to recalculate sunlit leaf area in the high nutrient treatment and vice versa.). This had the effect of reducing the difference in sunlit leaf area in the upper canopy between treatments to 20%. Likewise, increasing LAUC in the low fertilization treatment increased the amount of sunlit leaf area in the upper canopy by 22% (Figure 28D, gray lines). Importantly, allocating more leaf area to positions higher in the canopy where leaves contain more nitrogen (Figure 24A and B) would have the effect of allocating additional leaf nitrogen to canopy positions experiencing high light conditions and enhancing photosynthetic nitrogen use efficiency (Figure 28A).
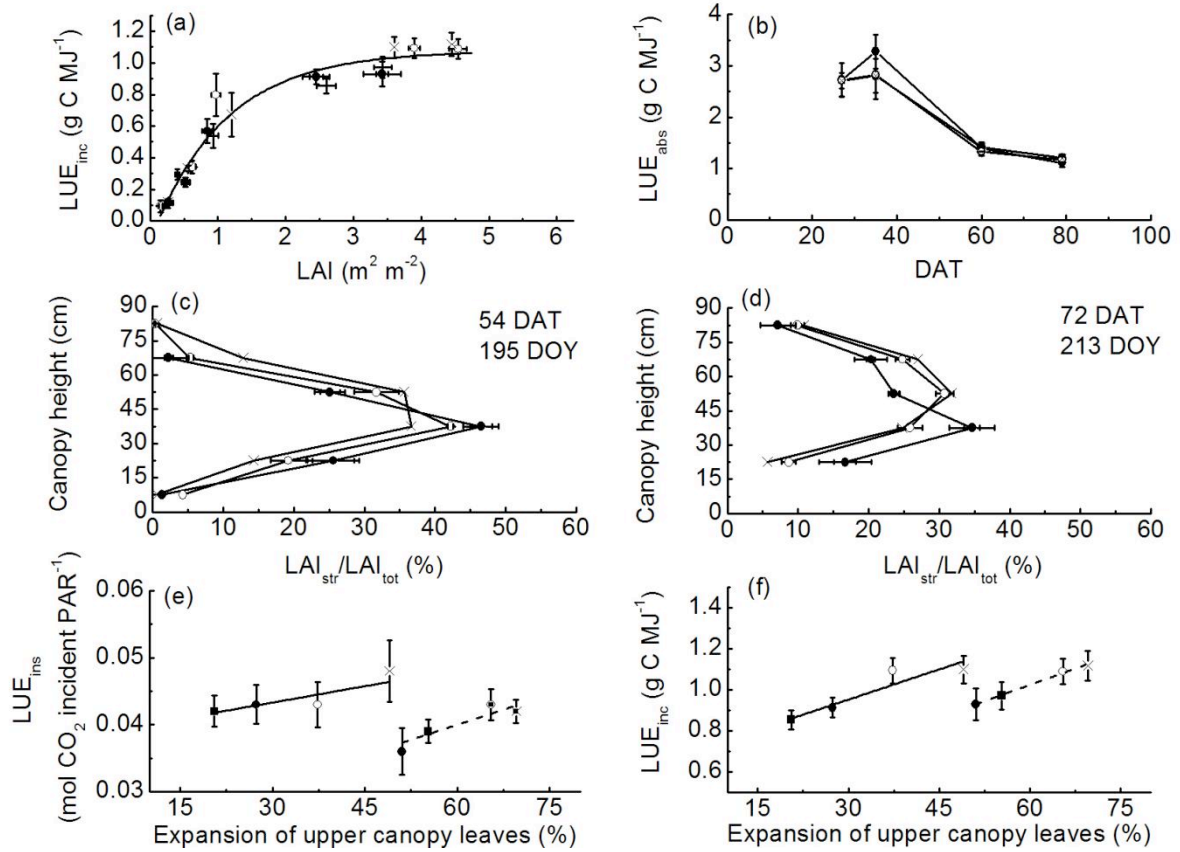
Figure 27: (A) Correlation between canopy light use efficiency (LUE$_{inc}$) and leaf area index, (B) seasonal development of LUE$_{abs}$, (C) and (D) proportion of stratified leaf area height > 45 cm to total canopy area. (E) Instantaneous canopy light use efficiency (LUE$_{ins}$) and expansion of upper canopy leaves (based on plot C and D), and (F) LUE$_{inc}$ and expansion of upper canopy leaves during elongation (solid line) and grain-filling stage (dot line). Bars indicated S.E., n = 3 to 6.
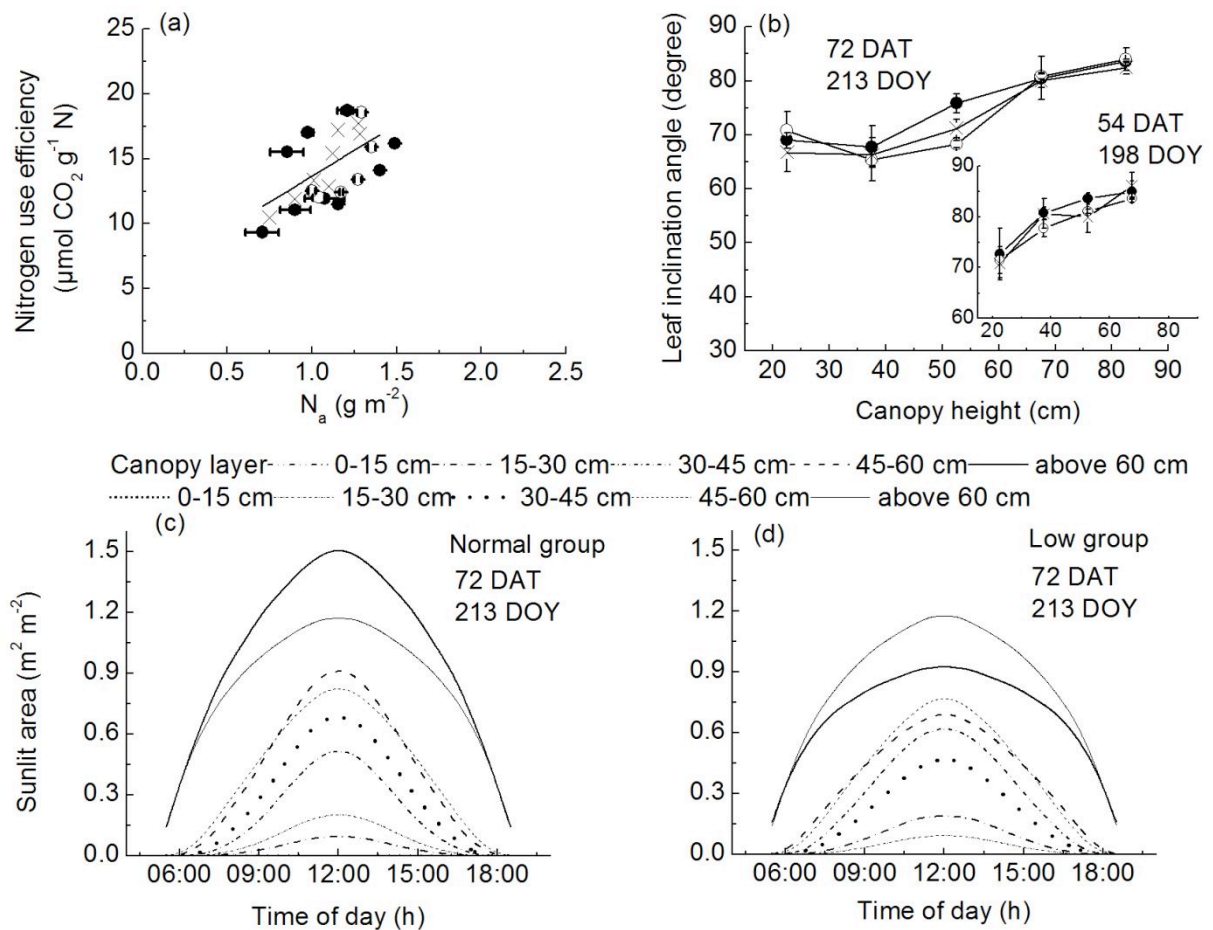
Figure 28: (A) Correlation between nitrogen use efficiency and leaf nitrogen content per leaf area, and **(B)** leaf inclination angle comparisons in canopy positions at elongation and grain-filling stages. **(C)** and **(D)** Changes of sunlit leaf area at canopy layers from sunrise to sunset during grain-filling stage for low and normal groups using actual measured vertical leaf distributions (black lines) or using reversed leaf distributions (grey lines). Bars indicate S.E., n = 3 to 6.

4.5. Discussion

In this study, carried out in South Korea in the summer of 2013, paddy rice plants (*Oryza sativa* L. cv. Unkwang) were grown under three levels of nitrogen fertilization, and the effects of fertilization on biomass accumulation were investigated. Not surprisingly and corresponding to previous research (Yang et al., 2015), aboveground biomass accumulation in paddy rice fields responded positively to increased levels of fertilization, although the positive effects of increased nitrogen seemed to be saturated at levels of 115 kg N ha^{-1}, since addition of 180 kg N ha^{-1} led to no further increase in production (Figure 22A). 80% of the total fertilizer addition was applied two days prior to transplanting and the remaining 20% was applied 19 DAT. Only slight aboveground biomass differences between treatments were

observed throughout the tillering phase, which lasted until approximately 30 DAT. With the onset of the elongation growth phase following 30 DAT, however, aboveground biomass in the two treatments receiving supplemental N was greatly accelerated relative to the unfertilized plots. The productivity gap between fertilized and unfertilized plots continued to widen until peak biomass was reached at the end of the elongation stage (~64 DAT), at which time aboveground biomass in the two fertilized treatments was approximately 60% greater than in the plots receiving no supplemental nitrogen. Following peak biomass, aboveground biomass in the fertilized plots declined more rapidly through flowering and grain-filling stages that in the unfertilized plots, and at 100 DAT the advantage in the fertilized plots had fallen to approximately 40%. Similar to biomass accumulation, there was only a small discrepancy in grain yield between the normal and high groups, but they produced 58% and 73% more grain, respectively, than the low fertilization treatment.

In general, during tillering, plots in all nutrient treatments exhibited low GPP_{max} and GPP_{int}, both of which rapidly increased after ~32 DAT, reaching a peak at the end of the reproductive stage and then declining until the end of ripening stage or at harvest (Figure 22B). Following tillering (after 32 DAT) ample fertilization management significantly promoted GPP_{max} and biomass production relative to unfertilized plots, and the GPP_{max} advantage of fertilized plots continued to increase throughout the elongation stage. Observed GPP_{max} values in our research (21.4 to 27.4 $\mu mol\ m^{-2}\ s^{-1}$) were compatible with reports of 21.8 ± 3.7 $\mu mol\ m^{-2}\ s^{-1}$ in South Korea (Lindner et al., 2015). The integrated GPP (GPP_{int}) under normal field management in our study (9.9 to 11.3 g $m^{-2}\ d^{-1}$; Table 10) fell within the reported range of Asia traditional paddy system 10.36 to 15.2 g $m^{-2}\ d^{-1}$ (Miyata et al., 2000; Alberto et al., 2012; Lee, 2015). Reported variability in carbon gain capacity of paddy rice can probably be ascribed to ecological conditions where rice was planted such as field management practice and fertilizer application rate, and also to endogenous variations in the rice genotypes selected.

We sought to determine the mechanistic basis for the observed productivity enhancement with supplemental fertilization. Crop productivity is largely determined by the amount of solar radiation intercepted by the canopy and the efficiency with which that absorbed energy is converted to carbohydrates in the process of photosynthesis (Monteith, 1972; Goward and Huemmrich, 1992; Inoue et al., 2008). This notion has been formalized in the concept of light utilization efficiency, which in the content of crop production, has been defined as carbon uptake divided by irradiance, both integrated over some period of time. As pointed out by Gitelson and Gamon (2015), carbon uptake can be variously defined as net photosynthesis, gross or net primary production, and irradiance as incident or absorbed PAR. LUE_{inc} is defined here as daily GPP (g C m^{-2} ground) integrated over the daylight hours, divided by incident PAR (MJ), integrated over the same period.

LUE_{inc} was measured five times during the growing season (Figure 22C) and increased rapidly in all treatments as canopy leaf area increased during the tillering and elongation stages of development, then leveled off as the canopy approached full closure. Beginning during tillering, LUE_{inc} in the fertilized plots exceeded that in the unfertilized treatment by 20-30%, a differential that persisted into the flowering and grain-filling stages. Research in soybean reported maximum LUE_{inc} of 1.2 g C MJ^{-1} (Gitelson and Gamon, 2015) and approximately 1.0 g C MJ^{-1} in rice (Atwell et al., 1999), which are similar to our values in this rice study (1.12 g C MJ^{-1} for fertilized and 0.92 g C MJ^{-1} for unfertilized plots).

LUE_{inc} is a representative reflection of crop ecophysiology responding to varying growth environment, and is influenced by multiple factors such as leaf area development, canopy light interception, light conversion efficiency, and leaf photosynthetic physiology associated with nitrogen investment in leaves and diffusional limitations. We will examine each of these factors that contribute to LUE_{inc} to better understand how fertilized rice plants utilize supplemental N to enhance their growth rates and biomass accumulation.

4.5.1. The role of leaf photosynthetic capacity in determining LUE$_{inc}$

Enhanced nitrogen supplied through supplemental fertilization, if allocated to individual leaves, might be expected to increase net photosynthetic rates by increasing the amounts of rate limiting enzymes. The importance of N_a in establishing photosynthetic performance is highlighted by data in Figure 25. A_{max}, across all fertilization treatments and over the course of the season, is a linear function of N_a (Figure 25A) as often reported previously (Yoshida 1981; Campbell et al., 2001A; Niinemets, 2007). Furthermore, as reported by Evans and Loreto (2000) and Bernacchi et al. (2002) the primary determinants of photosynthetic competence, V_{cmax} and J_{max}, are also linearly related by N_a (Figure 25B and C), resulting in a strong linear relationship between the two (Figure 25C, inset) with a slope 1.3 that falls within the range reported for a variety of C_3 species (Niinemets et al., 2009A; Wullschleger, 1993). This linear relationship between N_a and photosynthetic components is explained by the importance of nitrogen in determining amounts of rate-limiting enzymes in the Calvin cycle (especially Rubisco) and the electron transport chain. Both stomatal and mesophyll conductances also increase linearly with N_a (Figure 25E and F) but a mechanistic basis for this dependency is less obvious; however, it reveals the high degree of coordination between leaf biochemistry and diffusional limitations, which forms the basis of, for example, the empirical model of stomatal conductance developed by Ball et al. (1987). One of the consequences of this coordination between g_s and A_{max} is to maintain values of C_i across all treatment within a fairly narrow range (240 to 260 mmol mol^{-1}).

Clear treatment differences are apparent in the allocation of available nitrogen to photosynthetic processes early in the growing season. During tillering stage, N_a in the normal and high fertilization treatment was approx. 32% higher than in the low treatment (Figure 23A). N_a subsequently declined in all treatments, but the decline was particularly pronounced in fertilized plots, such that treatment differences in N_a narrowed, and by 47 DAT, midway through the elongation phase, significant differences were no longer apparent.

These differences in leaf nitrogen were reflected in photosynthetic performance at the individual leaf level. Light-saturated net photosynthesis at 30°C ($A_{max,30}$) of upper canopy leaves was approximately 16% greater in fertilized plots during tillering, but as N_a declined through the growing season, treatment differences in $A_{max,30}$ were greatly reduced (Figure 23B). Similarly, higher rates of both $V_{cmax,30}$ and $J_{max,30}$ (Figure 23C) observed in fertilized treatments during tillering were largely eliminated during later growth stages as N_a declined more rapidly in fertilized than unfertilized plots.

Figure 24 illustrates profiles through the canopy of N_a and photosynthetic parameters during the elongation and grain-filling developmental stages. During elongation, plants in fertilized plots clearly allocated more nitrogen to within canopy leaves than plants in the unfertilized treatment (Figure 24A) but, surprisingly, these differences were not reflected in parallel changes in $A_{max,30}$ (Figure 24C) with depth in the canopy. $V_{cmax,30}$ values of lower canopy leaves were less in plants without supplemental fertilizer, reflecting lower N_a, but $J_{max,30}$ values did not differ at this stage between treatments. The absence of a nitrogen effect on $A_{max,30}$ may therefore reflect the fact that within-canopy leaves were operating on the RuBP-regeneration portion of the A-C_i response curve (Bernacchi et al., 2002; Yamori et al., 2011), where reductions in $V_{cmax,30}$ would not be reflected in the photosynthesis measurement. Lower canopy leaves, in which photosynthesis is often light-limited, would benefit from preferentially allocating limiting nitrogen to light-harvesting proteins (i.e., $J_{max,30}$) at the expense of Rubsico ($V_{cmax,30}$). Later in the season, during grain-filling, canopy profiles of N_a and photosynthetic parameters were largely indistinguishable across treatments (Figure 24B, D, F, H, J).

Canopy area development and the total amount of free nitrogen content have been considered limiting factors in mediating canopy carbon gain (Leuning et al., 1995). Establishing a dynamic balance between reduced canopy area and sufficiently high nitrogen invested in leaves is a survival strategy under limited nitrogen conditions (Anten, 1995; Niinemets,

171

2007). Consistent with this, rice plants in the low fertilization group were able to maintain leaf nitrogen levels, especially in uppermost leaves, comparable to leaves in plants with supplemental nitrogen (Figure 23A; Figure 24A and B), but only by limiting the development of total canopy leaf area (Figure 22D). This nitrogen allocation strategy explains the narrowed difference in leaf N among nutrient groups in the elongation and grain-filling stages.

Independent of leaf biochemistry, CO_2 diffusion resistance in leaves, both stomatal and in the mesophyll, can significantly constrain carbon fixation by reducing the CO_2 partial pressure at the site of fixation. As mentioned above, as photosynthetic capacity increased with increasing N_a, the total limitation imposed by diffusional constraints declines (Figure 26C). A comparison of Figure 25E and F indicates that g_m increases more rapidly with increasing N_a than does g_s, such that the ratio of the two ($g_{s,30}$:$g_{m,30}$) declines (Figure 26D). Thus, the relative importance of g_m in limiting net photosynthesis declines with increasing nitrogen and stomatal limitations becomes increasingly significant. The percent limitation imposed by stomata is somewhat scattered, varying between 17 and 27%, but shows no clear dependence on N_a (Figure 26B), while mesophyll limitations clearly become less pronounced as N_a increase (Figure 26A), which was also previously reported (Monti et al., 2009; Tosens et al., 2012). Thus, diffusional limitations, particularly those imposed by the mesophyll, became more important as the growing season advanced and leaf nitrogen declined. Although diffusional limitations increased through the growing season, and represented a significant limitation (up to almost 45%) during grain-filling, there were no clear treatment differences in either mesophyll or stomatal limitations (Table 10).

In summary, large treatment differences in leaf photosynthetic physiology were apparent only in the early stages of development. Plants in the unfertilized paddies were generally able to maintain leaf nitrogen levels and photosynthetic capacities comparable to fertilized plants, but only at the expense of reduced canopy leaf area, discussed below.

4.5.2. Differences in seasonal canopy development between fertilization treatments

In addition to leaf photosynthetic properties that help determine LUE_{inc} through their role in controlling GPP_{max} and GPP_{int}, LUE_{inc} also depends strongly on the amount of light absorbed by the canopy, which depends on LAI (Leuning et al., 1995) and to a lesser extent, leaf angle distribution and leaf clumping.

In the first few weeks after transplanting, canopy development was slow, but by the beginning of the leaf elongation stage of development (ca. 30 DAT) canopy leaf area in the fertilized treatment had clearly accelerated relative to that in unfertilized plots, and this LAI advantage was maintained through flowering and grain-filling (Figure 22D). As a result, on any given day, fertilized canopies were able to absorb significantly more above-canopy PAR than unfertilized plots throughout the leaf elongation, flowering and grain-filling stages. Since GPP is strongly influenced by absorbed PAR, seasonal changes in both GPP_{max} and GPP_{int} (Figure 22B) paralleled changes in LAI (Figure 22D), increasing rapidly through the elongation phase and then leveling off during flowering and grain-filling. Inasmuch as LUE_{inc} is driven primarily by GPP_{int}, it is not surprising that LUE_{inc} differences between fertilization treatments also persisted throughout the growing season (Figure 22C).

Treatment differences in LAI, PAI and light absorption coefficients at two different growth stages are apparent in Figure 21 and Figure 27. During elongation (ca. 54 DAT) K_L values were similar across all treatments, while both LAI and PAI were approximately 50% greater in the fertilized plots than in the unfertilized treatment. The percentage of incoming PAR absorbed by canopies in each treatment was calculated using Equation 17 and PAI and K_L values from Table 10, and the unfertilized plots absorbed 44% of incoming PAR, significantly less than the normal or high nutrient plots (59% and 55%, respectively). High canopy light interception in fertilization group was directly documented by canopy reflectance NDVI which exponentially correlates to absorption of PAR by canopy (Figure 21A). Field measurement of light interception across three nutrient groups corresponded well to canopy

173

level spectrum reflectance, meaning NDVI could be one powerful biophysical index to reflect variation of canopy light interception due to soil nutrient availability. The observed lower canopy light interception ratio in the low treatment was actually ascribed primarily to lower canopy leaf area. Three weeks later, in the grain-filling stage (ca. 74 DAT), when all canopies were further developed, K_L values were much larger, and K_L in the unfertilized plots was comparable to the normal or high nutrient treatments, perhaps reflected in similarities in leaf angle distributions (Figure 28B). K_L measured during grain-filling stage fell in the range of 0.2-0.3 for erect canopy and 0.6-0.8 for prostrate canopy in rice (Sheehy and Mitchell, 2013), and favorably conformed to reports in two cultivars Nipponbare and Chugoku 117 with 0.24 and 0.5 at elongation and grain-filling stage, respectively (Saitoh et al., 2002) and 0.4 at end of elongation stage (Lee et al., 2006). Research in crops indicates that leaves in the upper part of the canopy tend to be more erect, with high leaf inclination angle, while lower positioned leaves tend to be displayed more horizontally in order to intercept transmitted light more efficiently (Anten et al., 1995). During the measuring seasons, averaged leaf angle distributions at each layer were similar among nutrient groups (Figure 28B), which might relate to similar light attenuation coefficient (Table 10), since variation in K_L value is commonly associated with leaf angle (Atwell et al., 1999; Sheehy and Mitchell, 2013). Compared to elongation stage, plants during grain-filling had significantly higher LAI, PAI and light extinction coefficients and thus absorbed a much higher fraction of incident PAR than earlier. Although PAR absorption by fertilized plots (92% and 91% in normal and high treatments, respectively) remained higher than in the unfertilized paddies (85%), treatment differences had clearly narrowed compared to earlier growth phases. The greatest benefit arising from increased nitrogen availability is the burst in productivity early in the elongation stage that stimulates rapid canopy development and increasing LAI (Figure 22D). Thus, development of aboveground biomass is accelerated in fertilized plots, enabling them to maintain their LAI advantage throughout development. This leads to greater PAR absorption

in fertilized plots, enhancing both GPP_{int} and LUE_{inc}. Thus, GPP_{max} increased rapidly between DAT 30-60 (Figure 22B) despite the fact that A_{max} (net assimilation at the leaf scale) and LUE_{abs} both were already declining (Figure 23B and Figure 27B), implying that the observed increase in GPP is not a result of improved photosynthesis at the leaf level, but rather it is due to increased PAR absorption.

Light use efficiency based on absorbed light by canopy (LUE_{abs}) across three nutrient groups were not constant over growing season, with higher level at active tillering phase and lowering level going on after that stage. Light use efficiency might not be constant and change as crop species develop (Gimenez et al., 1994; Alberto et al., 2013), with a maximum existing during vegetative stage and lower at early and late seasons in crops (Hall et al., 1995). Our reports favorably compared to theirs. LUE_{abs} of post-anthesis of spikelet fluctuated in a range from 0.73 to 1.22 g C MJ^{-1} and that of elongation growth between 1.52 and 2.1 g C MJ^{-1} (Campbell et al., 2001B). Similar seasonal tendency was also reported in paddy rice by Inoue et al. (2008). LUE_{abs} of grain-filling plants in our research ranged within their reports, while relatively high levels at elongation stage in our research were observed. Large fluctuations in seasonal LUE_{abs} in fast-growing rice crop are within our anticipation, since crop physiology and resource use strategy change significantly within short time period especially growth stage transit from active tillering to elongation and flowering stage (Figure 22). Variations in GPP (product of LUE_{abs} and intercepted PAR) can not be solely interpreted by either LUE_{abs} or intercepted light. Decline in LUE_{abs} partially interpret phenomena of GPP saturation at higher LAI that decline of LUE_{abs} might counteract benefits gained from increasing canopy light interception.

In addition to allocating more resources to leaf area development, plants in the fertilized treatments also produced a higher percentage of the leaves in the upper layers of the canopy during both elongation and grain-filling stages (Figure 27C and D). Recent research reported potential enhancement of carbon gain capacity arising from the enlargement of mid-upper

canopy leaves in cucumber (Chen et al., 2014). In our study, in all treatments at the elongation stage, the canopy layer with the highest amount of leaf area was the 15-cm thick layer centered at 37.5 cm height. In the low nutrient treatment, leaf area distribution was symmetrical, with approximately 26.9% of leaf area displayed in lower canopy layers, below 30 cm height, and 27.2% in layers above 45 cm. In fertilized plots, leaf area distribution was skewed towards upper layers, with 38.9% above 45 cm and only 15.0% below 30 cm in the normal nutrient plots, while in the high fertilization treatment the values were 37.2% and 23.4% in the upper and lower portions of the canopy, respectively. Later, during grain-filling, as canopy height increases, differences were maintained as only 27.4% of leaf area in low N plots was found above 60 cm height while 50.2% occurred below 45 cm. Corresponding numbers for the normal treatment were 34.7% and 30.4% and for the high fertilization treatment, 37.6% and 33.4%.

Positioning a higher percentage of leaf area in upper layers of the canopy exposes a greater amount of leaf area in fertilized plants to full sunlight conditions. This effect can be seen in Figure 28C and D, which presents modeling results using the multi-layer light interception model of Caldwell et al. (1986) comparing the amount of sunlit leaf area in low and normal fertilization plots during grain-filling and examines the effect of vertical leaf distribution. Total light absorption by the fertilized canopies was about 7% higher (92% in normal vs. 85% in low) but it is clear that far more leaf area is potentially exposed to sunlit conditions in the normal fertilization plots. Most of this difference is clearly the result of higher total leaf area, but we used the model to investigate the effect of altering the vertical leaf distribution. When the sunlit leaf area of the normal fertilization canopy was re-calculated using the vertical leaf distribution associated with the low nutrient canopy, the total amount of sunlit leaf area was unchanged, but more of the sunlit area was located in the lower canopy layers. When the leaf distribution of the normal canopy was used to re-calculate sunlit leaf area in the low fertilization canopy, the reverse was true. Depending on the vertical distribution of leaf

nitrogen, discussed below, these shifts in the vertical distribution of sunlit leaves could have implications for canopy carbon uptake. Since there is a steep gradient in N_a (and photosynthetic capacity) within rice canopies (Figure 24) the ability of fertilized rice plants to display more sunlit leaves in upper canopy layers, where leaves have higher leaf nitrogen and photosynthetic capacity, should provide an additional advantage to rice in fertilized paddies. Because there is a significant amount of residual nitrogen (i.e., nitrogen allocated to non-photosynthetic processes, x-intercept in Figure 25A) leaf nitrogen use efficiency (mmol CO_2 g^{-1} N) increases with increasing N_a (Figure 28A) particularly when incident PAR is high, as in upper canopy leaves. Similarly, leaf LUE also increases with increasing leaf nitrogen (data not shown), providing an additional advantage to displaying more leaf area in upper layers of the canopy. The linear correlations found between the percentage of leaf area in the upper canopy and both LUE_{ins} (Figure 27E), and LUE_{inc} (Figure 27F) supported promising role of deployment of leaf area allocation in crop canopies to optimally adjust gross carbon fixation.

4.5.3. Promoted canopy leaf area by fertilization depends on leaf number per bundle and relates to nitrogen-facilitated photosynthesis occurring initially

Differences in the rate of canopy leaf area development appear to be a key component in determining treatment differences in GPP and LUE_{inc}. It appears that supplemental nitrogen supplied during tillering enhances leaf nitrogen concentrations in early emerging leaves (Figure 23A), which manifests itself in higher amounts of photosynthetic enzymes (Figure 23C) and higher rates of light-saturated photosynthesis (Figure 23B). It appears that the initial photosynthetic advantage enjoyed by fertilized plants provides an initial burst of biomass production that is allocated to rapid production of new leaves. As shown in Table 2, relatively early in the elongation phase (DAT 43), the mean number of leaves per planted bundle (five plants) in the normal fertilization treatment (101) is 75% greater than in unfertilized paddies (57). This difference is also reflected in the mean leaf biomass per bundle, which was 50%

higher in the normally fertilized treatment than in the unfertilized plots, and 60% higher in the high nitrogen treatment. A comparative study in the first year of growth of eight perennial grasses observed that plants under nutrient-rich habitat had higher SLA (Elberse and Berendse, 1993), which increases the above ground LAI significantly (Knops and Reinhart, 2000). In our study there were no clear differences in leaf SLA among the three nutrient treatments (Figure 23A) or in canopy level SLA (not shown). Higher leaf area in fertilized paddies therefore mainly resulted from increased leaf numbers per planted bundle (Table 9), dramatically promoted by fertilization, rather than treatment differences in leaf thickness or morphology. This early advantage in leaf number and canopy leaf area development stimulated GPP_{int} and LUE_{inc} (Figure 27A) and allowed the fertilized plots to maintain their LAI advantage for the remainder of the growing season, despite having leaf photosynthetic characteristics similar to unfertilized paddies.

Very large gradients of light intensity exist within plant canopies, with light attenuation as large as 90% in bottom layers especially in dense canopies (Rosenberg et al., 1983). In our study, maximum light attenuation of 92% was observed late in the season, during grain-filling, in the normal fertilization plots. Research in several crop species has demonstrated that light distribution is commonly coupled to nitrogen patterns within canopies (Hirose and Werger, 1987), and that nitrogen extinction coefficients are higher under conditions of low N supply (Milroy et al., 2001; Moreau et al., 2012). In our study, higher values of K_N in the low nutrient group at both elongation and grain-filling stages were evident (Table 10), in agreement with previous reports. Leaf nitrogen distribution at the grain-filling stage was less uniform (i.e., higher K_N) than during leaf elongation in all nutrient treatments, which parallels seasonal changes in light extinction (K_L). Thus, nitrogen allocation patterns as the canopy developed reflected increasing light gradients.

4.6. Conclusions

Sustainable rice production system is treated as capable of producing high yield production with less nitrogen and water resource consumption and minimized impacts on environment sustainability. A sustainable rice production system is currently challenging by critical global environmental problems caused by surplus fertilizer application and greenhouse gas emission. Harvest high biomass production from this fast-growing crop coincident with environmental protection needs a priori establishment of fundamental knowledge with respect to plant growth, regulation and adaption to anthropogenic intervention. Biomass accumulation by plant is a direct result of photosynthesis which could be stimulated by soil nitrogen addition. Disentangling ecophysiological mechanisms influencing regulations of rice plant growth and carbon fluxes is still open area need to fill in. In this research, we attempt to understand ecophysiological traits that relate to plant efficient carbon gain, and to determine important factors need to be concerned in sustainable rice production system.

During active tillering stage, fertilization manipulations enhanced leaf N content and consequently contributed to higher photosynthesis rates, presumably due to significantly higher rate-limiting photosynthetic proteins. An important consequence of greater assimilation rates was the more rapid production of new leaves, resulting in higher leaf number per planted bundle and head start in canopy area size which is a promising resource use strategy to maximize canopy light interception and thereby plant carbon gain capacity and biomass accumulation. Rapid increase in GPP dismissed and approached saturation when canopy was closing intensively, even though more light could be intercepted. DPP saturation at higher LAI could be partially explained by continuous decline of light use efficiency after active tillering stage. Whereas, allocate more leaves at upper part of canopy is seeming to be promising growth strategy to enhance carbon gain, since more leaves are exposed to full sunlight environment and those leaves assemble more nitrogen concentration with lowering CO_2 diffusion resistance. We suggest that basic knowledge of coordinated adjustments

between structure and leaf physiology should be in concert in sustainable rice production system.

4.8. Appendices

Appendix A. Chloroplast CO$_2$ compensation point

CO$_2$ response curves at different measuring light intensities (PAR of 500, 200 and 100 μmol m^{-2} s^{-1}) and at leaf temperature of 30°C at tillering and grain-filling stage were obtained using growth chamber acclimated plants. CO$_2$ curves were commenced after leaves had acclimated to the cuvette microenvironment (CO$_2$ 400 μmol mol^{-1} and measuring PAR 1500 μmol m^{-2} s^{-1}) after which CO$_2$ concentration was changed progressively in the sequence 400, 200, 150, 100 to 50 μmol mol^{-1}. Relative humidity was controlled to ca. 60%. Assimilation rate and stomatal conductance data were recorded after new steady-state readings were obtained. At least three replicate CO$_2$ curves were obtained. Chlorophyll fluorescence was measured simultaneously. Fully expanded leaves in different age classes, distinguished by distinct differences in photosynthetic capacity, were selected for study. Leaf physiology was not altered by the experimental manipulations at different CO$_2$ concentrations as indicated by complete recovery afterward to the initial A$_{max}$ at 400. Leaves adjacent to those used for CO$_2$ curve measurements were then enclosed in the leaf cuvette at O$_2$ concentration of ca. 1% provided by an external gas cylinder (99% N$_2$) in stable flow rate identical to working frequency of pump of Walz GFS-3000 system, and CO$_2$ response determinations were repeated. Chloroplast CO$_2$ compensation point was defined as the intercellular CO$_2$ concentration where downward extension of linear phase of each photosynthesis-CO$_2$ response curve cross-transit (Figure 29B).

Appendix B. Estimation of linear electron transport rate (J$_p$)

While measuring gas exchange, chlorophyll fluorescence was simultaneously assessed with a Walz PAM-Fluorometer 3050-F to monitor dynamics of the quantum yield of photosystem II (Φ$_{PSII}$) in response to varying CO$_2$ concentrations. Only those fluorescence data exhibiting a clear saturation plateau after application of a saturating actinic pulse were considered in the

calculations described below. The electron transport rate (ETR) passing through photosystem II (J_F) was calculated using the equation of Genty et al. (1989),

$$J_F = \Phi_{PSII} \cdot \alpha \cdot \beta \cdot Q,$$ **Equation 23**

where Q is incident PAR, α is leaf absorptance (0.84 for rice adopted here from Agarie et al. (1996), and β is the fraction of excitation energy absorbed by PS II.

Partitioning J_F into component J_P with flow through PS II and I to support Rubisco carboxylation and oxygenation and an alternative component, J_A, which supports electron consumption by O_2-dependent acceptors (i.e., the Mehler reaction, nitrite reduction, and oxaloacetate reduction) and O_2-independent acceptors (i.e., cyclic electron transport around PS II) is physiologically meaningful under saturating light in cereals (Loreto et al., 1994). The electron transport rate calculated from chlorophyll fluorescence measurements, J_F, is the sum of J_P plus J_A. The component J_P which is required to calculate mesophyll conductance of the leaf can be expressed as:

$$J_p = J_F \cdot (1 - b_F),$$ **Equation 24**

where b_F is the ratio of J_A to J_F. Rearranging,

$$b_F = 1 - J_p/J_F,$$ **Equation 25**

The value of b_F is assumed to be constant in unstressed plants at normal atmospheric CO_2 and 21% or lower O_2. The value of b_F, and therefore the value for J_p, can be obtained in the following manner. Equation 23 can be re-expressed as follows:

$$J_F = \sigma \cdot \Phi_{CO2} \cdot \alpha \cdot \beta \cdot Q,$$ **Equation 26**

Where σ is the ratio of Φ_{PSII} to Φ_{CO2}, the efficiency of CO_2 fixation, Φ_{CO2} is defined as G/Q where G, gross photosynthesis. Substituting for Φ_{CO2},

$$J_F = \sigma \cdot G \cdot \beta,$$ **Equation 27**

Assuming a conservative value for the number of electrons required for NADPH synthesis and the amount of NADPH required for regeneration of one molecule of ribulose-1,5-bisphosphate (RuBP), i.e., 4 electrons consumed for one molecule of CO_2 fixed in the absence of photorespiration, $J_P = 4G$. Substituting this value for J_P and the value for J_F from Equation 27 into Equation 25,

$$b_f = 1 - J_P / J_F = 1 - 4G/(G \cdot \sigma \cdot \beta) = 1 - 4/(\sigma \cdot \beta), \qquad \textbf{Equation 28}$$

We estimated the value of σ by calculating Φ_{PSII} and Φ_{CO2} over a range of varying ambient CO_2 concentrations and light intensities under low O_2 (to infer the alternative electron transport rate, ETR, occurring under normal atmosphere conditions) and then plotting them against one another (Figure 29A). The slope of the relationship, i.e., σ was found to be 8.5, which fell in the range reported in the herbaceous under relatively high light and normal air conditions (Flexas et al., 2007; Genty et al., 1989; Laisk and Loreto, 1996; Loreto et al., 1994) and parallel with the average (slope of black line) (Figure 29A). The fraction of absorbed light used by PS II, β, varies between 0.45 and 0.6 in herbaceous and tree species (Laisk and Loreto, 1996), and similar values between 0.39 and 0.51 have been reported for several C_3 species (Flexas, 2007). We assume that the absorbed radiation is equally distributed between PS I and PS II, i.e., $\beta = 0.5$. With $\sigma = 8.5$ and $\beta = 0.5$, the value of b_F for our data is 0.06, meaning that J_A is only a few percent of J_P to compensate variations in the NADPH synthesis as compare to the linear flow.
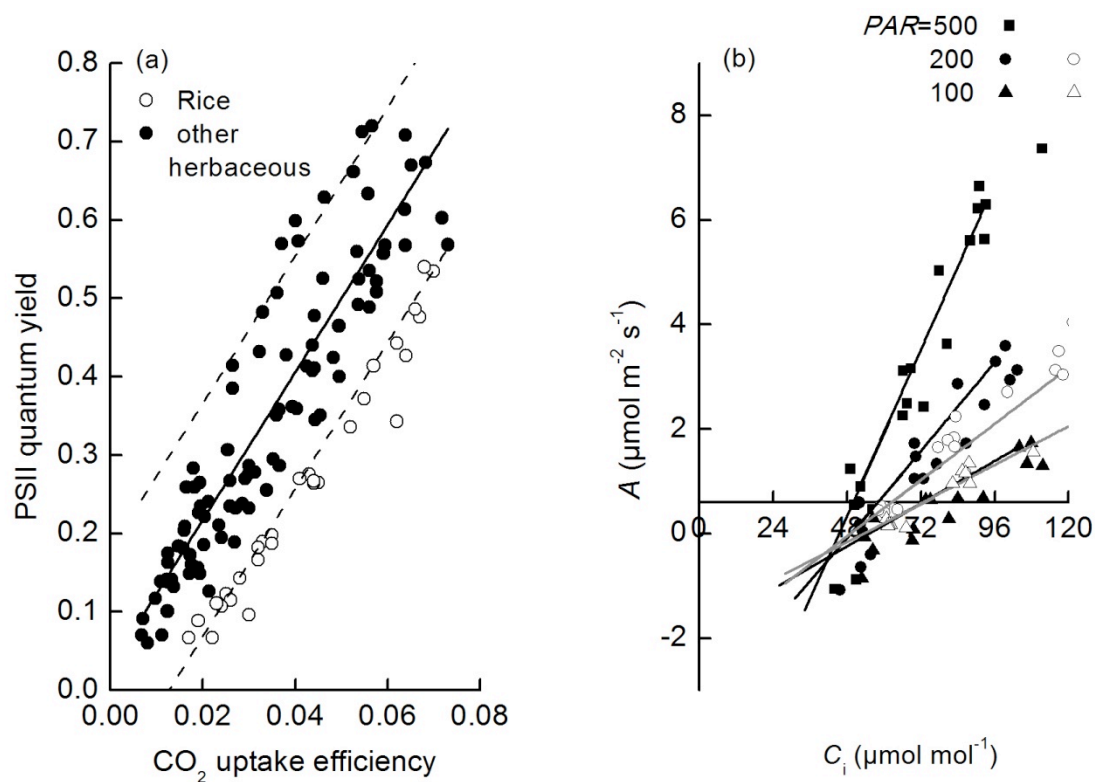
Figure 29: (A) Relationship between quantum yield of PS II and efficiency of CO$_2$ fixation under varying ambient CO$_2$ concentration and light intensity with O$_2$ approximately 1% in rice (open circle) and other herbaceous (black circle). (B) CO$_2$ response curves at measuring light intensities of 500, 200, 100 μmol m^{-2} s^{-1} and leaf temperature 30°C during tillering (filled symbols) and grain-filling stage (open symbols). n = 5 to 6. Linear fits to each data set were made to estimate the C$_i$ value at which response curves intersect, indicative of G* of 44.4 ± 1.3 μmol mol^{-1}.

4.9. References

Adachi, S., Nakae, T., Uchida, M., Soda, K., Takai, T., Oi, T., Yamamoto, T., Ookawa, T., Miyake H., Yano M., and Hirasawa T. 2013. The mesophyll anatomy enhancing CO_2 diffusion is a key trait for improving rice photosynthesis. J. Exp. Bot. 64, 1061-1072. doi: 10.1093/jxb/ers382

Alberto, M.C.R., Hirano, T., Miyata, A., Wassmann, R., Kumar, A., Padre, A., Amante, M. 2012. Influence of climate variability on seasonal and interannual variations of ecosystem CO2 exchange in flooded and non-flooded rice fields in the Philippines. Field Crops Res. 134, 80-94. doi: 10.1016/j.fcr.2012.05.002

Alberto, M.C.R., Buresh, R.J., Hirano, T., Miyata, A., Wassmann, R., Quilty, J.R., Correa, T.Q., Jr., Sandro, J. 2013. Carbon uptake and water productivity for dry-seeded rice and hybrid maize grown with overhead sprinkler irrigation. Field Crops Res. 146, 51-65. doi: 10.1016/j.fcr.2013.03.006

Anten, N.P.R., Schieving, F., Werger, M.J.A. 1995. Patterns of light and nitrogen distribution in relation to whole canopy carbon gain in C_3 and C_4 mono–and dicotyledonous species. Oecologia 101, 504–513. doi: 10.1007/BF00329431

Atwell, B.J., Kriedemann, P.E., Turnbull, C.G.N. 1999. Sunlight: an all pervasive source of energy-light use efficiency. In Plants in Action: Adaption in nature, performance in cultivation. Macmillan Education Australia Pty Ltd, Melbourne, Australia.

Bernacchi, C.J., Portis, A.R., Nakano, H., von Caemmerer, S., Long, S.P. 2002. Temperature response of mesophyll conductance. Implications for the determination of rubisco enzyme kinetics and for limitations to photosynthesis in vivo. Plant Physiol. 130, 1992-1998. doi: 10.1104/pp.008250

Caldwell, M.M., Meister, H.P., Tenhunen, J.D., Lange, O.L. 1986. Canopy structure, light microclimate and leaf gas exchange of Quercus coccifera L. in a Portuguese macchia:

measurements in different canopy layers and simulations with a canopy model. Trees–Struct Funct. 1, 25–41. doi: 10.1007/BF00197022

Campbell, C.S., Heilman, J.L., McInnes, K.J., Wilson, L.T., Medley, J.C., Wu, G.W., Cobos D.R. 2001A. Diel and seasonal variation in CO_2 flux of irrigated rice. Agric. For. Meteorol. 108, 15-27. doi: 10.1016/S0168-1923(01)00225-8

Campbell, C.S., Heilman, J.L., McInnes, K.J., Wilson, L.T., Medley, J.C., Wu, G., Cobos, D.R. 2001B. Seasonal variation in radiation use efficiency of irrigated rice. Agric. For. Meteorol. 110, 45-54. doi: 10.1016/S0168-1923(01)00277-5

Chen, T.W., Henke, M., de Visser, P.H.B., Buck-Sorlin, G., Wiechers, D., Kahlen, K., Stützel, H. 2014. What is the most prominent factor limiting photosynthesis in different layers of a greenhouse cucumber canopy? Ann. Bot. doi: 10.1093/aob/mcu100.

Choudhury, B.J. 1987. Relationships between vegetation indices, radiation absorption, and net photosynthesis evaluated by a sensitivity analysis. Remote Sens. Environ. 22, 209-233. doi:10.1016/0034-4257(87)90059-9

Ehleringer, J., Pearcy, R.W. 1983. Variation in quantum yield for CO_2 uptake among C_3 and C_4 plants. Plant Physiol. 73, 555-559. doi: 10.1104/pp.73.3.555

Elberse, W.T., Berendse, F. 1993. A comparative study of the growth and morphology of eight grass speciesfrom habitats with different nutrient availabilities. Funct. Ecol. 7, 223-229. doi: http://www.jstor.org/stable/2389891

Ethier, G.J., Livingston, N.J. 2004. On the need to incorporate sensitivity to CO_2 transfer conductance into the Farquhar-von Caemmerer-Berry leaf photosynthesis model. Plant Cell Environ. 27, 137-153. doi: 10.1111/j.1365-3040.2004.01140.x

Flexas, J., Diaz-Espejo, A., Galmés, J., Kaldenhoff, R., Medrano, H., Ribas-Carbo, M. 2007. Rapid variations of mesophyll conductance in response to changes in CO_2 concentration around leaves. Plant Cell Environ. 30, 1284-1298. doi: 10.1111/j.1365-3040.2007.01700.x

Flexas, J., Ribas-Carbó, M., Diaz-Espejo, A., Galmés, J., Medrano, H. 2008. Mesophyll

conductance to CO_2: current knowledge and future prospects. Plant Cell Environ. 31, 602-621. doi: 10.1111/j.1365-3040.2007.01757.x

Flexas, J., Barbour, M.M., Brendel, O., Cabrera, H.M., Carriquí, M., Diaz-Espejo, A., Douthe,C., Dreyerc, E., Ferrio,J.P., Gago,J., Gallé,A., Galmés,J., Kodama, N., Medrano,H., Niinemets,Ü., Peguero-Pina,J.J., Pou,A., Ribas-Carbó, M., Tomás, M., Tosens T., Warren, C.R. 2012. Mesophyll diffusion conductance to CO_2: an unappreciated central player in photosynthesis. Plant Sci. 193, 70-84. doi: 10.1016/j.plantsci.2012.05.009

Foulkes, M.J., Reynolds, M.P. 2015. Breeding challenges: improving yield potential. In, Sadra, V., Calderini, D. (Eds), Crop Physiology: Application for breeding agronomy. Elsevier, USA, pp 397-422.

Gimenez, C., Connor, D., Rueda, F. 1994. Canopy development, photosynthesis and radiation-use efficiency in sunflower in response to nitrogen. Field Crops Res. 38, 15-27. doi: 10.1016/0378-4290(94)90028-0

Genty, B., Briantais, J.M., Baker, N.R. 1989. The relationship between the quantum yield of photosynthetic electron transport and quenching of chlorophyll fluorescence. Biochim. Biophys. Acta 990, 87-92. doi: 10.1016/S0304-4165(89)80016-9

Gitelson, A.A., Gamon, J.A. 2015. The need for a common basis for defining light-use efficiency: Implications for productivity estimation. Remote Sens. Environ. 156, 196–201. doi:10.1016/j.rse.2014.09.017

Goward, S.N. and Huemmrich, K.F. 1992. Vegetation canopy PAR absorptance and the normalized difference vegetation index: an assessment using the SAIL model. Remote Sens. Environ. 39, 119-140. doi:10.1016/0034-4257(92)90131-3

Hall, A., Connor, D., Sadras, V. 1995. Radiation-use efficiency of sunflower crops: effects of specific leaf nitrogen and ontogeny. Field Crops Res. 41, 65-77. doi: 10.1016/0378-4290(94)00108-O

Harley, P.C, Tenhunen, J.D., Lang, O.L. 1986. Use of an analytical model to study limitation

on net photosynthesis in *Arbutus unedo* under field conditions. Oecologia 70, 393-401. doi: 10.1007/BF00379502

Harley, P.C., Loreto, F., DiMarco, G., Sharkey, T.D. 1992. Theoretical considerations when estimating the mesophyll conductance to CO_2 flux by the analysis of the response of photosynthesis to CO_2. Plant Physiol. 98, 1429-1436. doi: 10.1104/pp.98.4.1429

Harley, P.C., Tenhunen, J.D. 1991. Modeling the photosynthetic response of C_3 leaves to environmental factors. In Modeling Crop Photosynthesis: from Biochemistry to Canopy (eds K.J. Boote, R.S. Loomis), Crop Science Society of America, Madison, WI. pp. 1-16

Hirose, T., Werger, M.J.A. 1987. Maximizing daily canopy photosynthesis with respect to the leaf nitrogen allocation pattern in the canopy. Oecologia 72, 520–526. doi: 10.1007/BF00378977

Hui, D., Luo, Y., Cheng, W., Coleman, J.S., Johnson, D., Sims, D.A. 2001. Canopy radiation- and water-use efficiencies as affected by elevated [CO_2]. Glob. Change Biol. 7, 75–91. doi: 10.1046/j.1365-2486.2001.00391.x

Inoue, Y., Peñuelas, J., Miyata, A. and Mano, M. 2008. Normalized difference spectral indices for estimating photosynthetic efficiency and capacity at a canopy scale derived from hyperspectral and CO_2 flux measurements in rice. Remote Sens. Environ. 112, 156-172. doi:10.1016/j.rse.2007.04.011

Knops, J.M.H., Reinhart, K. 2000. Specific leaf area along a nitrogen fertilization gradient. Am. Midl. Nat. 144, 265-272. doi: 10.1674/0003-0031(2000)144[0265:slaaan]2.0.co;2

Laisk, A., Loreto, F. 1996. Determining photosynthetic parameters from leaf CO_2 exchange and chlorophyll fluorescence (ribulose-1,5-bisphosphate carboxylase/oxygenase specificity factor, dark respiration in the light, excitation distribution between photosystems, alternative electron transport rate, and mesophyll diffusion resistance. Plant Physiol. 110, 903-912. doi: 10.1104/pp.110.3.903

Leuning, R., Kelliher, F.M., De Pury, D.G.G., Schulze, E.D. 1995. Leaf nitrogen, photosynthesis, conductance and transpiration: scaling from leaves to canopies. Plant Cell Environ. 18, 1183–1200. doi: 10.1111/j.1365-3040.1995.tb00628.x

Lee, B. 2015. Remote sensing-based assessment of gross primary production in agricultural ecosystems. Doctor degree dissertation, University of Bayreuth, pp. 41-62.

Lee, D.-Y., Kim, M.-H., Lee, K.-J. and Lee, B.-W. 2006. Changes in radiation use efficiency of rice canopies under different nitrogen nutrition status. Korean Journal of Agricultural and Forest Meteorology, 8, 190-198.

Loreto, F., Marco, G.D., Tricoli, D., Sharkey, T.D. 1994. Measurements of mesophyll conductance, photosynthetic electron transport and alternative electron sinks of field grown wheat leaves. Photosynth. Res. 41, 397-403. doi: 10.1007/BF02183042

Milroy, S.P., Bange, M.P., Sadras, V.O. 2001. Profiles of leaf nitrogen and light in reproductive canopies of cotton (*Gossypium hirsutum*). Ann. Bot. 87, 325–333. doi: 10.1006/anbo.2000.1344

Miyata, A., Leuning, R., Denmead, O.T., Kim, J., Harazono, Y. 2000. Carbon dioxide and methane fluxes from an intermittently flooded paddy field. Agric. For. Meteorol. 102, 287-303. doi: 10.1016/S0168-1923(00)00092-7

Monteith, J.L. 1972. Solar radiation and productivity in tropical ecosystems. J. Appl. Ecol. 9, 744–766. doi: http://www.jstor.org/stable/2401901

Monteith, J.L. 1977. Climate and the efficiency of crop production in Britain. Philos. T. Roy. Soc. B. 281, 277–294. doi: 10.1098/rstb.1977.0140

Moreau, D., Allard, V., Gaju, O., Gouis, J.L., Foulkes, M.J., Martre, P. 2012. Acclimation of leaf nitrogen to vertical light gradient at anthesis in wheat is a whole–plant process that scales with the size of the canopy. Plant Physiol. 160, 1479–1490. doi: 10.1104/pp.112

Monti, A., Bezzi, G. and Venturi, G. 2009. Internal conductance under different light conditions along the plant profile of Ethiopian mustard (*Brassica carinata* A. Brown.). J. Exp. Bot. 60, 2341-2350. doi: 10.1093/jxb/erp032

Muir, C.D., Hangarter, R.P., Moyle, L.C., Davis, P.A. 2014. Morphological and anatomical determinants of mesophyll conductance in wild relatives of tomato (*Solanum sect. Lycopersicon, sect. Lycopersicoides*; Solanaceae). Plant Cell Environ. 37, 1415-1426. doi: 10.1111/pce.12245

Nay-Htoon B. 2015. Water use efficiency of rainfed and paddy rice ecosystem. Ph.D dissertation, Nature Science of the University of Bayreuth.

Niinemets, Ü. 2007. Photosynthesis and resource distribution through plant canopies. Plant Cell Environ. 30, 1052-1071. doi: 10.1111/j.1365-3040.2007.01683.x

Niinemets, Ü., Díaz-Espejo, A., Flexas, J., Galmés, J., Warren, C.R. 2009A. Importance of mesophyll diffusion conductance in estimation of plant photosynthesis in the field. J. Exp. Bot. 60, 2271-2282. doi: 10.1093/jxb/erp063

Niinemets, Ü., Díaz-Espejo, A., Flexas, J., Galmés, J., Warren, C.R. 2009B. Role of mesophyll diffusion conductance in constraining potential photosynthetic productivity in the field. J. Exp. Bot. 60, 2249-2270. doi: 10.1093/jxb/erp036

Niinemets, Ü., Keenan, T.F. 2012. Measures of light in studies on light-driven plant plasticity in artificial environments. Front. Plant Sci. 3, 1-21. doi: 10.3389/fpls.2012.00156

Parry, M.A.J., Reynolds, M., Salvucci, M.E., Raines, C., Andralojc, P.J., Zhu, X.G, Price, G.D., Condon, A.G, Furbank, R.T. 2011. Raising yield potential of wheat. II. Increasing photosynthetic capacity and efficiency. J. Exp. Bot. 62, 453–467. doi: 10.1093/jxb/erq304

Rosenberg, N. J., Blad, B.L., Verma S.B. 1983. Microclimate: the biological environment, second edition. John Wiley & Sons, New York, pp 495.

Saitoh, K., Yonetani, K., Murota, T. and Kuroda, T. 2002. Effects of flag leaves and panicles on light interception and canopy photosynthesis in high-yielding rice cultivars. Plant. Prod. Sci. 5, 275-280. doi: 10.1626/pps.5.275

Sharkey, T.D., Bernacchi, C.J., Farquhar, G.D., Singsaas, E.L. 2007. Fitting photosynthetic carbon dioxide response curves for C_3 leaves. Plant Cell Environ. 30, 1035-1040. doi: 10.1111/j.1365-3040.2007.01710.x

Sheehy., J.E., Mitchell, P.L. 2013. Designing rice for the 21st century: the three laws of maximum yield. Discussion Paper Series 48. Los Nanos, Internationl Rice Research Institute, p19 .

Tosens, T., Niinemets, U., Vislap, V., Eichelmann, H. and Castro Diez, P. 2012. Developmental changes in mesophyll diffusion conductance and photosynthetic capacity under different light and water availabilities in Populus tremula: how structure constrains function. Plant Cell Environ. 35, 839-856.

Warren, C.R., Adams, M.A. 2006. Internal conductance does not scale with photosynthetic capacity: implications for carbon isotope discrimination and the economics of water and nitrogen use in photosynthesis. Plant Cell Environ. 29, 192-201. doi: 10.1111/j.1365-3040.2005.01412.x

Wullschleger, S.D. 1993. Biochemical limitations to carbon assimilation in C_3 plants–a retrospective analysis of the A/C_i curves from 109 species. J. Exp. Bot. 44, 907-920. doi: 10.1093/jxb/44.5.907

Yamori, W., Nagai, T., Makino, A. 2011. The rate-limiting step for CO_2 assimilation at different temperatures is influenced by the leaf nitrogen content in several C3 crop species. Plant Cell Environ. 34, 764-777. doi: 10.1111/j.1365-3040.2011.02280.x

Yang, J., Gao, W., Ren, S.R. 2015. Long-term effects of combined application of chemical nitrogen with organic materials on crop yields, soil organic carbon and total nitrogen in fluvo-aquic soil. Soil Tillage Res. 151, 67-74. doi: 10.1016/j.still.2015.03.008

Yoshida, S. 1981. Fundamentals of rice crop science. The International Rice Research Institiute, Manila, Philippines. pp. 130-146.

5. Appendix

Additional publications not included in this thesis

Otieno, D., **Lindner, S.**, Muhr, J., Borken, W., 2012: Sensitivity of Peatland Herbaceous Vegetation to Vapor Pressure Deficit Influences Net Ecosystem CO_2 Exchange. Wetlands 32, 895–905.

Kettering, J., Park, J.H., **Lindner, S.**, Lee, B., Tenhunen, J., Kuzyakov, Y., 2012: N fluxes in an agricultural catchment under monsoon climate: A budget approach at different scales. Agriculture, Ecosystems and Environment 161, 101– 111.

Arnhold, S., **Lindner, S.**, Lee, B., Martin, E., Kettering, J., Nguyen, T.T., Koellner, T., Ok, Y.S., Huwe, B., 2014: Conventional and organic farming: Soil erosion and conservation potential for row crop cultivation. Geoderma 219–220, 89–105.

Xue, W., Nay–Htoon, B., **Lindner, S.**, Dubbert, M., Otieno, D., Ko, J., Werner, C., Tenhunen, J. (2016): Soil water availability and capacity of nitrogen accumulation influence variations of intrinsic water use efficiency in rice. Journal of Plant Physiology 193, 26–36.

Xue, W., **Lindner, S.**, Nay–Htoon, B., Harley, P., Huwe, B., Ko, J., Otieno, D., Muraoka, H., Werner, C., Tenhunen, J., (under review): Differentiation in paddy versus rainfed rice in factors influencing carbon gain, water use and grain yield under monsoon climate in South Korea. (submitted to Journal of Plant Research)

(Eidesstattliche) Versicherungen und Erklärungen

(§ 8 S. 2 Nr. 6 PromO)

Hiermit erkläre ich mich damit einverstanden, dass die elektronische Fassung meiner Dissertation unter Wahrung meiner Urheberrechte und des Datenschutzes einer gesonderten Überprüfung hinsichtlich der eigenständigen Anfertigung der Dissertation unterzogen werden kann.

(§ 8 S. 2 Nr. 8 PromO)

Hiermit erkläre ich eidesstattlich, dass ich die Dissertation selbständig verfasst und keine anderen als die von mir angegebenen Quellen und Hilfsmittel benutzt habe.

(§ 8 S. 2 Nr. 9 PromO)

Ich habe die Dissertation nicht bereits zur Erlangung eines akademischen Grades anderweitig eingereicht und habe auch nicht bereits diese oder eine gleichartige Doktorprüfung endgültig nicht bestanden.

(§ 8 S. 2 Nr. 10 PromO)

Hiermit erkläre ich, dass ich keine Hilfe von gewerblichen Promotionsberatern bzw. -vermittlern in Anspruch genommen habe und auch künftig nicht nehmen werde.

Bayreuth, _____

Steve Lindner